INELFE

BISCAY GULF WESTERN INTERCONNECTOR

HYDROSEDIMENTARY STUDIES REPORT

FINAL REPORT

ARTELIA Eau & Environnement
Branche MARITIME
6 rue de Lorraine
38130 - Echirolles
Tel. : +33 (0) 4 76 33 40 00
Fax : +33 (0) 4 76 33 43 33

DATE : MARCH 2018 **REF :** 8 71 37343

N° 8 71 37343 - Biscay Gulf Western Interconnector – Hydrosedimentary studies report – Final report					
02	Revision with client comments + inclusion of alternative Spanish route and alternative HDD canyon crossing route	ALZ	SAL	SAL	29/03/2018
01	Revision with client comments + inclusion of Spanish landfall	ALZ	SAL	SAL	14/02/2018
00	First issue	CCL - ALZ	SAL	SLX	30/10/2017
Version	Description	Redaction	Checked	Approved	Date

TABLE OF CONTENTS

TABLES

FIGURES

EXECUTIVE SUMMARY

The overall aim of the Biscay Gulf Western Interconnector metocean and hydrosedimentary studies is to provide input for the identification of a suitable route for the submarine interconnector and the determination of appropriate burial depths/cable protection methods to ensure the security of the asset during its operational lifetime.

To achieve this, ARTELIA investigated coastal stability, seabed mobility and vertical seabed changes at landfall areas (at French and Spanish sides) as well as at the coastal area of Capbreton canyon, and seabed mobility and vertical seabed changes along the 283 km long offshore cable route (see following figure for location of the studied areas).

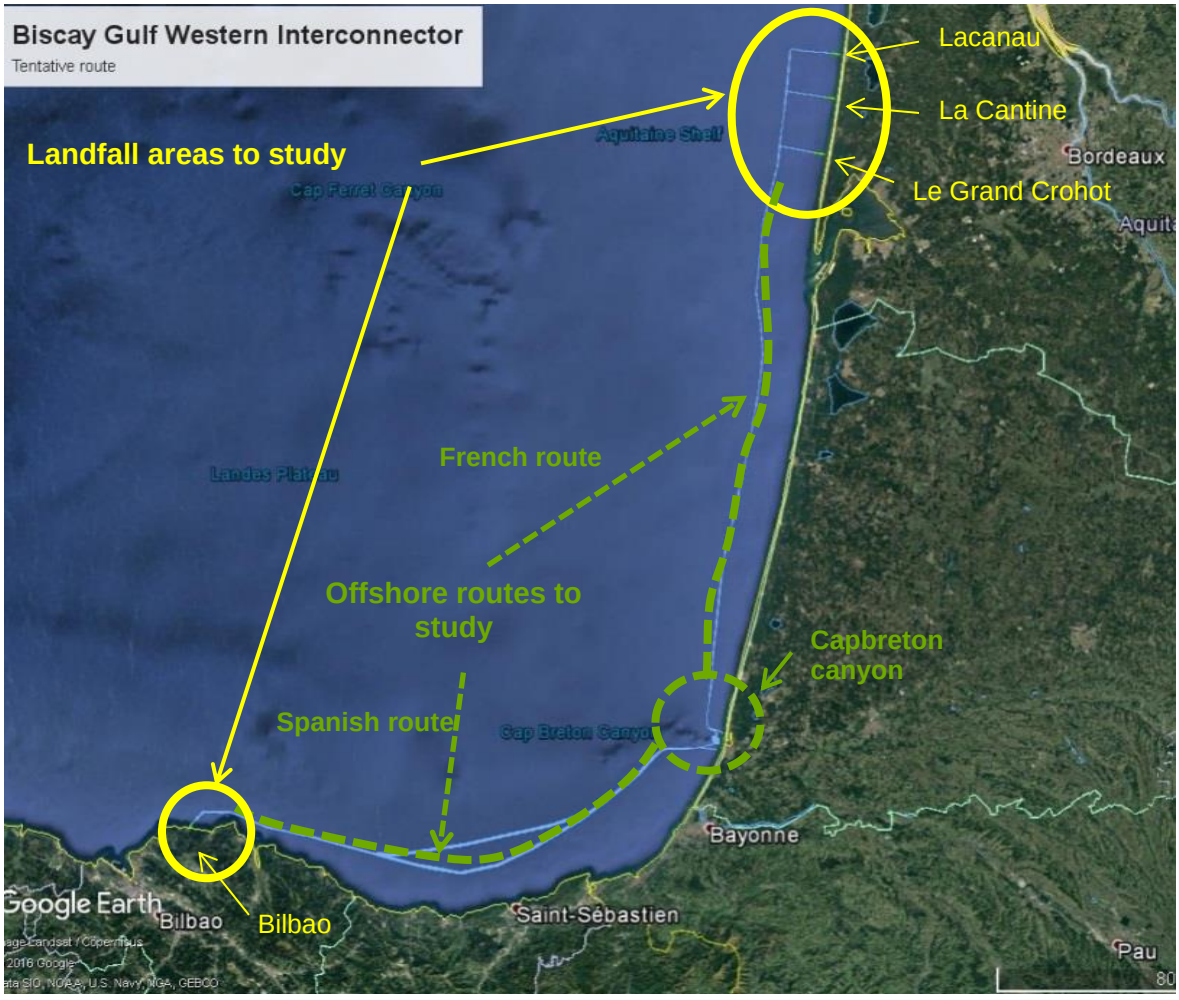

Figure 1. Overview of the main route of the cable including its coastal zone crossing Capbreton canyon and the French and Spanish landfall areas

In order to assess the sea bed level variability and the maximum extent of the potential vertical seabed variations at each zone of interest, specific methodologies have been implemented depending on the areas, as following:

- For the three French landfall locations :
  - Characterization of seabed nature from comprehensive geophysical and geotechnical surveys;

- Long term evolution of the shoreline (past and future);
- Long term changes of beach profiles;
- Cross-shore profile evolution during storm events.

- For Capbreton canyon:
  - Specific studies of the interaction between the canyon head and the shore through analysis of bathymetric data in collaboration with:
    - I-SEA for the provision of satellite imagery,
    - the city council of Capbreton for the provision of in situ bathymetric surveys and
    - Mr Hervé Gillet from the University of Bordeaux for his knowledge and expertise of the area.

- For the offshore routes :
  - Characterization of seabed nature and movable sediment thickness from comprehensive geophysical and geotechnical surveys;
  - Assessment of potential seabed level change.

- For the Spanish landfall location:
  - Characterization of seabed nature and movable sediment thickness from comprehensive geophysical and geotechnical surveys;
  - Conclusion on the potential vertical variation of the movable seabed layer.

Conclusions of the hydro-sedimentary study are the following.

Nature and characteristics of sedimentary features of movable seabed and hydro-sedimentary study results in terms of vertical seabed variation for **the three French landfalls**:

- Seabed along the three studied French landfalls is made of sand (fine to medium);
- Thickness of movable sediment layer is greater than 5 m;
- Long term vertical seabed variations:

  At each landfall location, the comparison between initial profile and predicted profiles in 2050 and 2067 leads to a first assessment of the vertical variation of the sea bed during the cable life span;

  Assessed vertical variations are the greatest at Lacanau, reaching -3.8 m, at the higher part of the profile (at the foot of the dune) as well as at its lower one (by 10 m water depth);

  For the 2 other profiles, assessed vertical variations are about -1.5m at the foot of the dune and -1m by 5 m water depth.
- Short term vertical seabed variations (due to storm conditions) :

  Sbeach modelling is used to assess the short term vertical evolutions below 10 m CD due to profile reshaping under Hercule storm conditions (major storm that occurred in January 2014);

Shoreline retreat due to the storm is highest at Lacanau (about 30 m) and smallest at La Cantine (less than 10 m) and Grand Crohot (almost nil). Sand is taken on the beach and moved offshore, leading to short term vertical variations (erosion above sea level, accretion below sea level) of 1 to 4 meters depending on the profile.

Nature and characteristics of sedimentary features of movable seabed and hydro-sedimentary study results in terms of vertical seabed variation for **coastal route section crossing the Capbreton canyon**:

- Cyclic vertical seabed variations:

  V**ertical amplitude of sea bed changes in front of canyon head is important for bathymetry above -30 m CM.** It can reach:

  - **5 m in very shallow waters** (intertidal beach + upper subtidal beach i.e. depths from +2 m to -5 m);
  - **8 m in greater depths** (-5 m to -30 m) due to interactions between the subtidal beach and the the canyon head;
  - **A maximum 12 m vertical change is observed at the north-east corner of the canyon head** at depths of 15-25 m.

  Variations of seabed level in this area are cyclic and mostly due to migration of sand bars onshore/offshore with respect to wave conditions. Maximum vertical variations are important during a cycle, but no trend of long term evolution of seabed (erosion or / and accretion) has been highlighted so far.

  If the cable route is crossing this area, it can be expected that sometime during its lifespan, the cable will be buried under a sandbar, therefore 8 or 10 meters below the seabed surface.

Nature and characteristics of sedimentary features of movable seabed and hydro-sedimentary study results in terms of vertical seabed variation along the **offshore main cable route**:

Results are summarized in the following table. Sections 2 and 3 of the main route are most at risk from bed level change:

- about +/-2 m in section 2 due to sand dune migration at a rate of 7 to 33 m per year,
- about +/- 8 m to 10 m at the canyon head cyclically and mostly due to migration of sand bars onshore/offshore with respect to wave conditions (cf section 2.3).

Within these sections at high risk of bed level change, the rate of sand bar migration is sufficiently rapid for the features to move across the cable route during the proposed lifetime of the asset, and to bury or expose the cable of the equivalent of their height.

Table 1 – Subsections mobility along the Main Route

Section	Subsection	Metocean analysis point	Bed forms	Thickness of erodible layer	D50 (mm) of surficial layer	Seabed mobility (% of the year)	Seabed level change
MR 1	1	N02	Sand ripples Δr < 7 cm	Larger than 5 m	Sand, 0.29 – 0.40	From 35% to 50%	Maximum bed level change is likely to be of the order of 10 cm
	2	N02				About 35%	
	3	L01				About 18%	
MR 2	4	L02, L03	Sandy ribbons and isolated sand dune like bed forms with height of 2 meters	Larger than 5 m	Sand + Gravel, 0.29 – 1.2	From 13% to 30%	Maximum bed level change is likely to be around 2m, which is the height of the largest seabed features. These features migrate at a rate of 7 to 33m per year
	5	L04, L05, L06				< 20%	
MR 3	6		Sand ripples Δr < 5 cm	2.5 to 5 m	Sand, 0.18 – 0.32	Important rate of mobility	Formation and migration of sand ripples/ height of sand ripples < 5 cm outside the canyon head and seabed level changes of +/- 8 m to 10 m at canyon head
MR 4	7		No bed forms identified	From1 to 2 m, with local outcrops	Sand, silt and clay		Negligible bed level change
	8	L07					
	9	L08, L09, L10				<0.65%	
	10					No seabed mobility	
	11	L11			Sand, 0.09 to 0.9	Weak seabed mobility	Negligible bed level change
	12	L12				Weak seabed mobility	

Nature and characteristics of sedimentary features of movable seabed and hydro-sedimentary study results in terms of vertical seabed variation along the **HDCC route** are summarized in the following table.

Table 2 – Potential mobility along the HDCC route

Section	Metocean analysis point	Bed forms	Thickness of erodible layer	D50 (mm) at surficial layer	Seabed mobility (% of a year)	seabed level change
KP 0 to KP 3.432	**S09**	No evidence of bedforms	**Mostly greater than 3m**	Fine to medium sand, **D_{50} = 0.18 mm**	High potential of seabed mobility due to local wave climate on canyon sides , from 40 to 59%	No evidence of seabed level change. Lack of data to conclude
KP 3.432 to KP 5.315	**Canyon walls and canyon floor**	**Steep slopes** at canyon walls (reaching 59 deg) **Sediment slump/ slides**	**No sediment along canyon wall and where the CS outcrops**	Gravelly sand at canyon floor	No mobility due to hydraulic forcingon the canyon walls and canyon floor	Evidence of **slumping seabed** in vicinity of the canyon walls
KP 5.315 to KP 8.599	**S08**	No evidence of bedforms. Two local CS outcropping	**Mostly greater than 3 m** Except between KP 6.383 to KP 6.606 when CS outcrops	Fine to medium sand, **D_{50} = 0.18 mm**	High potential of seabed mobility due to local wave climate on canyon sides , from 69 to 83%.	No evidence of seabed level change. Lack of data to conclude.

The available data do not allow us to conclude on the seabed level change along the HDCC route on each side of the canyon. Indeed, seabed material can be mobilized through hydraulic forcing but no evidence of such seabed mobility (such as bedforms) is observed. Differential bathymetric data are needed to provide quantitative information.

What is important to note is the slumping/slides, observed along the canyon walls, that have to be linked with the flushing of sediments observed at the canyon's head), mechanisms typical of submarine canyons.

Nature and characteristics of sedimentary features of movable seabed and hydro-sedimentary study results in terms of vertical seabed variation along the **ARSW route**:

Table 3 – Potential mobility along ARWS

Section	Metocean analysis point	Bed forms	Thickness of erodible layer	D50 (mm) at surficial layer	Seabed mobility (% of a year)	seabed level change
ARSW	L08, L10	Bedrock outcropping Evidence of **trawl marks**	Relatively thin layer of surficial sediments over bedrock may not allow sufficient depth of burial for the proposed cable.	Fine sand , Sandy clay D50 < 0.2 mm	Very low potential of seabed mobility (< 0.4%)	Negligible bed level change.

The results show that the ARSW has a very thin layer of surficial sediments and that these sediments are not likely to be moved by the hydraulic conditions mainly due to the deep water depths.

The major constraint along this route is the relatively thin layer of surficial sediments over the bedrock that may not provide sufficient depth of burial for the proposed cable.

Nature and characteristics of sedimentary features of movable seabed and hydro-sedimentary study results in terms of vertical seabed variation for **Spanish landfall**:

- Seabed along the Spanish landfall is mainly bedrock with isolated patchy sand and gravel veneer;
- Thickness of movable sediment in sand and gravel pouch reaches 2.5 m;
- Assessment of potential depth of seabed mobility: Wave action enable reworking of medium to coarse sand trapped and accumulated in bedrock cavities. This hydrodynamic forcing induces formation of sand ripples at seabed surface. Potential seabed level change is of the order of height of sand ripples.

Table 4 – Potential mobility at Spanish landfall

Section	Metocean analysis point	Bed forms	Thickness of erodible layer	D50 (mm) at surficial layer	Seabed mobility (% of a year)	Seabed level change
SL[1]	Sp02, Sp01	Mainly bedrock, with isolated patchy sand and gravel veneer/ Ripples at seabed surface of sand pouch Height < 10cmr	Reaches 2.5m	Sand and Gravel trapped in bedrock cavities. D50 = 0.5 mm at surficial layer	Surficial sand in sandy pouch are possibly reworked 41% of the year	In sandy pouch made of sediment trapped in bedrock cavities, seabed changes are equal to height of sand ripples < 10 cm.

No significant seabed level change are expected at the Spanish landfall, due to the rocky nature of the seabed.

Finally, according to a simple comparison of historical aerial pictures we can assume the apparent stability of the coastline at the Spanish landfall area. Shoreline accretion or recession at the Spanish landfall is expected to be negligible over the cable life span.

[1] SL for Spanish Landfall

DEFINITION, ABREVIATION AND NOTATIONS

ARSW	Additional Route in Spanish Waters
BRGM	Bureau de Recherches Géologiques et Minières
BSF	Below Sea Floor
CC	Climate Change
CM	*Cote Marine* - Altimetric reference corresponding to the Chart Datum (CD)
CS	Consolidated Seabed
HAT	Highest Astronomical Tide
HDCC (or HDDC)	Alternative route Crossing the Canyon
HDD	Horizontal Directional Drilling
IGN69 /NGF	Terrestrial French altimetric reference -Correlations between the different altimetric systems are given by the SHOM for the main harbours along the French coast
LAT	Lowest Astronomical Tide
MHWS	Mean High Water Spring
MLWS	Mean Low Water Spring
MR	Main Route
MSL	Mean Sea Level
LCHF	Laboratoire Central d'Hydraulique de France
OCA	Observatoire de la Côte Aquitaine
ONF	Office National des Forêts
SHOM	Service Hydrographique et Océanographique de la Marine
SL	Spanish Landfall

Table 5 – Names and acronyms in French and English for astronomical tide levels

Coefficient	French		English	
	Pleine mer	**Basse mer**	**High water**	**Low water**
120	PHMA Plus Haute Mer Astronomique	PBMA Plus Basse mer Astronomique	HAT Highest Astronomical Tide	LAT Lowest Astronomical Tide
95	PMVE Pleine Mer de Vive-Eau	BMVE Basse Mer de Vive-Eau	MHWS Mean High Water Spring	MLWS Mean Low Water Spring
70	Pleine Mer de Marée Moyenne	Basse Mer de Marée Moyenne	MHW Mean High Water	MLW Mean Low Water
45	PMME Pleine Mer de Morte-Eau	BMME Basse Mer de Morte-Eau	MHWN Mean High Water Neap	MLWN Mean Low Water Neap
20	Pleine Mer de Morte-Eau Exceptionnelle	Basse Mer de Morte-Eau Exceptionnelle	LAHW Extreme Neap Tide High Water	HALW Extreme Neap Tide Low Water
-	NM Niveau moyen		MSL Mean Sea Level	

1. PURPOSE OF THE STUDY AND OBJECTIVES OF THE HYDRO-SEDIMENTARY STUDIES

1.1. CONTEXT OF THE STUDY

RTE launched a consultation about metocean and hydro-sedimentary studies in the frame of various projects concerning the interconnectors for the electricity supply (laying and protection of the submarine cables).

INELFE, a consortium between RTE and REE (Red de Eléctrica de España, its Spanish counterpart), has awarded ARTELIA for the studies of the Biscay Gulf Western Interconnector (BGWI) project (Figure 2).

Figure 2. Route of the interconnector (blue line)

The length of the marine cable route is approximately 280 km (180 km in French waters and 100 km in Spanish waters). The cable route is located between 10 and 20 km offshore from the coast, except at the landfalls and the Capbreton canyon crossing. The possible route position corresponding to the routes surveyed in 2016 is provided in Appendix 1 of [1].

The metocean and hydro-sedimentary studies aim to:

- Give input to the designers for defining the position of the cable (route and burying depth within de pre-defined corridor);
- Optimise the laying of the cable (schedule, Weather Down Time to go on site…);
- Inform the requirement for cable protection.

The present report deals with the hydro-sedimentary study. It describes the methodology, the models developed and the results of the hydro-sedimentary study in terms of sea bed elevation variation at the landfalls and along the offshore route, including the crossing of the Capbreton Canyon. It is organized as follows :

- Chapter 2 refers to the French landfalls and the Capbreton area,
- Chapter 3 analyses the hydrosedimentary dynamics along the offshore route and
- Chapter 4 refers to the Spanish landfall.

1.2. OBJECTIVES OF THE HYDRO-SEDIMENTARY STUDY

The overall aim of the Biscay Gulf Western Interconnector metocean and hydrosedimentary studies is to provide input for the identification of a suitable route for the submarine interconnector and the determination of appropriate burial depths/cable protection methods to ensure the security of the asset during its operational lifetime.

To achieve this, it is necessary to understand the following issues associated with sediment dynamics and sea bed morphology:

- Coastal/seabed stability at landfall areas and in the area of Capbreton canyon.

  Four locations are proposed for the landfall of the cable: 3 on the Aquitaine coast (at Lacanau, La Cantine and Le Grand Crohot) and 1 on the Spanish Basque coast (close to Bilbao). At these four locations, the rates of the coastal line retreat (or accretion) in the medium (50 years) term have to be assessed, as well as short term profile response to storm events (how much beach lowering occurs).

  This will help to determine how deep the cable needs to be buried to ensure that it would not be exposed during its operational lifespan.

  Then, to engineer the bypass of the Capbreton canyon head, INELFE engineering team needs to understand both the nearshore morphology in this area and how dynamic the seabed is. In this study, attention is given to the area inshore from the canyon head to provide seabed level elevations variations in response to storms or longer term profile evolution. For these assessments, ARTELIA has collaborated with I-SEA for satellite imagery and with Mr. Hervé Gillet from the University of Bordeaux, for his knowledge and expertise in this area of the Aquitaine coast.

- Seabed mobility and bed level changes along the offshore cable route.

  It will be necessary to identify areas along the entire cable route where the seabed is mobile and under which conditions mobility occurs. However, the primary output should indicate areas that are subject to significant bed level changes, rather than simply whether the surface sediments are mobile. This could include ongoing migration of bedforms and other medium scale seabed features that cause bed levels to change.

  Offshore routes sections studied in this report are the Main Route, the Alternative Route in Spanish Waters (ARSW) and the HDCC (Horizontal Drilling Crossing Canyon) route.

.

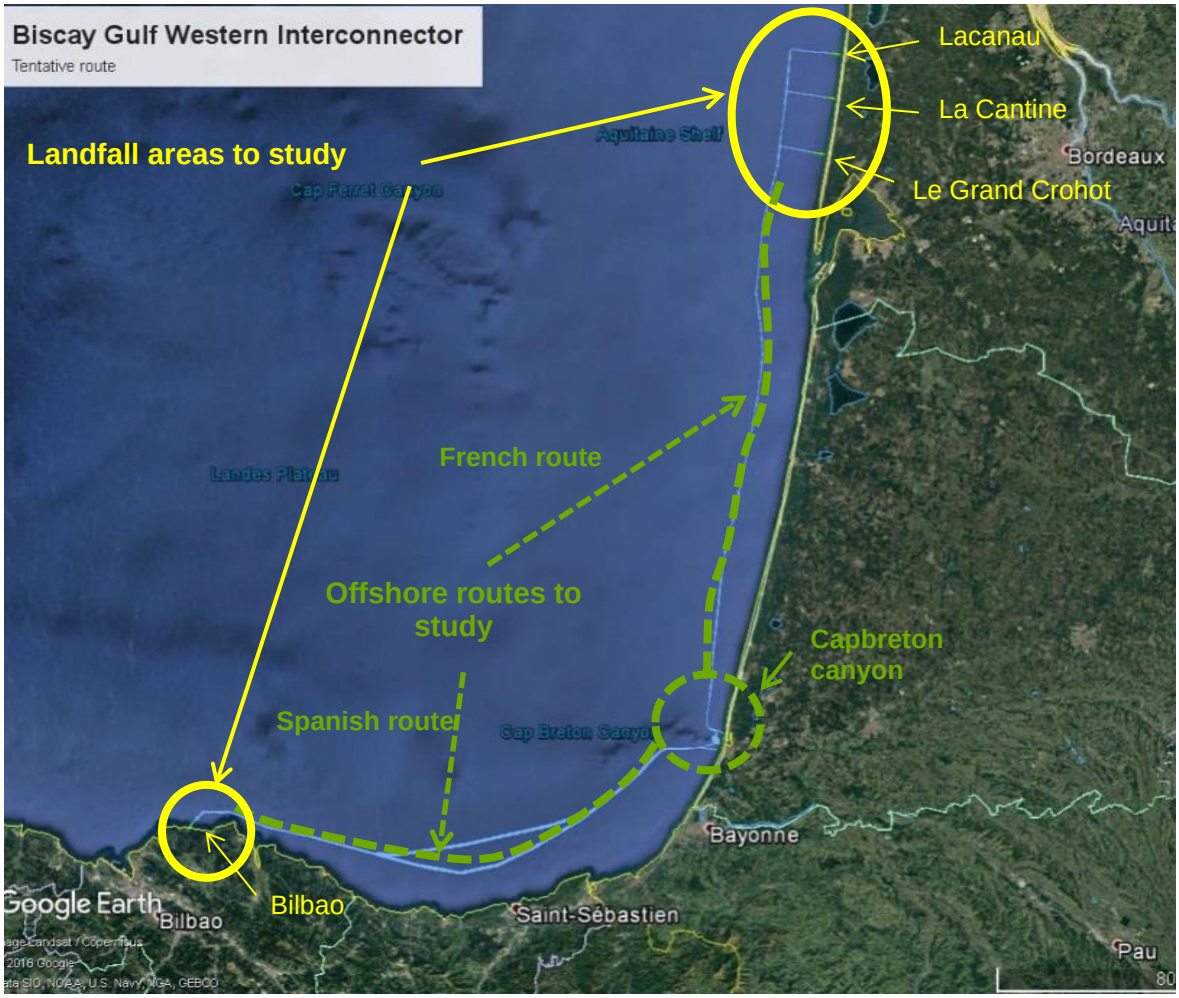

***Figure 3.* Overall view of the cable route**

2. COASTAL STABILITY AT FRENCH LANDFALLS AND CAPBRETON AREA

2.1. INTRODUCTION

Two French coastal areas are to be studied: the landfall area located between Lacanau and Lège (Aquitaine coast), and the Caprebton area (between the canyon's head and the shore area)

In order to assess the sea bed level variability and the maximum extent of the potential vertical variations at these coastal areas, specific methodologies have been implemented depending on the areas, as follows:

- For French landfalls :
  - Long term evolution of the shoreline (past and future);
  - Cross-shore profile evolution during storm events (short term) ;
  - Long term changes of beach profiles.

- For Capbreton canyon
  - Specific studies of the interaction between the canyon's head and the shore through collaboration with:
    - I-SEA for the provision of satellite imagery,
    - the city council of Capbreton for the provision of in situ bathymetric surveys and
    - Mr Hervé Gillet from the University of Bordeaux for his knowledge and expertise of the area.

2.2. FRENCH LANDFALLS

2.2.1. Location of French landfalls

The three French landfalls to study are located on Aquitaine coast in Southwestern France, between Lacanau city and Lège city. Lacanau, a French municipality in the Gironde department in Nouvelle-Aquitaine region, is located between the Gironde estuaries (70 km further north) and the Bassin d' Arcachon (50 km further south).

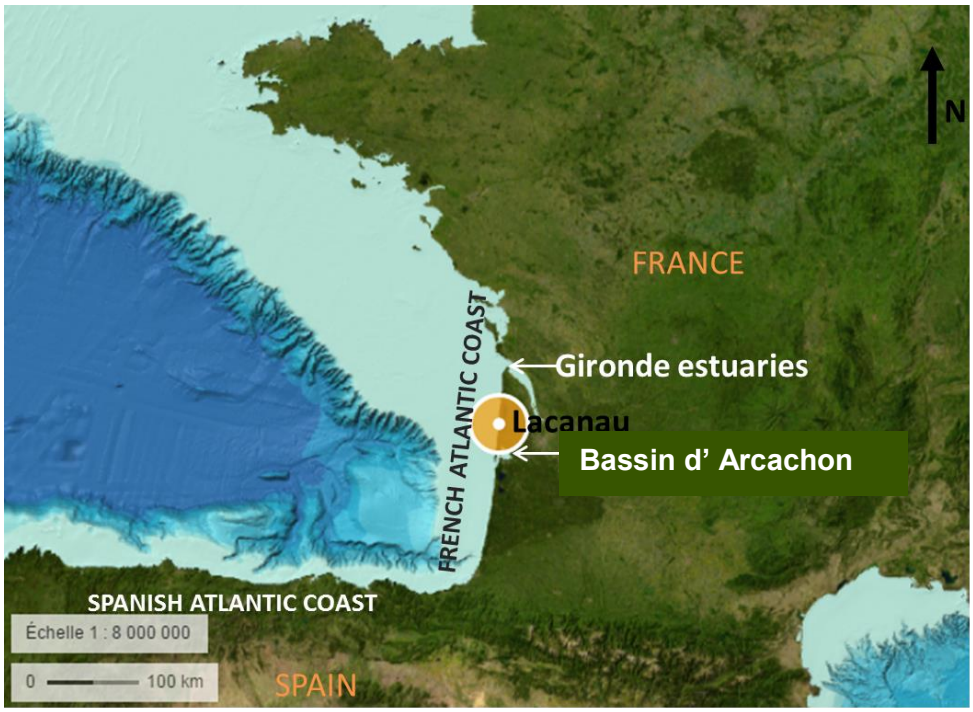

Figure 4. Lacanau area

The French landfalls area is characterized by a very straight coast oriented ~5°N. The three locations under study are, from North to South:

- Lacanau, located immediately to the North of the urban city of Lacanau Ocean;
- La Cantine,located about 10 km south, in front of a natural shoreline;
- Le Grand Crohot, located about 20 km south (from the first location), in front of a naturel area too.

The following pictures illustrate the 3 potential landfalls locations.

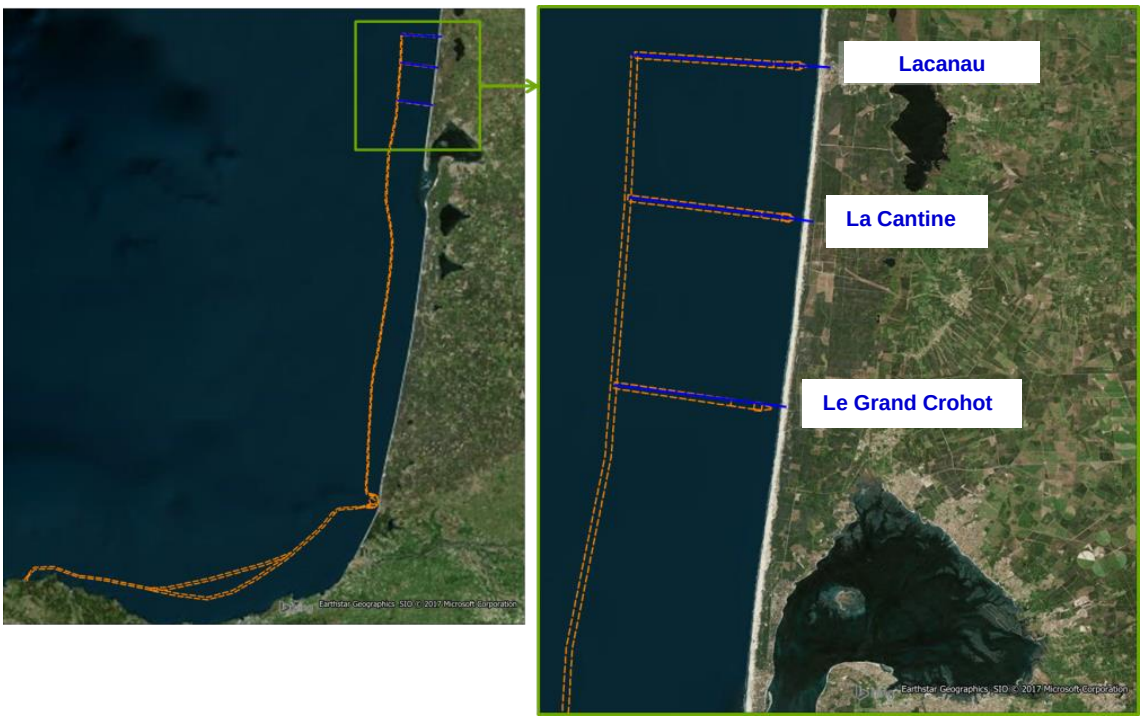

***Figure 5.* Cable route overview and French landfall locations**

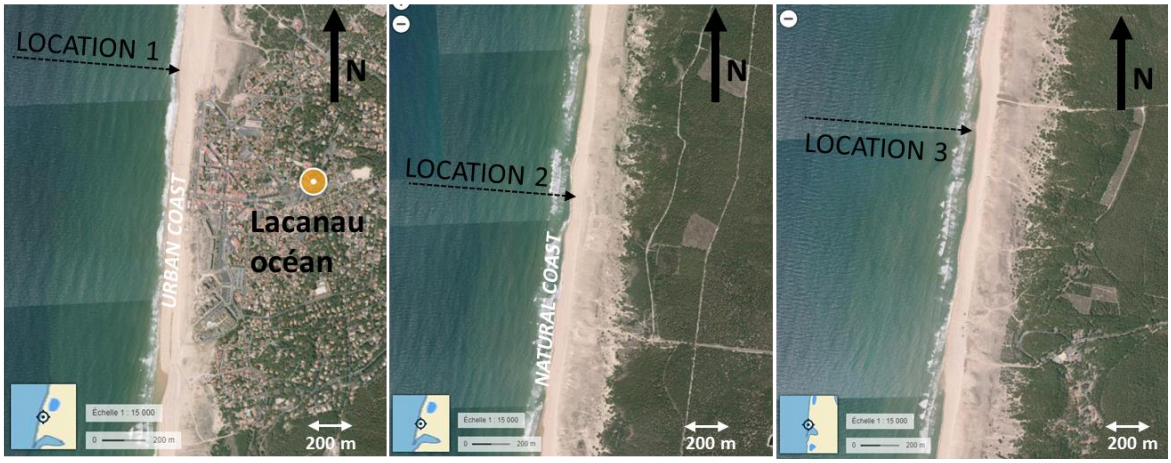

***Figure 6.* French landfalls locations**

2.2.2. Geomorphology of the area

The following figure presents the overall bathymetry of the French landfalls area issued from the SHOM. The bathymetry is regular with isobaths almost parallel to the coastline, without outstanding features.

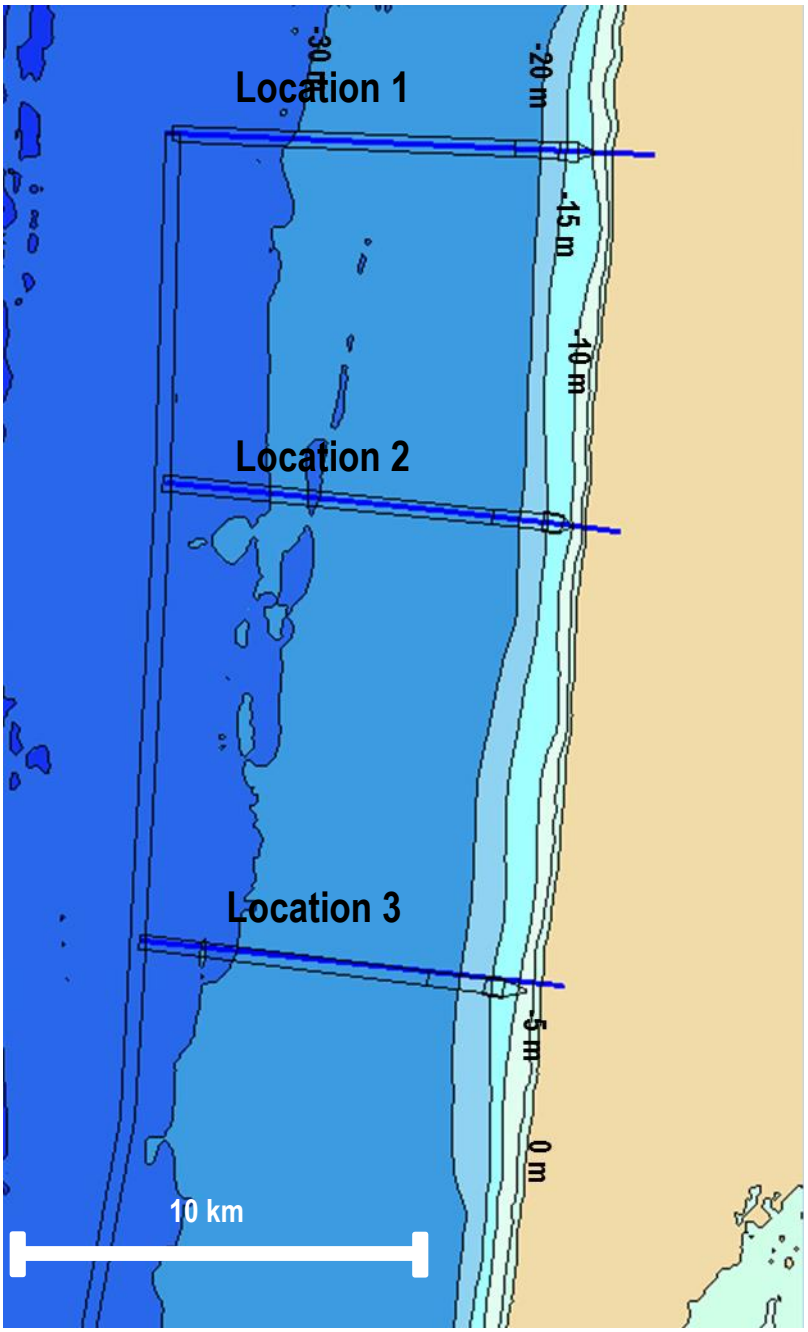

Figure 7. Bathymetry in French landfall area (source : SHOM)

The area is also quite homogeneous from a sedimentary point a view.: it is included in the hydrosedimentary cell n°3 of the Aquitaine coast (see Figure 8 Figure 7) between the Bassin d' Arcachon bay and the Anse Gurp.

The hydro-sedimentary cells are defined by the homogeneity of their typical cross section and the homogeneity of sedimentary transports.

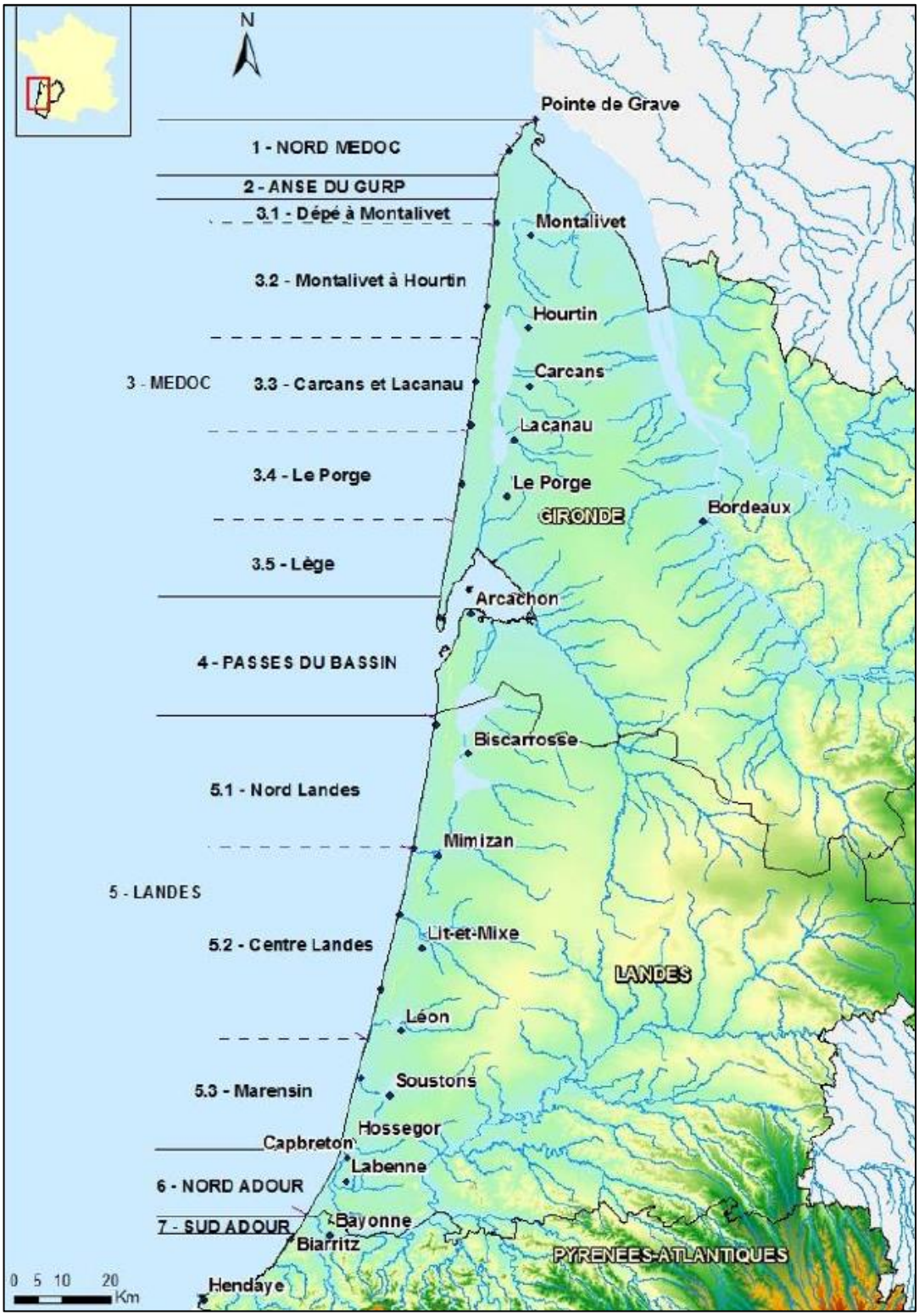

Figure 8. ***Hydro-sedimentary cells defined along the Aquitaine coast (BRGM)***

The typical cross section of the Aquitaine coast is presented in Figure 9 and is composed of:

- A regular slope in deep water area up to the near shore area;
- A system of one or many longshore bars and troughs in the nearshore area;
- A foreshore including the wet and dry beach;
- A system of sandy or vegetated dunes.

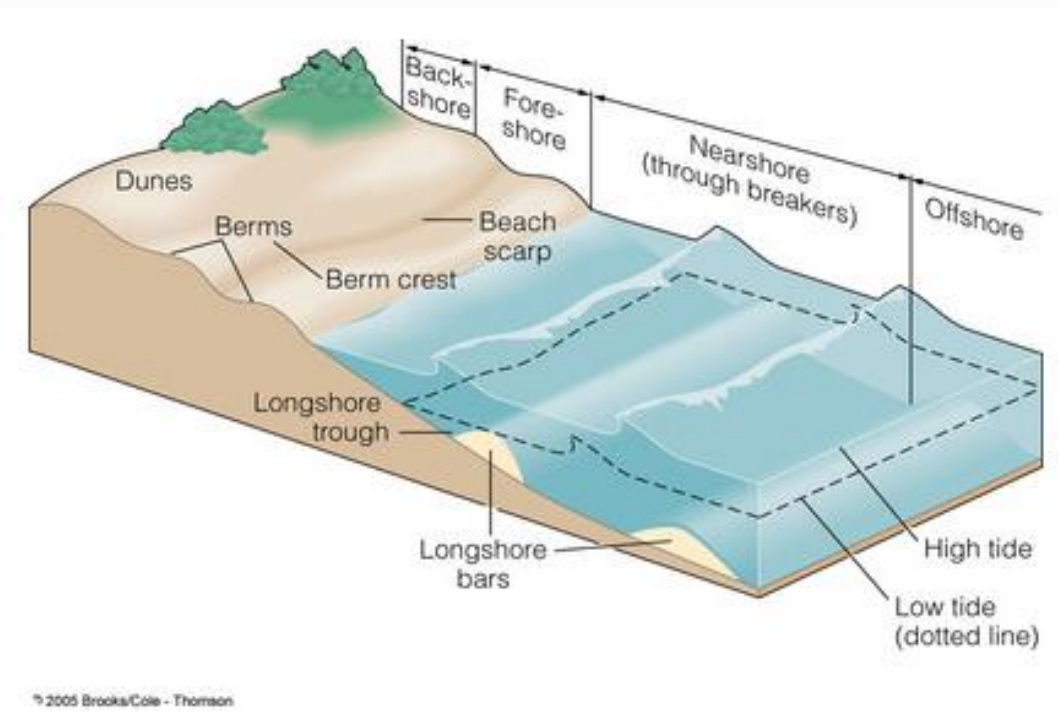

Figure 9. Typical cross-section along the Aquitaine shoreline

2.2.3. Local granulometry

According to [3], the local dune sand has a mean grain diameter between 0.150 mm and 0.350 mm, which is characteristic of fine to medium sand according to the Wentworth sediment classification, which is presented in Table 6 below.

Table 6 - The Wentworth sediment classification

Grain diameter range (mm)	Classification	
>256	Boulder	Gravel
64 - 256	Cobble	
4 - 64	Pebble	
2 - 4	Granule	
1 - 2	Very coarse sand	Sand
0.5 - 1	Coarse sand	
0.25 - 0.5	Medium sand	
0.125 - 0.250	Fine sand	
0.0625 - 0.125	Very fine sand	
0.004 - 0.0625	Silt particle	Mud
< 0.004	Clay particle	

On the beach, the mean grain diameter is between 0.300 mm and 0.500 mm, characteristic of a medium sand. A *Laboratoire Central d'Hydraulique de France* (LCHF) report issued in 1979 gives a mean diameter greater than 0.300 mm from the berm to the isobaths -2 m CD in front of Lacanau where hydrodynamics is high due to wave breaking.

From -2 m CD and -20 m CD, mean diameter is between 0.125 mm and 0.300 mm, characteristic of fine sand.

For deeper sea beds, the sediment becomes medium to coarse sand.

This description of sandy sea bed is in accordance with [11], as illustrated on the following figure.

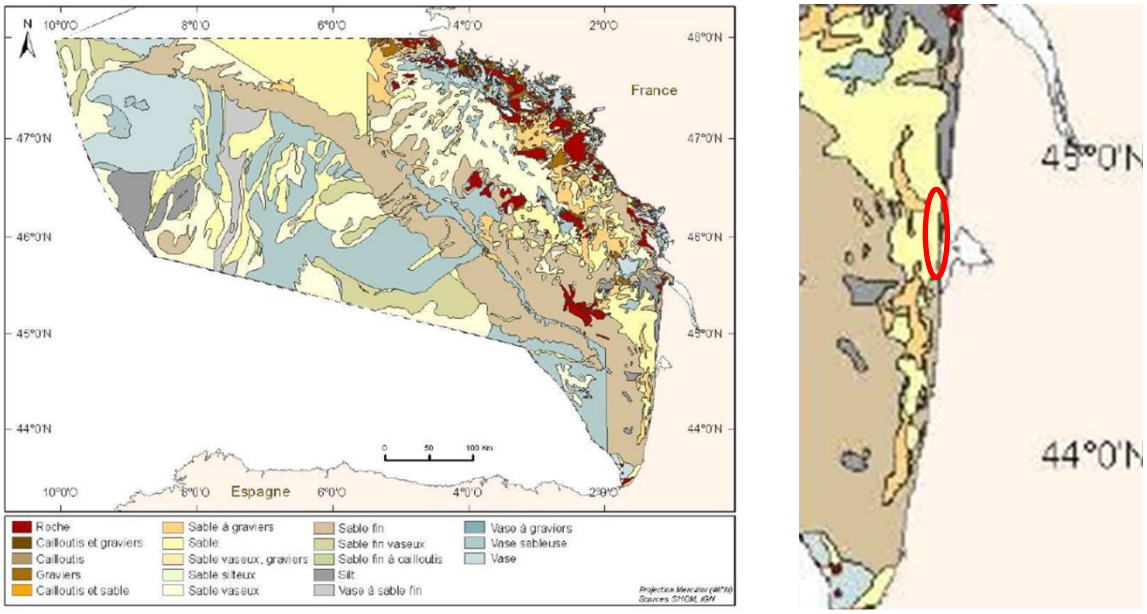

Figure 10. Mapping of the nature of sediment along the Aquitaine Coast, from [11]

2.2.4. Morphodynamic evolution of the area

2.2.4.1. Mechanisms of morphodynamic evolution

This section aims at understanding the mechanisms that govern the hydro-sedimentary dynamics in front of French landfalls area.

Along the Aquitaine coast and in particular in front of French landfalls area, waves are the primary forcing mechanism for morphodynamic evolution and especially so during storm conditions. Tidal currents are not strong enough to shape alone the seabed but can be involved in transport of sediments already resuspended under wave action.

Figure 11 presents a schematic representation of the main forcing mechanisms for sedimentary dynamics that shape the Bay of Biscay (from [11]).

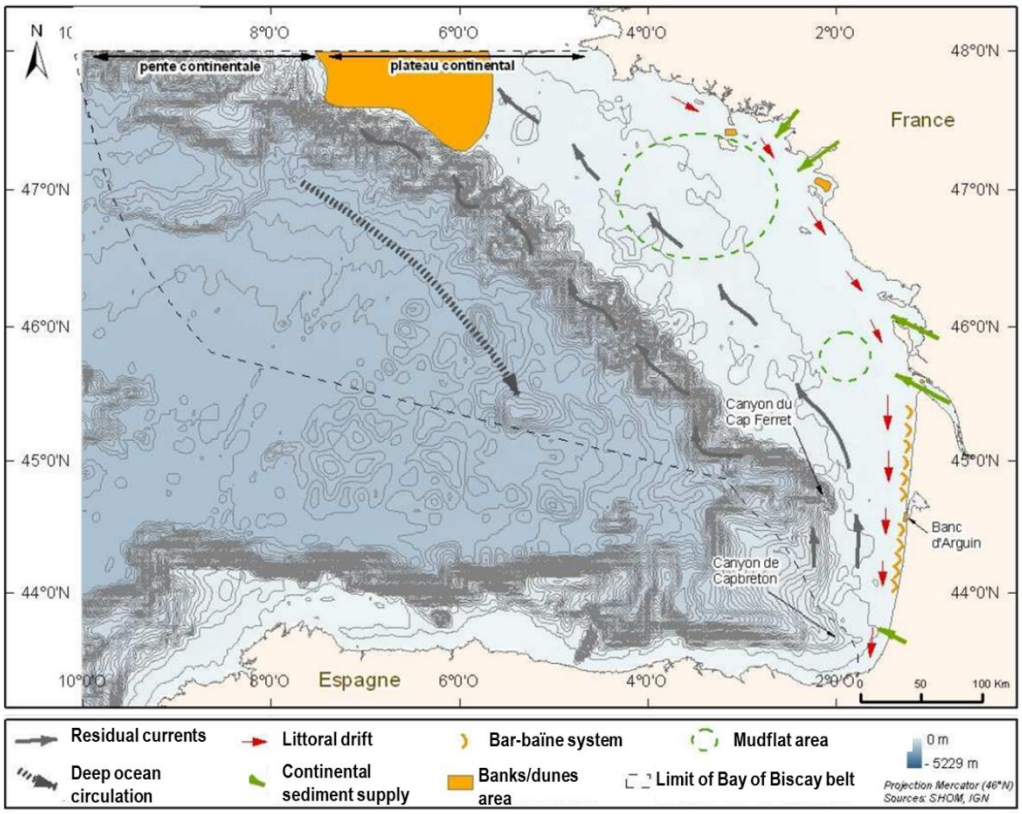

Figure 11. Main sedimentological transits and locations of the main structures of the Bay of Biscay, from [11]

The strongest dynamics are located nearshore, between the shoreline and the closure depth, which is taken to be the offshore limit of *significant seasonal* variation of the beach or seabed profile and is estimated to be around -11 to – 13m CD along the Aquitaine coast

It is noted that beyond closure depth, in much deeper water than this; large storm waves can still interact with the seabed and still stir sediments beyond this depth.

Two main types of sediment motions take part in the local morphodynamics :

- Sediment transport along the shoreline : the littoral drift ,
- Sediment transport along the cross shore profile.

Mid and long-term evolution of the shoreline is mainly due to gradient of littoral drift along the coast (this gradient can be natural or artificial if in presence of coastal structures perpendicular to the coast, like groins). Along the Aquitaine coast, the longshore transport is oriented from North to South (like in the area under study) but can possibly reverse locally in the vicinity of a bay or a headland.

Short term evolution is generally due to motions in cross-shore profile, which are seasonal or generated by storms. Processes involved in sediment motion are illustrated on Figure 13.

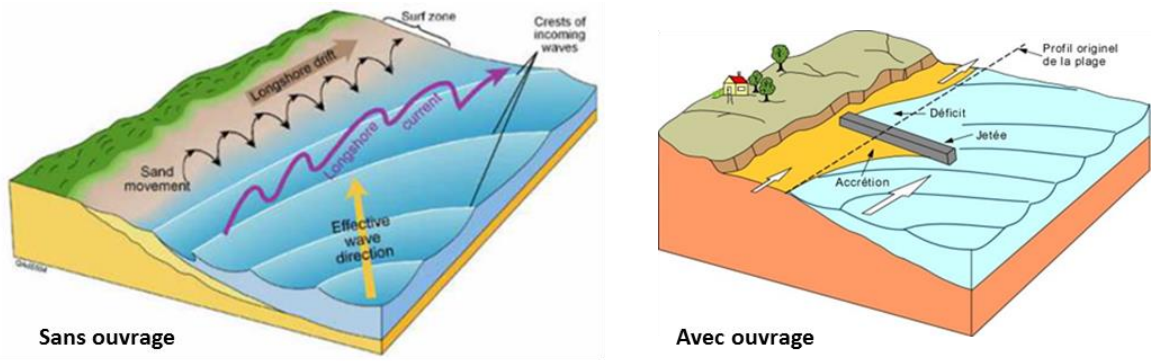

Figure 12. Principle of longshore transport ("littoral drift") in presence or not of a coastal structure

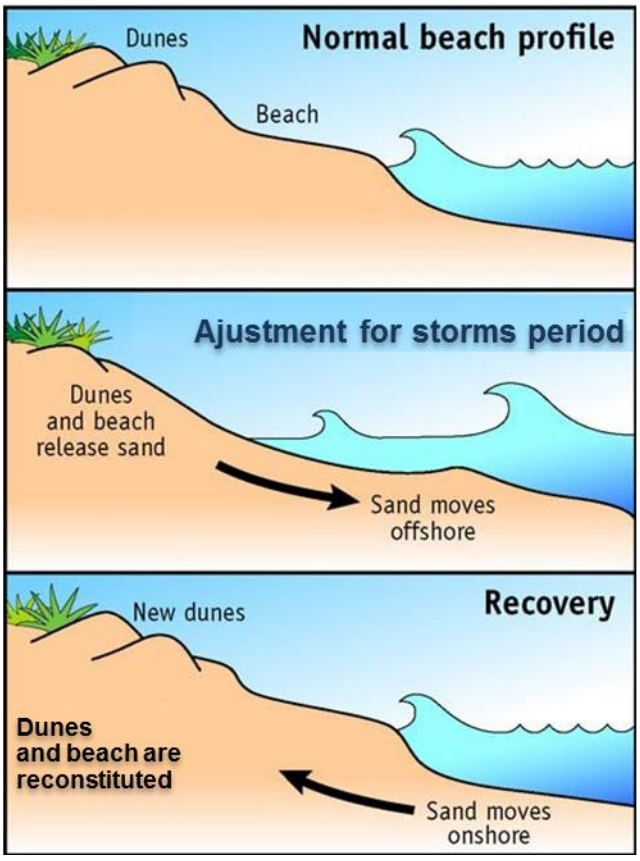

Figure 13. Movement in cross-shore profile

2.2.4.2. Hydrodynamic forcing

The hydrodynamic forcing mechanisms that control coastal evolution in the study area are described below.

2.2.4.2.1. Sea levels

Tidal level in the area:

Chart datum (0 CD) at Lacanau is located 3.2 m below the origin of the Nivellement Général de France system (0 NGF/ 0 IGN69) (from SHOM 2014).

Tide levels at Lacanau (SHOM) are presented in the following table.

Table 7 - Tidal levels in front of Lacanau

Type of tide	HAT	MHWS	MSL	MLWS	LAT
	Highest astronomical tide	Mean High Water Spring	Mean Sea Level	Mean Low Water Spring	Lowest Astronomical Tide
Water level (m IGN 69)	2.1	1.45	-0.51	-2.65	-3.22
Water level (m CD)	5.3	4.65	2.69	0.55	-0.02

50-year water level in Lacanau:

As the life span of cable is not greater than 50 years, we choose to consider events of 50 year return period (meaning with a yearly probability of exceedance of 1/50) as design event. According to CETMEF document [9], extreme sea level occurring with a 50 year return period reaches **3.40 m NGF/ 6.6m CD**.

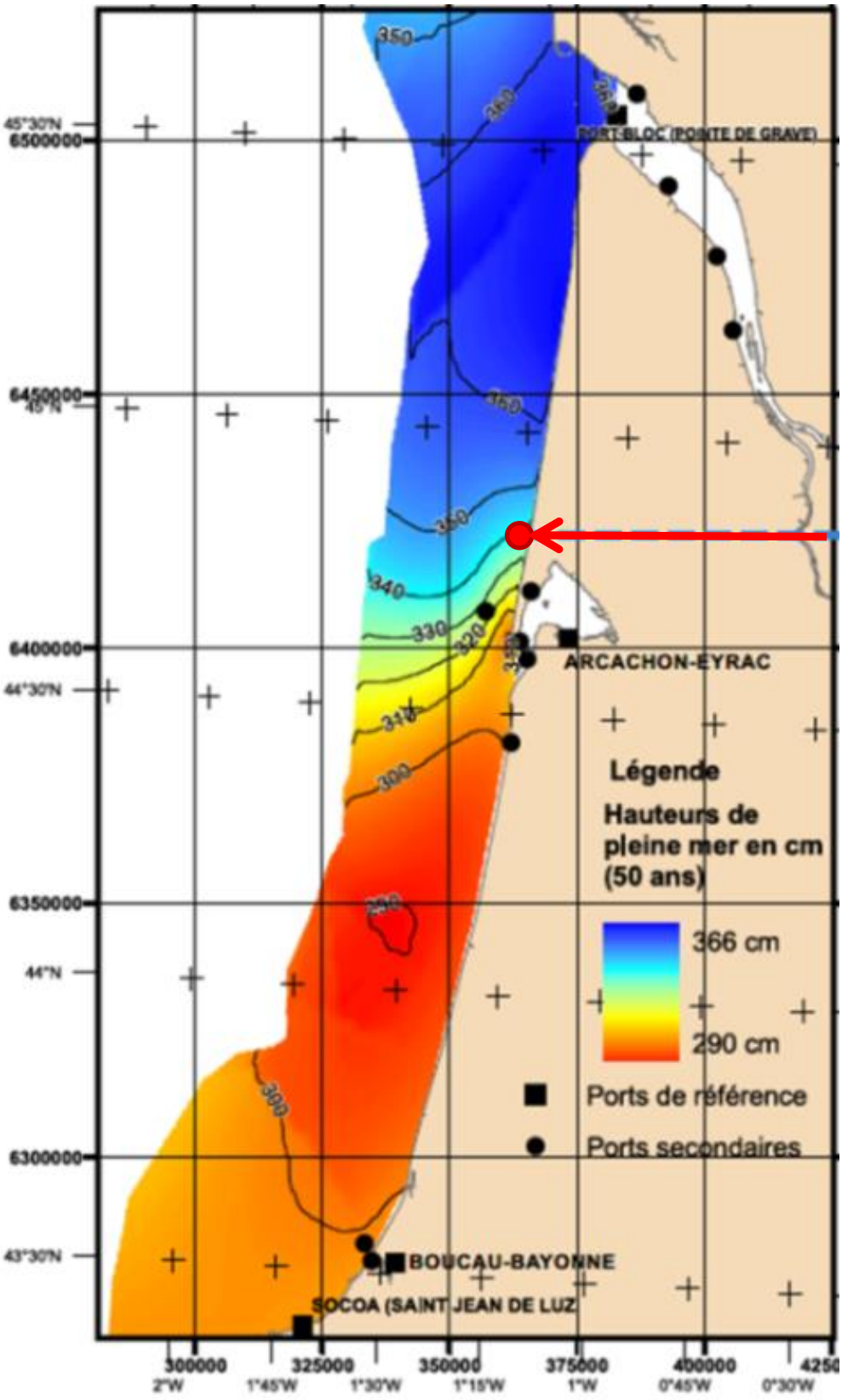

Figure 14. ***Map of the sea level reached with a 50 year return period (from CETMEF [9])***

2.2.4.2.2. Usual and extreme wave conditions

According to the wave analysis carried out in [1] at the specific locations plotted in Figure 15 the **usual wave conditions** in front of French landfalls area are the following:

As regards to the **offshore** wave climate, the wave direction is mainly West/North-West for every month. The highest waves occur during the winter season (December to February) with H_s higher than 3 m more than 10 % of the time. It corresponds to long period waves (T_p > 12 s). During the summer season (May to September), the waves remain lower than 3 m most of the time and the periods are shorter.

During the winter, the wave height H_s is mainly between 1.5 and 3 m (about 60% of the time for example in January) and is higher than 3 m (more than 25% of the time in January); the wave period exceeds 12 s.

When the summer season approaches, the H_s and the T_p tend to decrease to reach the most frequent values between 0.5 and 1.5 m and 8 to 10 s.

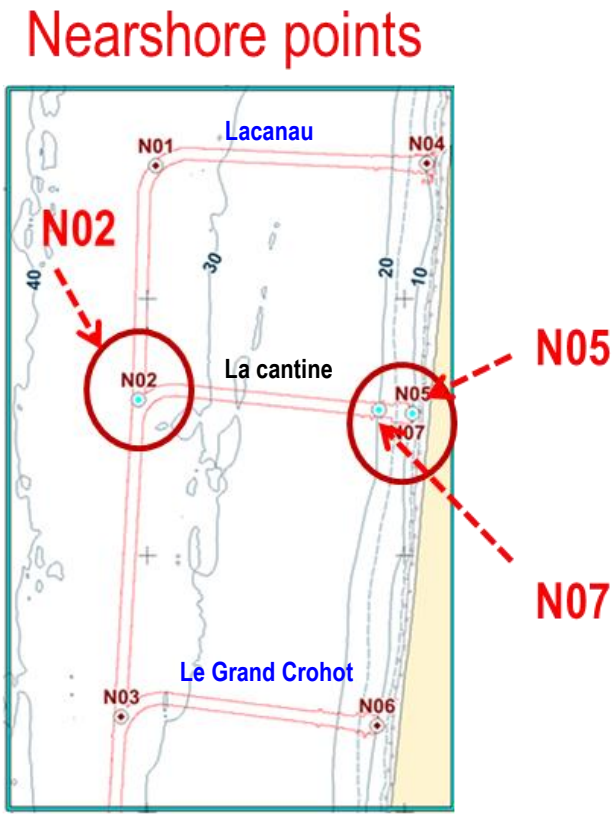

Figure 15. Locations of points where wave climate was analyzed, from [1]

Wave conditions are homogeneous between the three landfall locations under study. At points N05 and N07, the wave climates are consistent with the offshore climate. The main directions are West/West-North-West with a narrower spread around the main direction near the coastline (point N05 - Figure 16) due to refraction. The highest H_s and the longest periods (12-14 s) appear frequently during winter months whereas the summer season sees waves with lower H_s (0.5 to 1.5 m) and shorter period.

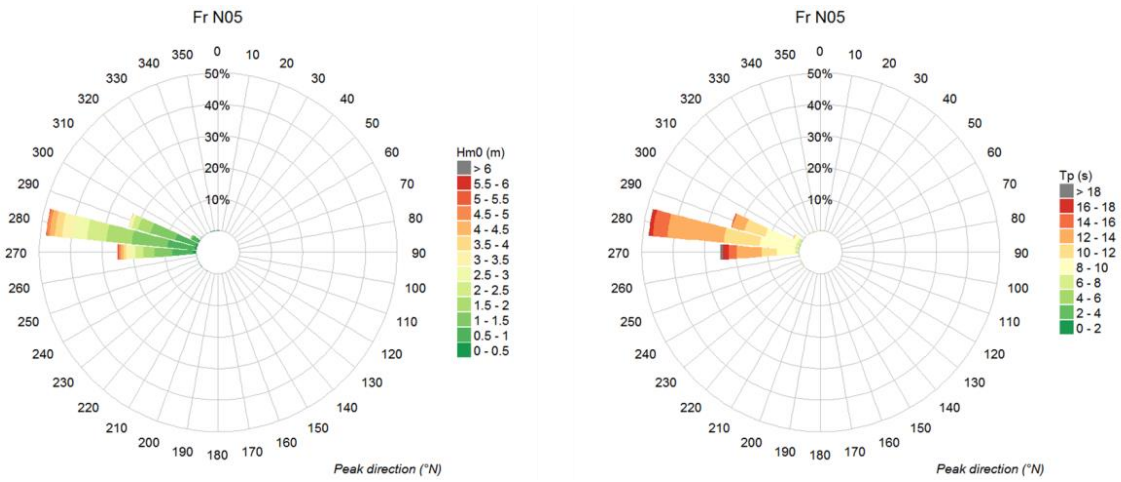

Figure 16. Annual wave rose – Point N05 – Coast - Landfall

In [1], a study of the **extreme wave climate** was carried out at the same locations. At point N07, according to the Figure 17, 50-year significant wave height Hs is assessed to be about 9.25 m (mean value of the confidence interval) and its corresponding period is about Tp = 15.7 s

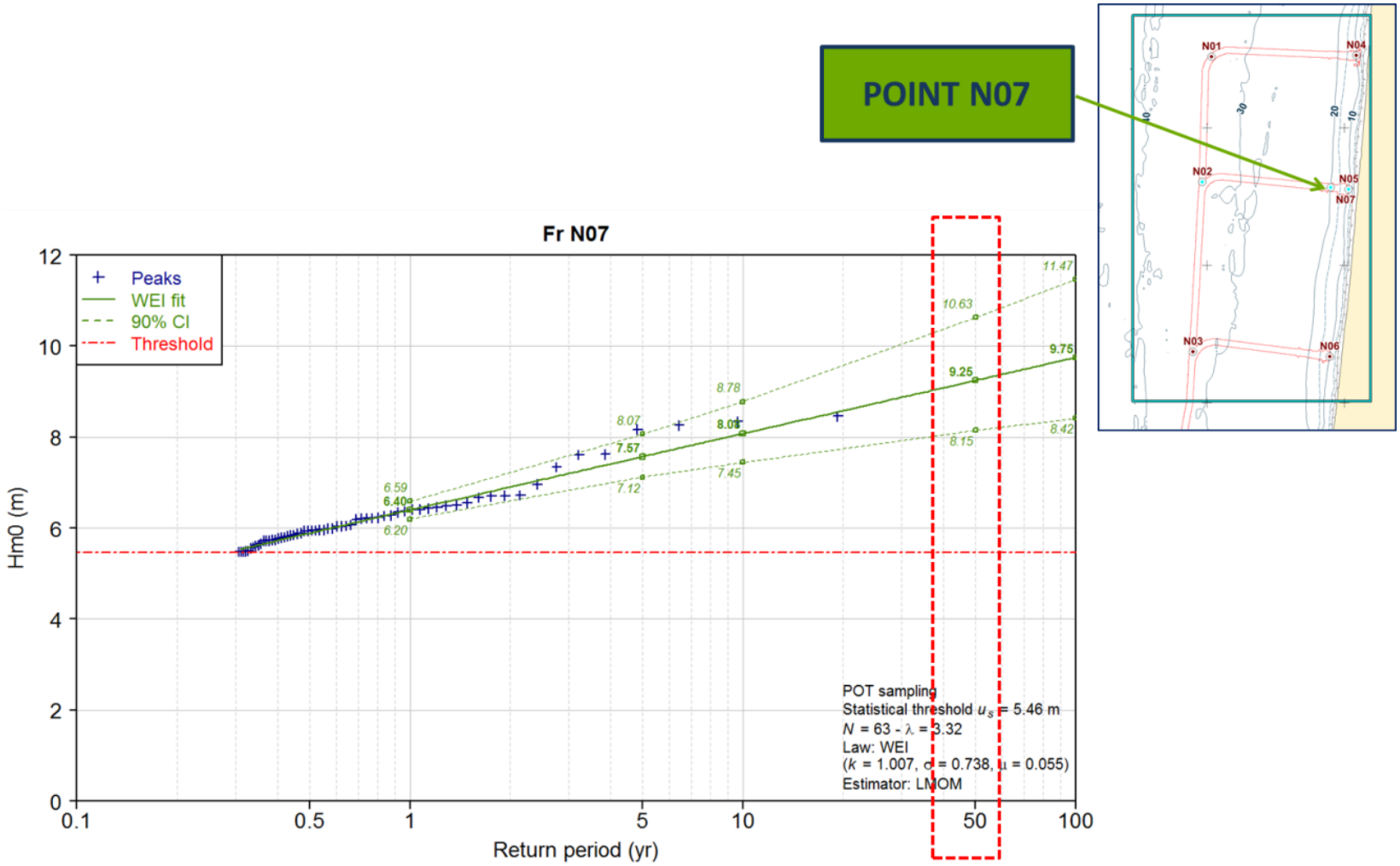

Figure 17. ***Point N07 – Extrapolation of storm peaks by a Weibull distribution, from [1], Appendix 5***

2.2.4.2.3. Hercule storm

Storms during winter 2013-2014, and particularly the storm called Hercule that occurred in early January 2014, caused significant changes to the shoreline along theAquitaine coast. Those changes were observed and reviewed in [15]. Shoreline retreat at Lacanau and Le Grand Crohot were notably recorded.

Assessment of short term evolutions in cross-shore beach profile under storm event have been carried (by modelling) in the frame of this study: it has considered wave conditions related to January 2014 Hercule storm.

Wave conditions are given by HOMERE database (at point 7247 by 25 m water depth). Time series of significant height and peak period are plotted in the Figure 18. It shall be noted the particularly long period of Hercule storm: larger than 20 s.

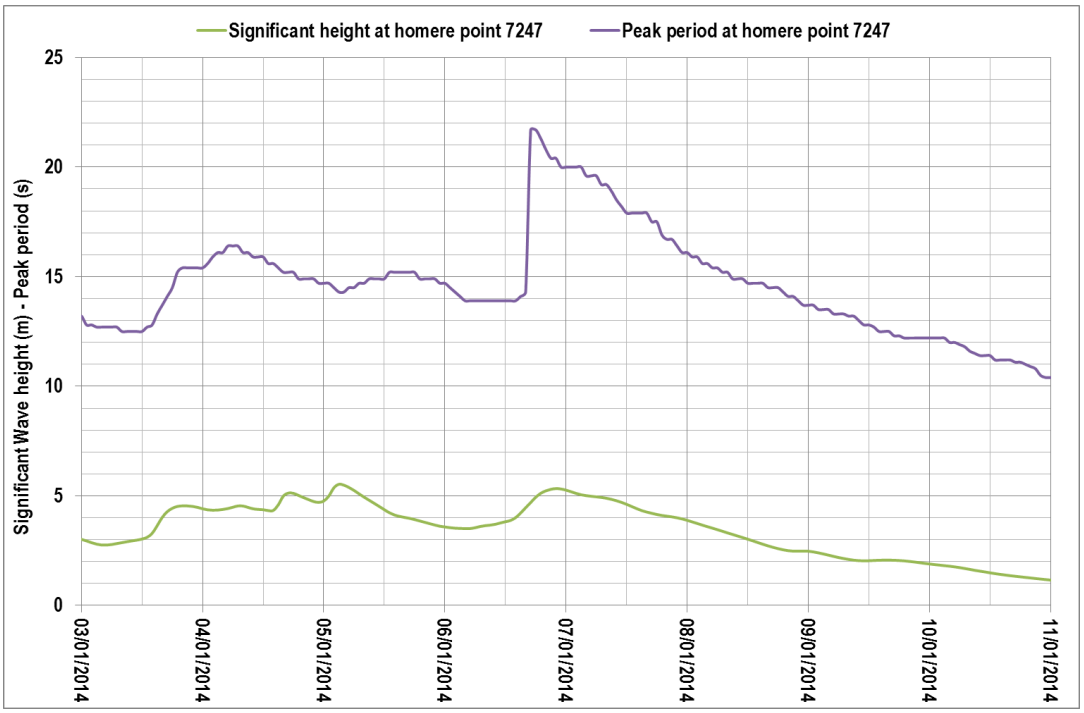

Figure 18. Time series of significant height and peak period from Homere database at point 7247 corresponding to Hercule storm occurred in January 2014

2.2.5. Description of seabed at the French landfall routes

2.2.5.1. Survey data

For the need of Biscay Gulf Western Interconnector project, full geophysical and geotechnical surveys have been carried out along the investigated cable route (including landfalls and coastal areas). Those surveys were mainly carried out in fall 2016 by MMT, a Swedish firm specialised in high-resolution marine surveys. Geotechnical surveys were completed during summer 2017 when needed.

The comprehensive geophysical and geotechnical survey were carried out to determine the seabed characteristics along the cable route and landfalls: bathymetry, morphology, presence of sedimentary features, nature and thickness of movable sediment layers…

INELFE provided ARTELIA with survey reports [10] and [16] that present the results of the investigations on the seabed: nature, the location, thickness and density of the movable sediment layer, granulometry analysis and resulting particle size distribution graphs at numerous locations along the route and the landfalls, and following topo bathymetric data.

A. Topo-bathymetric data

- Bathymetric data surveyed by boat along the cable route in September 2016, and analysed in the geophysical surveys report [10] in which it is mentioned that bathymetric descriptions are referenced to lowest astronomical tide (LAT). These bathymetric data cover seabed beyond -5 m CD.
- Bathymetric data in shallow water depth surveyed by divers to complete the MMT boat survey:
  - La Cantine : 3 november 2016
  - Lacanau : 2 August 2017
  - Le grand Crohot : 27 September 2017
- Topographic data surveyed by drone in September 2016.

Additionally, ARTELIA collected from the Observatoire de la Côte Aquitaine OCA (see http://www.observatoire-cote-aquitaine.fr/-Catalogue-de-donnees) the following historical data:

- Historical Aquitaine shoreline positions from 1966 to 2014, in GIS format;
- Historical topographic surveys (from 2001 to 2016) of the dune along 6 cross shore profiles in vicinity to the three studied French landfall locations, in GIS and text formats.

Finally, to complete the description of the area, ARTELIA used the Numerical Elevation Model HOMONIM (SHOM product) also used in the numerical modelling of waves and currents for the metocean study [1].

B. Granulometry along French landfall route

Sediment samples were collected at Lacanau, La Cantine and Le Grand Crohot: analyses of in situ granulometry allows to update data from literature quoted in subsection 2.2.3. Results are reported in [16] and summarized as following:

- Along the Lacanau landfall route, over the first 6 km from the inshore to the offshore, surficial sediment is made of sand, slightly silty and slightly gravelly in upper parts, presenting rare thin clay/silt band, and becoming very dense beyond 1.8 m Below Sea Floor (BSF). Median particle diameter is 0.3 mm, characteristic of medium sand. Going further offshore the median diameter increases to 0.35 mm.

- Along the Le Grand Crohot landfall route, nature of sea bed is quite similar: surficial sediment is sand, locally slightly gravelly and slightly silty as well. The sediment layer is typically dense at 0.56 m BSF, and becomes very dense at 1.16m BSF. Median particle diameter is 0.35 mm.

- Along the La Cantine landfall route, surficial sediment is sand too, locally slightly gravelly to very gravelly at depth and slightly silty. Median particle diameter of surficial layer is coarser, varying from 0.3 mm inshore to 0.47 mm 12 km offshore.

2.2.5.2. Cross-shore bathymetric profiles

The geographic coordinates are referred to the two following systems: Lambert 93 and WGS84 UTM30 North.

In order to characterize more accurately the sea bed elevation along the three studied landfall routes, the following method is implemented.

First, three cross-shore segments are defined, following the landfall routes provided by INELFE, and lengthened landward to reach the dunes in backshore. These cross-shore segments are drawn on Figure 19.

Coordinates in Lambert 93 and in UTM30 (WGS84) of the two extremities of each profile are given below:

		COORDINATES in Lambert 93 (L93)	
LACANAU PROFILE	Eastern extremity	369 786.6	6 442 800.0
	Western extremity	357 216.3	6 444 346.0
LA CANTINE PROFILE	Eastern extremity	368 158.7	6 433 096.6
	Western extremity	356 564.7	6 435 259.6
LE GRAND CROHOT PROFILE	Eastern extremity	366 090.3	6 421 073.0
	Western extremity	354 978.9	6 423 392.8

		COORDINATES in WGS84	
LACANAU PROFILE	Eastern extremity	642 410.2	4 985 150.6
	Western extremity	629 753.7	4 985 745.2
LA CANTINE PROFILE	Eastern extremity	641 800.0	4 975 100.0
	Western extremity	629 788.9	4 976 631.9
LE GRAND CROHOT PROFILE	Eastern extremity	640 359.8	4 936 198.1
	Western extremity	629 101.5	4 964 675.1

The collected topo-bathymetric data are gathered, treated to refer to the same altimetric reference (m CD) and synthetized in a georeferenced mosaic from which topo-bathymetric data are extracted along the three profiles.

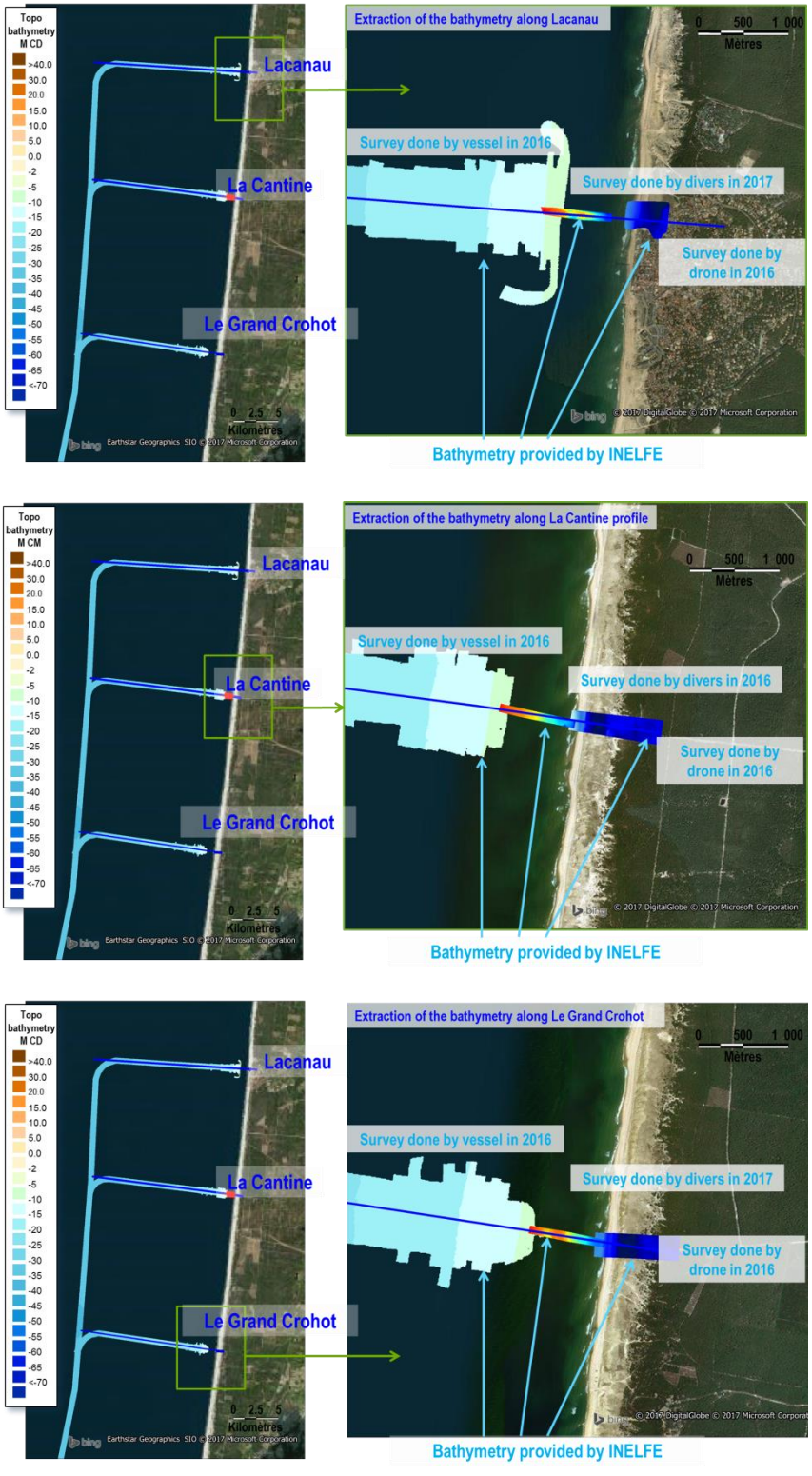

***Figure 19.* INELFE topo-bathymetry data available along the 3 French landfalls**

The resulting topo-bathymetric profiles are presented in Figure 20, Figure 21 and Figure 22. The dashed brown line represents the bathymetry surveyed by vessels by MMT in September-October

2016. The yellow line represents the dune surveyed by drone in September 2016 covering the upper part of the beach and the dune.

For La Cantine profile, local bathymetric survey carried out by divers in November 2016 completes in dashed blue line the profile description between MMT survey and drone survey CANO.

For Lacanau and Le Grand Crohot profiles, local bathymetric surveys of the shallow waters between vessel survey and drone survey were done in August and September 2017 and complete the profile descriptions in dashed blue line.

On each graph, are reported the local Mean Sea Level (MSL) in blue solid line as well as the Highest Astronomical Tide level (HAT) and Lowest Astronomical Tide level (LAT) in dashed blue line and an additional synthetic graph represents the horizontal variation of the water line location.

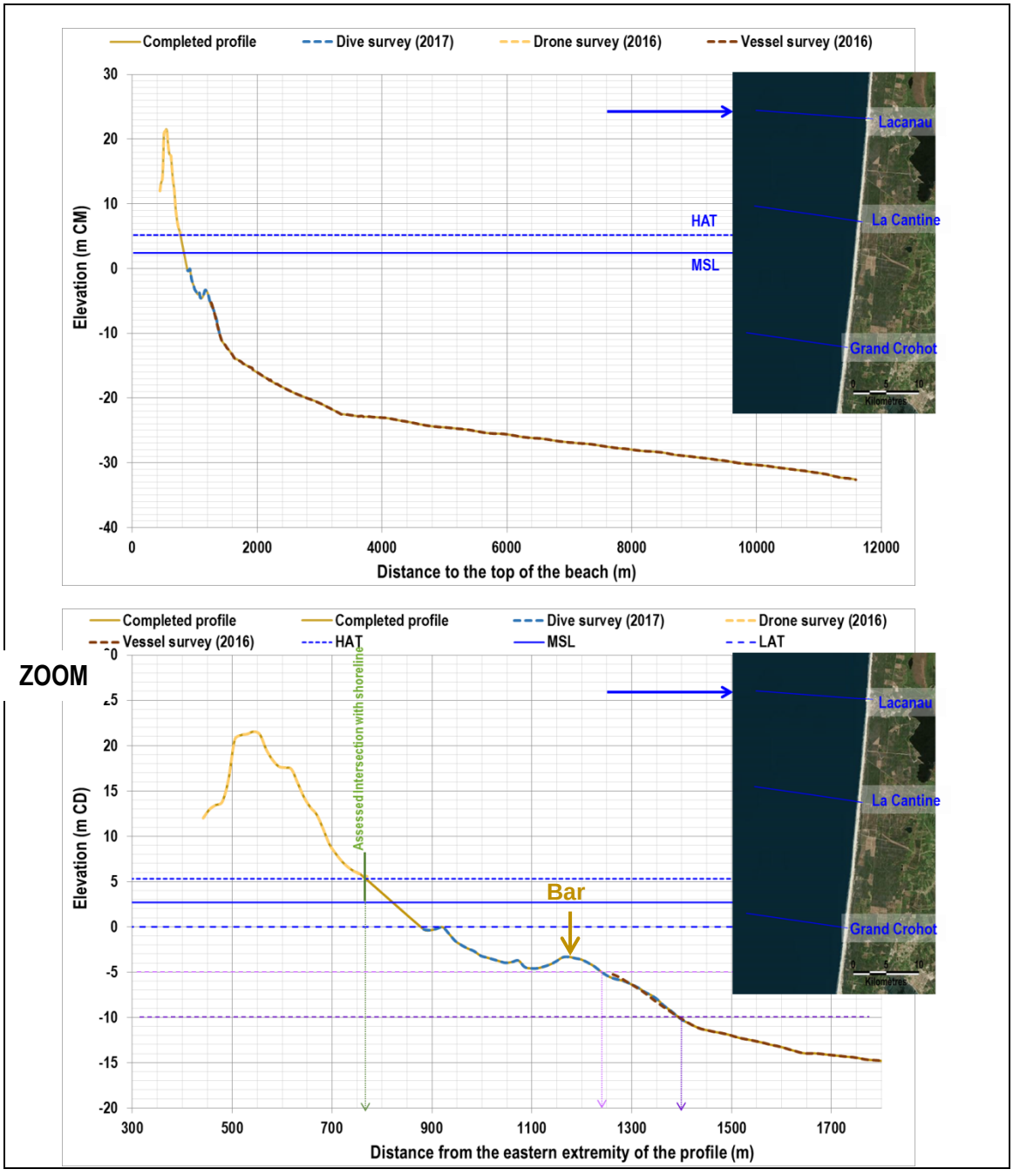

***Figure 20.* Topo-bathymetric profile along the Lacanau landfall route**

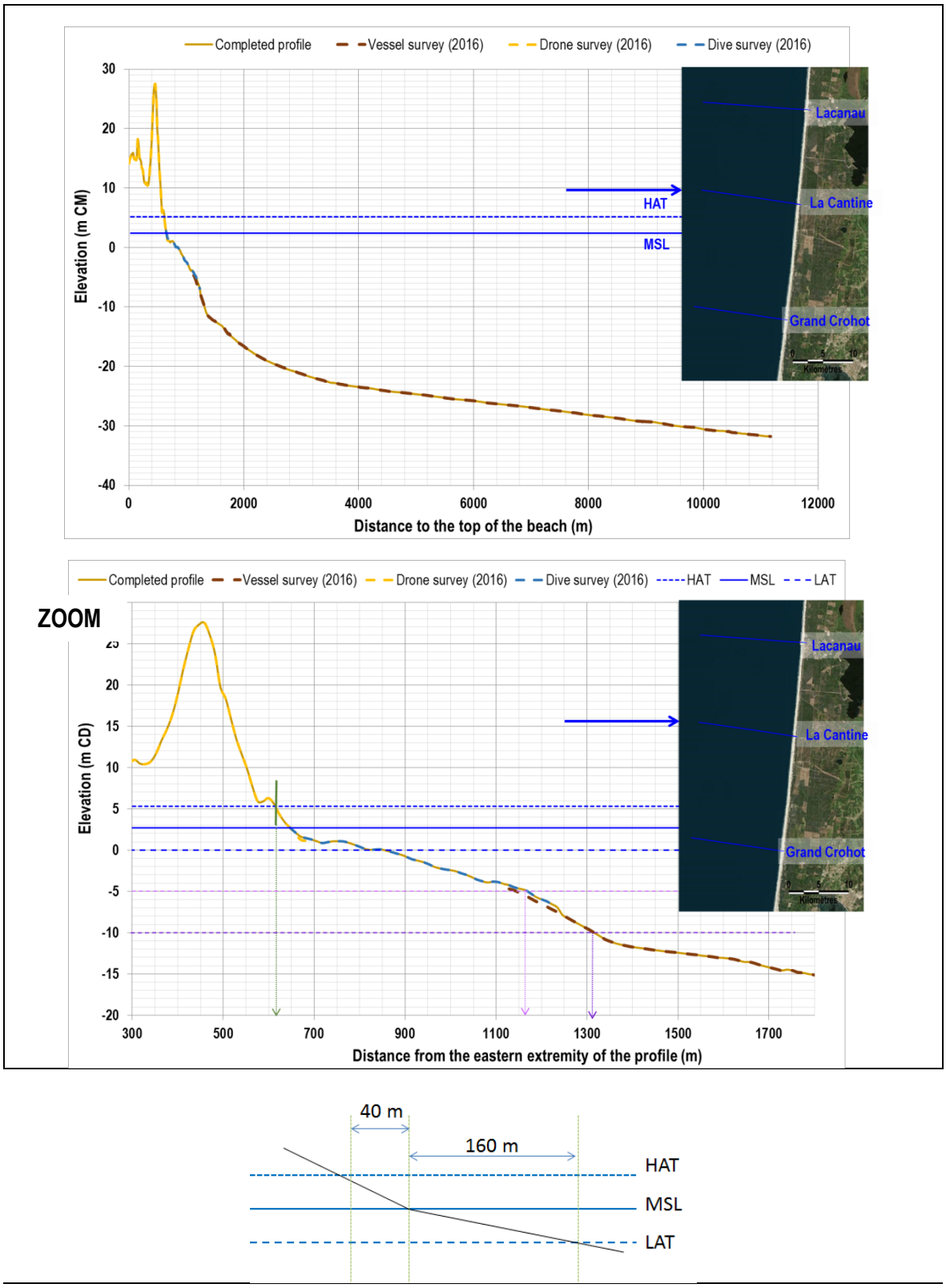

Figure 21. ***Topo-bathymetric profile along the La Cantine landfall route***

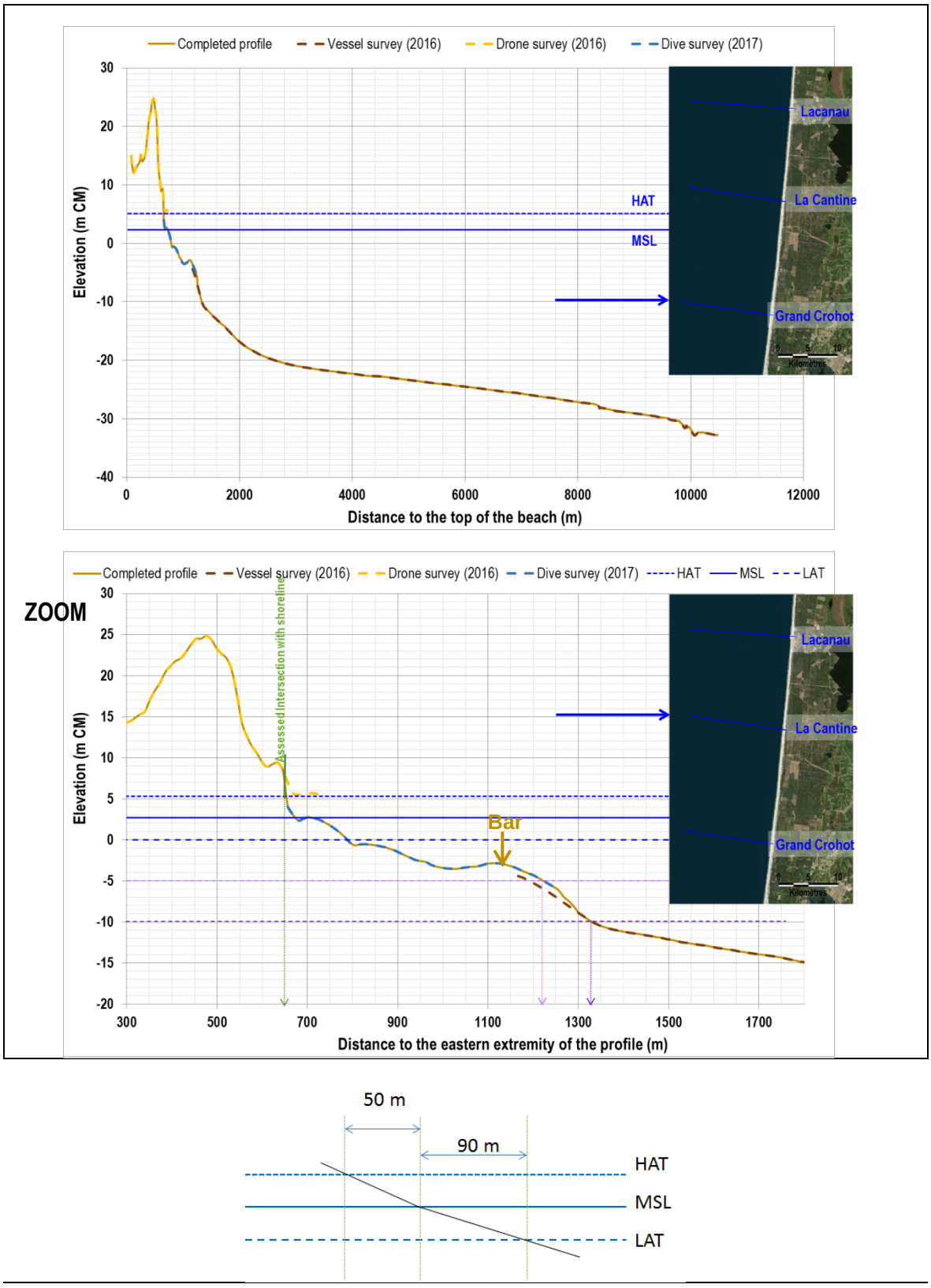

Figure 22. Topo-bathymetric profile along the Grand Crohot landfall route

The 3 resulting cross-shore profiles show a significant homogeneity of the sea bed shape from Lacanau to Le Grand Crohot, located 20 km south.

Each profile presents a first slope discontinuity between -10 m CD and to -15 m CD, splitting the profile in a deeper part characterized by a very gentle slope (< 0.15%), and a shallower part characterized by a greater slope reaching 3%. This slope discontinuity materializes what is generally considered as the beach toe, or closure depth and is taken to represent the seasonal limit of offshore profile variability.

Closure depth, assessed here by bathymetric profile observation can also be assessed by empirical formula depending on local wave climate, such as Hallermeier formula. This is done in subsection 2.2.8.1.

Profiles at Lacanau and Le Grand Crohot surveyed by divers in 2017 present an outer bar. The outer bar is located roughly 300 m offshore the isobath 0 m CD, and it is from 1m to 2m high. Its crest rises to -3 m CD.

The current absence of a bar on the La Cantine profile surveyd in 2016 does not mean that such a feature is never present at this location. It demonstrates that such features are temporal along this stretch of coast, subject to cross-shore wave action and its seasonality.

This surveyed situation actually serves to demonstrate the variable cross-shore profile response to nearshore hydrodynamics. Due to seasonality of such features, the cable can be buried or excavated of the height of the bar, meaning 1 to 2 m high.

2.2.6. Long term evolution of the shoreline (past and future)

Based on the historical shoreline positions provided by the OCA, a diachronic study of the shoreline evolution is carried out for each of the 3 studied landfall locations.

The aim of this study is the assessment of the shoreline retreat at 2067 horizon (in 50 years, corresponding to the approximate operational lifetime of the cable) at each landfall location.

2.2.6.1. OCA's Definition of the shoreline

The shoreline is an abstract line, defined by a convention on its location: corresponding to the low water mark, or to the highest one, its definition differs among the coastal scientists/experts community. The definition of the shoreline according to the OCA is given in [6] and is *the shoreline is the separation line between dune and beach, corresponding to one of the following situation:*

- *Foot of the dune cliff;*
- *Slope discontinuity;*
- *Limit of dune vegetation;*
- *Longshore protection structure.*

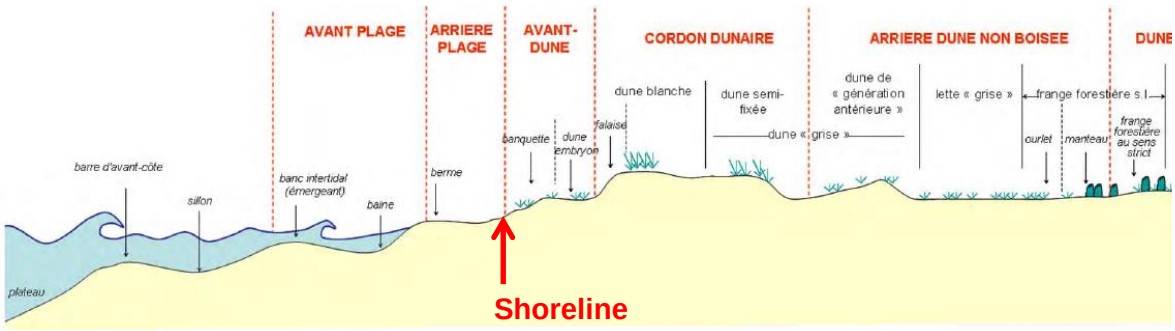

Figure 23. Position of the shoreline definition according to the OCA

This definition differs from the SHOM one who considers the shoreline as the Highest Astronomical Tidal water level corresponding to a tidal coefficient of 120 under normal weather conditions.

Using OCA's historical data (among which shoreline positions), we refer here to OCA's definition of the shoreline, illustrated on figure below.

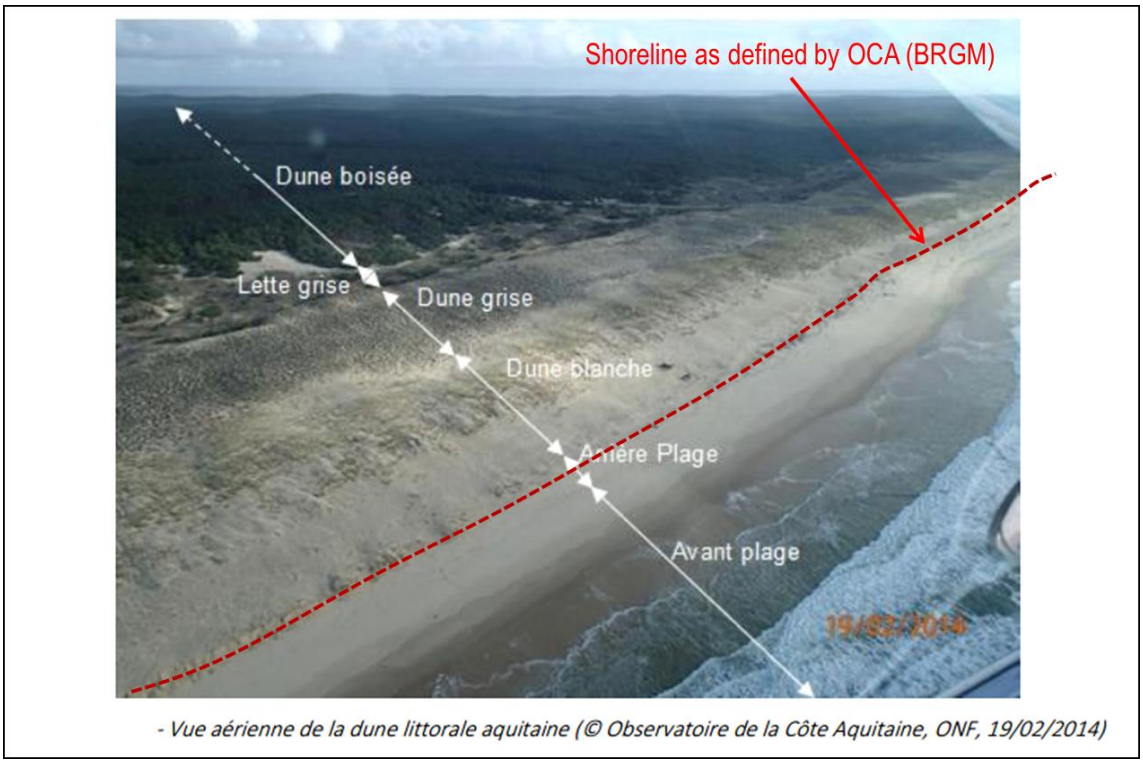

Figure 24. Illustration of the shoreline on Aquitaine Coast

2.2.6.2. Historical shoreline positions

The OCA digitalized historical shoreline positions along the Aquitaine coast for the following years: 1966, 1998, 2000, 2006, 2007, 2008, 2009, 2011, and 2014.

Figure 25 shows the mapping, at each landfall site, of the provided historical shoreline positions.

2.2.6.3. Shoreline position prediction in 2025 and 2050

In addition, shoreline positions predicted in 2016 by the BRGM for 2025 and 2050 [8] are reported on the maps.

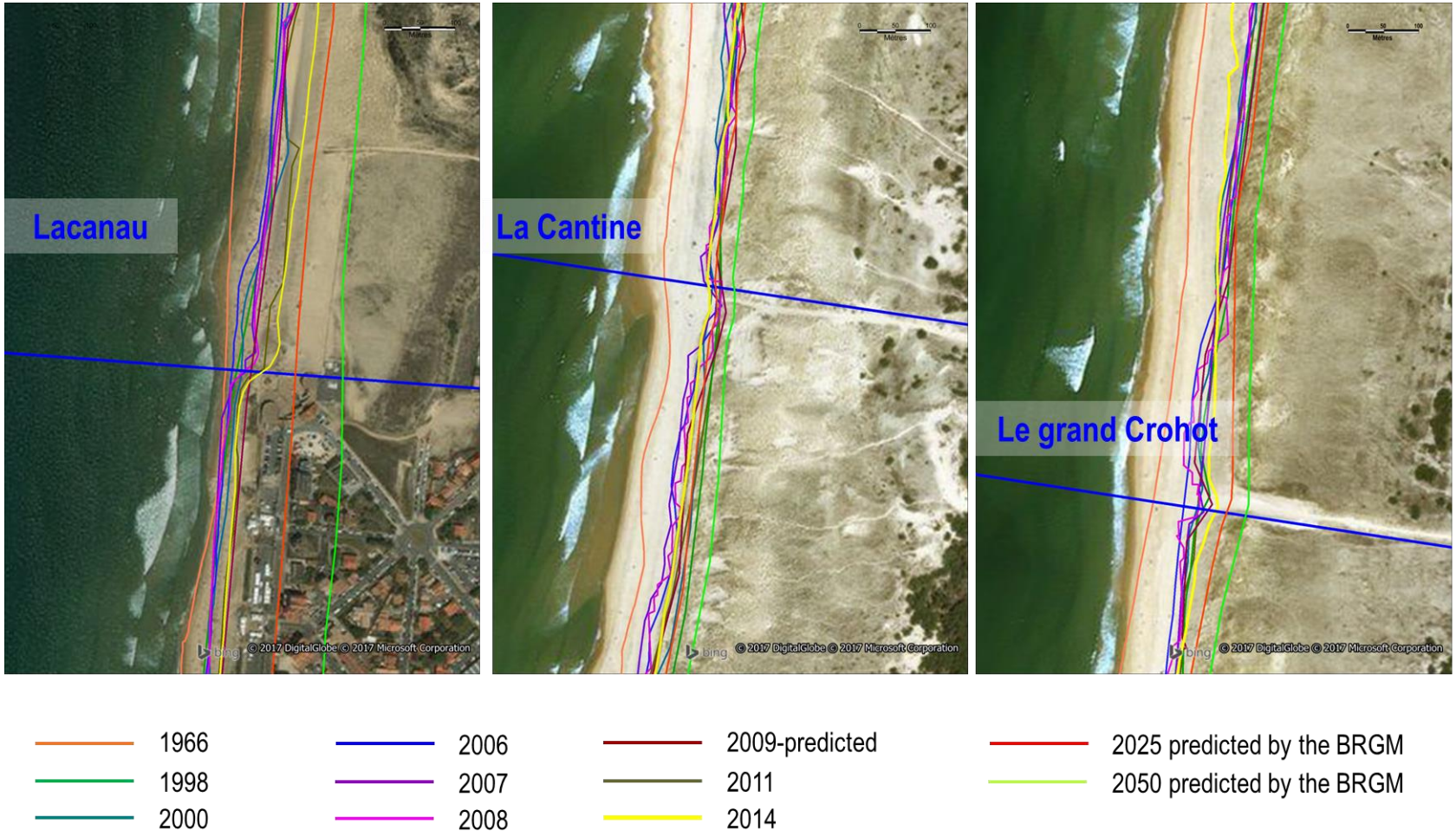

***Figure 25.** Mapping of the historical and predicted shoreline positions at the 3 studied landfall locations*

To predict these shorelines (2025 and 2050), the BRGM proceeded in 5 steps

Step 1:

Creation of a **reference shoreline dated from 2014** based on IGN ortho photograph dated from 2014 and profiles surveyed by the OCA, mapped after the storms that occurred during the winter 2013/2014. The reference shoreline is considered « without coastal protection »

Step 2:

Use of the DSAS[2] tool to **assess mean annual shoreline position evolution rates « Tx »** in meters, every 100m along the Aquitaine coast.

Step 3:

Interpretation of the gross predicted shoreline for 2025 and 2050 by expert opinion: takes into account field knowledge, feedback of previous studies, local strategies, hydro-sedimentary processes in order to determine more realistic evolution rates along the sandy coast.

Step 4:

Application of Lmax : lump-sum lane of **shoreline recession related to a major storm event**, defined from in situ observations made after the 2013-2014 storms.

Step 5:

Impact of climate change taken into account for the predicted shoreline position in 2050.

The BRGM assessed this impact is by considering that climate change will induce a sea level rise from 0.1 m (optimistic assumption) to 0.5 m (pessimistic assumption) in 2015 and by calculating the consecutive shoreline recession using Brüun rule.

According to the Brüun rule [21], sea level will rise slowly. This will allow the beach and the dune ridge to adapt to the phenomena through (Figure 26):

- Beach profile will be translated landward and be modified by a sediment transfer from the beach and the shallow coastal areas to deeper areas until the closure depth. Figure 26 illustrates the translation landward and the sediment transfer.
- This will induce shoreline recession and rise of the upper part of the beach similarly to the sea level rise.

[2] DASA: Digital Shoreline Analysis System

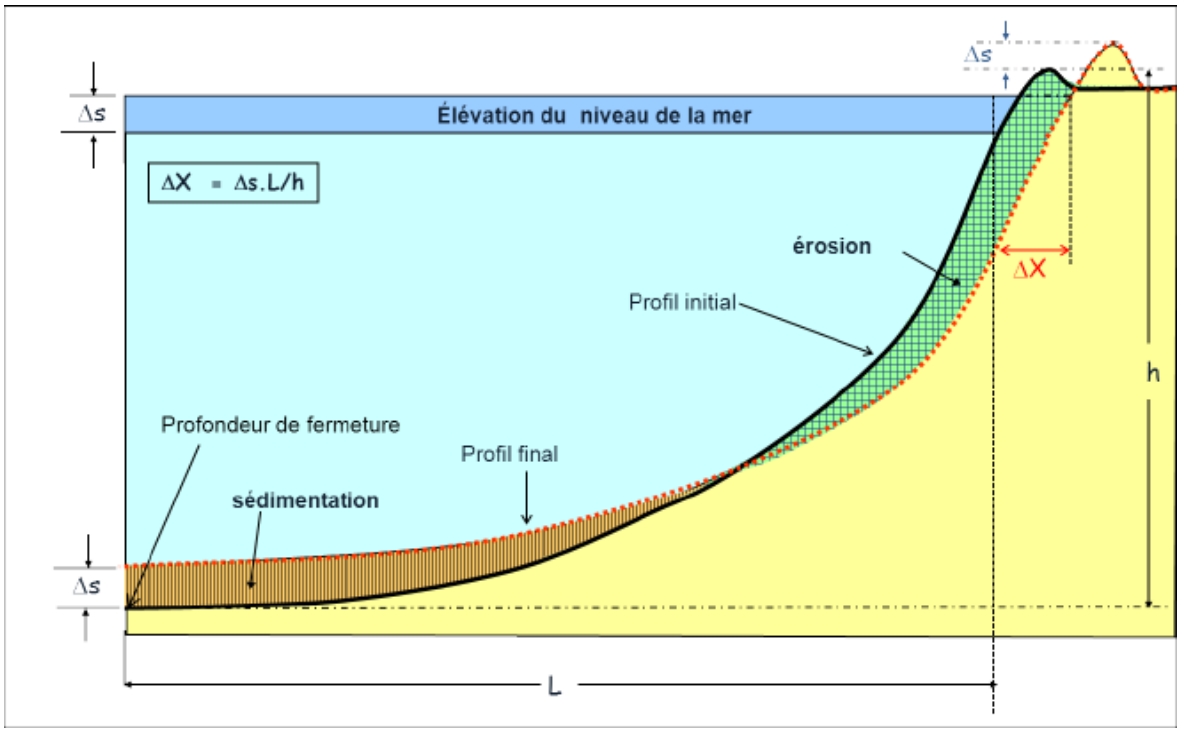

Figure 26. Brüun theoretical approach

Calculation of shoreline recession for 2050 using Brüun rule was carried out on 11 profiles along the Aquitaine coast, giving a mean recession value of 7 m under 0.1 m sea level rise assumption and 35 m under 0.5 m sea level rise assumption.

Considering this range of resulting recession values, the BRGM finally applied a mean recession due to the average sea level rise assumption of 0.3m. Thus **a 20 m wide lane of recession** is considered for 2050 to take into account the climate change on the sandy coast.

The resulting predicted shorelines are shown on Figure 25 (in orange and green lines).

Limits and uncertainties of the method

In [8], the authors warn about the sources of uncertainties inherent to this method:

- Uncertainties due to the resolution of satellite images;
- Uncertainties due to the Brüun method for calculation of the shoreline retreat due to climate change;

An assessment of the degree of uncertainty had been carried out in [8], and mapped on Figure 27. This assessment concludes that the level of uncertainty in the area of interest is low and hence the results presented herein are given with a high level of confidence.

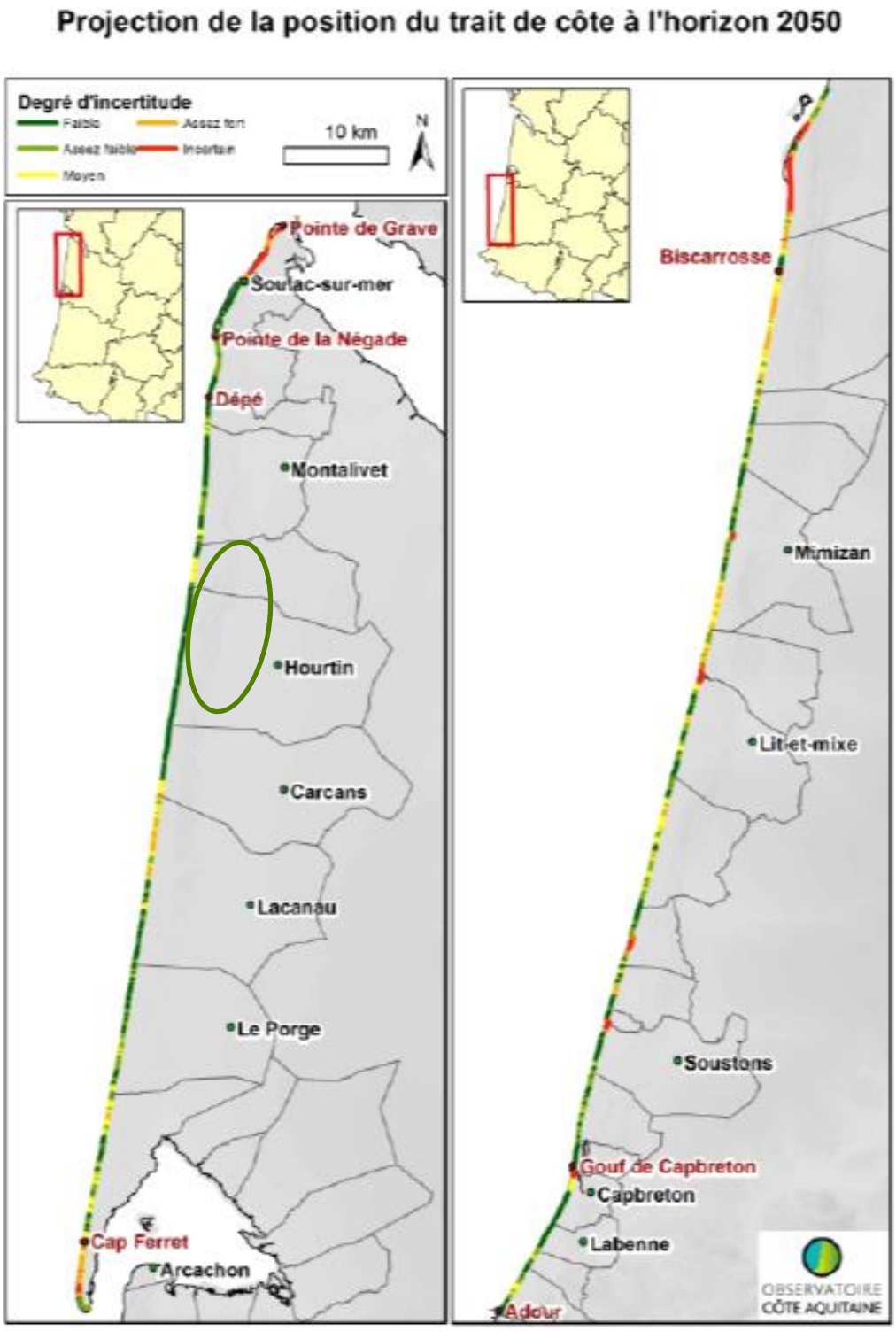

Figure 27. Mapping of the degree of uncertainty of the projected shoreline position in 2050

2.2.6.4. Assessment of shoreline retreat in 2067

Once mapped, the historical and predicted shorelines provided by the OCA are analyzed to determine historical and predicted variations of the shoreline retreat or accretion (in m) and evolution rate Tx (in m/year) from 1966 to 2050. This analysis is carried out by ARTELIA for each landfall site separately.

Thanks to this analysis, and considering the BRGM methodology described above (including shoreline recession due to major storm event, and climate change effects for 2050), the following parameters are calculated for each landfall location:

- Mean annual rate of evolution Tx from 2014 to 2067;
- Width of the recession lane due to climate change in 50 years.

Therefore, the shoreline reccession in 2067 is assessed for each landfall shoreline as : Distance = Tx . (year 2067 – year 2014) + L_{max} + L_{CC} :

- At Lacanau: -107.7 m from the 2014 shoreline location ;
- At La Cantine: - 35 m from the 2014 shoreline location;
- At Le Grand Crohot: - 45.6 m from the 2014 shoreline location.

The results of this assessment in terms of 2067 shoreline position are recorded in the table presented in Figure 28 and mapped in Figure 29

The following tables give the coordinates (in L93 and WGS84) of the intersection of the predicted 2067 shoreline at the three studied cross-shore profiles.

		COORDINATES in Lambert 93 (L93)	
LACANAU PROFILE	Eastern extremity	369 786.6	6 442 800.0
	Western extremity	357 216.3	6 444 346.0
	Position of the Shorline in 2067	369 225.8	6 442 871.9
LA CANTINE PROFILE	Eastern extremity	368 158.7	6 433 096.6
	Western extremity	356 564.7	6 435 259.6
	Position of the Shorline in 2067	367 638.2	6 443 202.5
LE GRAND CROHOT PROFILE	Eastern extremity	366 090.3	6 421 073.0
	Western extremity	354 978.9	6 423 392.8
	Position of the Shorline in 2067	365 582.9	6 421 178.9

		COORDINATES in WGS84	
LACANAU PROFILE	Eastern extremity	642 410.2	4 985 150.6
	Western extremity	629 753.7	4 985 745.2
	Position of the Shorline in 2067	641 845.4	4 985 180.1
LA CANTINE PROFILE	Eastern extremity	641 800.0	4 975 100.0
	Western extremity	629 788.9	4 976 631.9
	Position of the Shorline in 2067	640 985.5	4 975 413.4
LE GRAND CROHOT PROFILE	Eastern extremity	640 359.8	4 936 198.1
	Western extremity	629 101.5	4 964 675.1
	Position of the Shorline in 2067	639 845.2	4 963 264.7

		Historical evolutions *(from shorelines provided by OCA)*								Predicted evolutions *(OCA)*		Predicted evolutions in 50 years *(ARTELIA)*
LACANAU		1966-1988	1998-2000	2000-2006	2006-2007	2007-2008	2008-2009	2009-2011	2011-2014	2014-2025	2014-2050	2014-2067
	Distance (m)	-11 to -19.3	-4.2 to 4.5	5 to 9	-13 to -15.3	-2.3 to 1.5	-2.8 to -7	-10.9 to -7	-9.4 to -4	-20 to -34	-64 to -80.7	-88 to -107.7
	Tx (m/year)	-0.5 to -0.9	-2.1 to 2.25	0.8 to 1.5	-13 to -15.3	-2.3 to 1.5	-2.8 to -7	-5.5 to -3.5	-3.1 to -1.3	Tx = -0.96 to -1.07 Lmax = -9.5 to -22.2	Tx = -0.96 to -1.07 Lmax = -9.5 to -22 L_{CC}=-20	Tx = -0.92 to -1.07 Lmax = -9.5 to -22 L_{CC}=-29
LA CANTINE		1966-1988	1998-2000	2000-2006	2006-2007	2007-2008	2008-2009	2009-2011	2011_2014	2014-2025	2014-2050	2014-2067
	Distance (m)	-57.2	8.7	-1.2	6.8	-14.3	-0.7	2.6	11.1	-7.3	-26.6	-35
	Tx (m/year)	-2.60	4.35	-0.20	6.80	-14.30	-0.70	1.30	3.70	Tx =+0.03 Lmax = -7.6	Tx = +0.03 Lmax = -7.6 L_{CC}=-20	Tx = +0.03 Lmax = -7.6 L_{CC}=-29
LE GRAND CROHOT		1966-1988	1998-2000	2000-2006	2006-2007	2007-2008	2008-2009	2009-2011	2011_2014	2014-2025	2014-2050	2014-2067
	Distance (m)	-42 to -50	6.7 to13.5	-8 to 13	-19.6 to 4.8	-4.4 to 4	-5.7 to -9.6	6.3 to 10.5	5.1 to 18.5	-10.7 to -17.8	-30 to -37	-38.5 to -45.6
	Tx (m/year)	-1.9 to -2.3	3.35 to 6.75	-1.3 to 2.2	-19.6 to 4.8	-4.4 to 4	-5.7 to -9.6	3.15 to 5.25	1.7 to 6.2	Tx =+0.03 Lmax = -11 to -18.1 L_{CC}=-20	Tx =+0.03 Lmax = -11 to -18.1 L_{CC}=-20	Tx =+0.03 Lmax = -11 to -18.1 L_{CC}=-29

***Figure 28.** Record of the historical and predicted variations of the shoreline retreat or accretion (in m) and evolution rate Tx (in m/year), based on OCA data, BRGM prediction (2025 and 2050)and ARTELIA expertise (2067)*

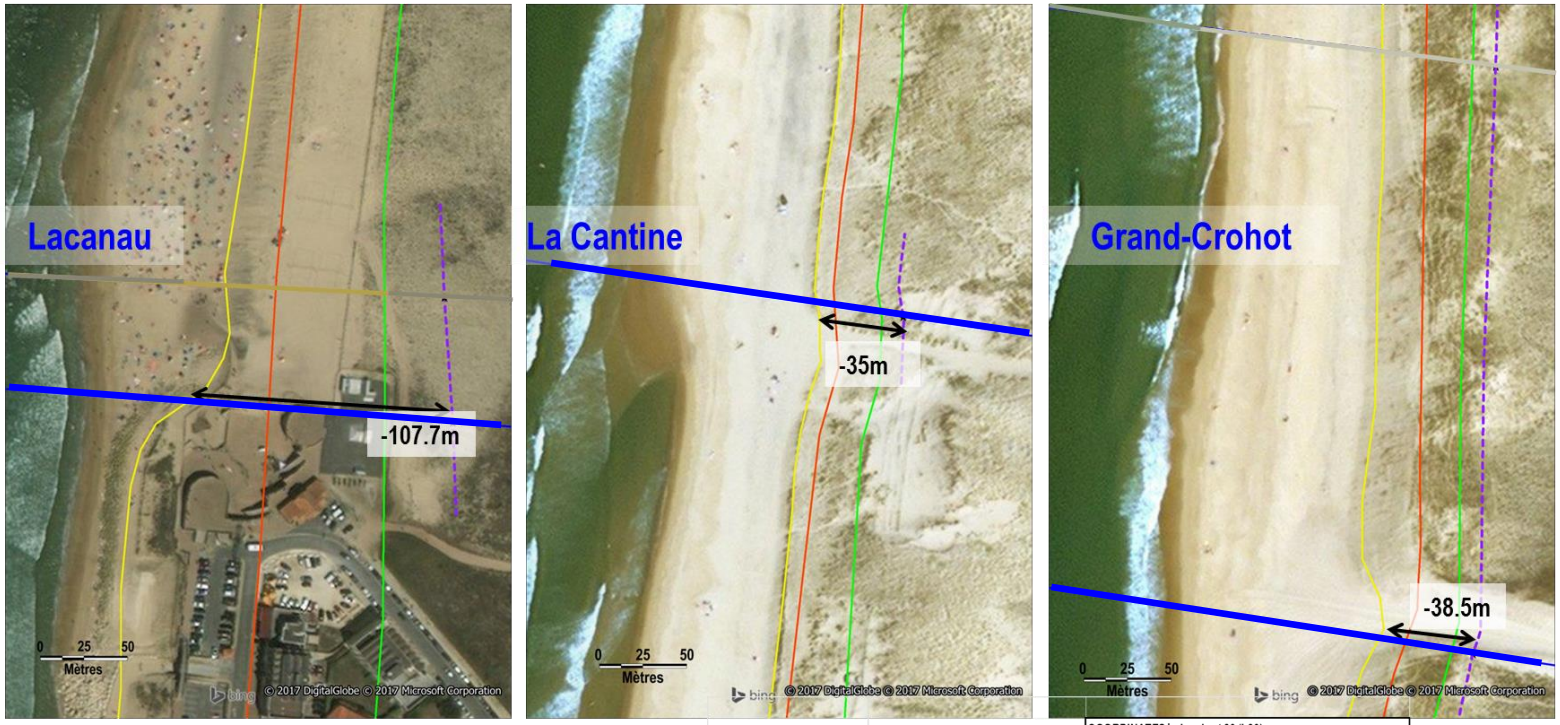

		COORDINATES in Lambert 93 (L93)	
LACANAU PROFILE	Eastern extremity	369 786.6	6 442 800.0
	Western extremity	357 216.3	6 444 346.0
	Position of the Shorline in 2067	369 225.8	6 442 871.9
LA CANTINE PROFILE	Eastern extremity	368 158.7	6 433 096.6
	Western extremity	356 564.7	6 435 259.6
	Position of the Shorline in 2067	367 638.2	6 443 202.5
LE GRAND CROHOT PROFILE	Eastern extremity	366 090.3	6 421 073.0
	Western extremity	354 978.9	6 423 392.8
	Position of the Shorline in 2067	365 582.9	6 421 178.9

***Figure 29.** Mapping of the predicted shoreline positions in 2025, 2050 and 2067 at the 3 studied landfall locations*

2.2.7. Long term changes of beach profiles

2.2.7.1. Long term translations of the 3 beach profiles

In absence of historical bathymetric surveys along the 3 defined profiles Lacanau, La Cantine and Le Grand Crohot, historical long term vertical variations of sea bed (below the dune foot) cannot be assessed on field data.

Therefore, the Brüun theoretical approach is applied to predict the long term changes of beach profiles at 50 years horizon.

In horizontal direction, current bathymetric profiles (Figure 20, Figure 21, Figure 22) are transposed landward over a distance corresponding to the shoreline recession values at 2067 assessed in section 2.2.6.

Then in vertical direction, each profile is transposed upward over a distance corresponding to the assumption taken for the sea level rise : 0.3 m for 2050, and 0.45 m for 2067.

A limit of this method is that this profile transposition(in vertical and horizontal directions) does not take into account the re-shaping of the profile (Figure 26), nor does it take account of the altered beach profile evolution following significant profile reshaping after a storm event, where the profile could become steeper and result in more rapid retreat. This short term evolutions due to storm events are studied in the next subsection.

The resulting predicted cross-shore profiles for 2050 and 2067 are shown in Figure 30, Figure 31 and Figure 32.

At each landfall location, the comparison between initial profile and predicted profiles in 2050 and 2067 leads to a first assessment of the vertical variation of the sea bed during the cable life span.

Assessed vertical variations are the greatest at Lacanau, reaching -3.8 m, at the higher part of the profile (at the foot of the dune) as well as at its lower one (by 10 m water depth).

For the 2 other profiles, assessed vertical variations are about -1.5m at the foot of the dune and -1m by 5 m water depth.

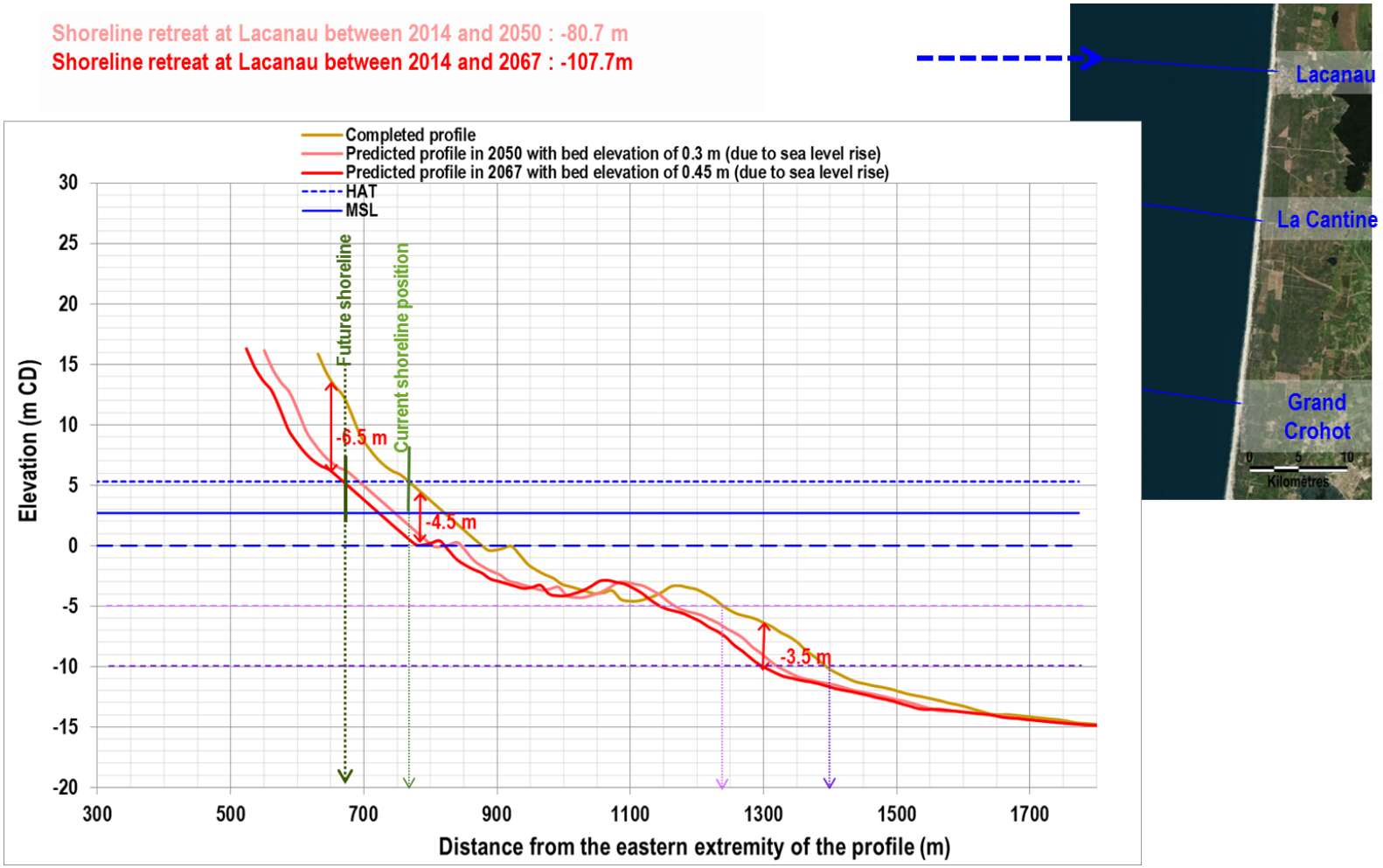

***Figure 30.** Appplication of the predicted shoreline retreat in 2050 and 2067 to Lacanau profile and observation of resulting vertical variations of the sea bed between 2014 and 2067.*

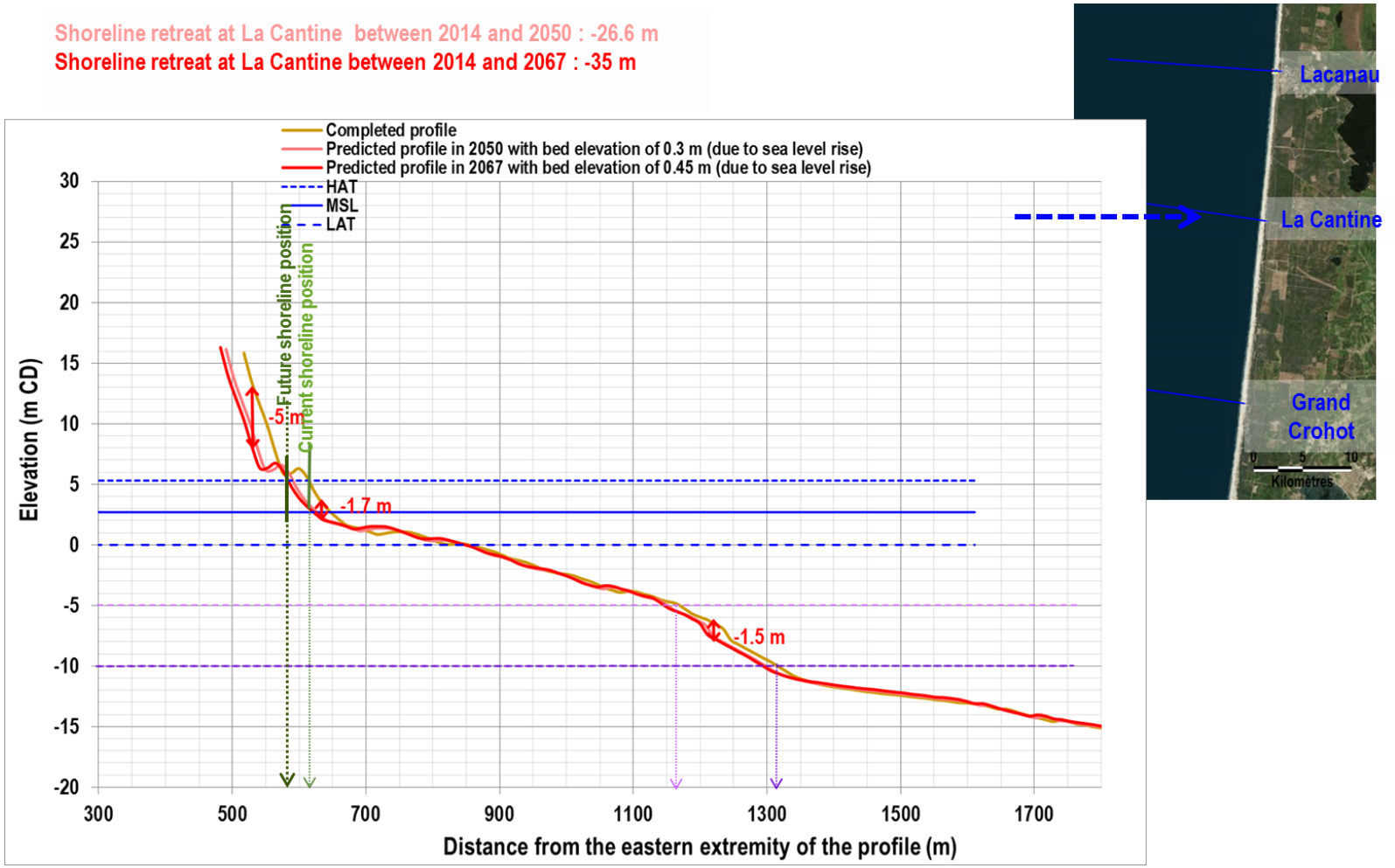

***Figure 31.** Appplication of the predicted shoreline retreat in 2050 and 2067 to La Cantine profile and observation of resulting vertical variations of the sea bed between 2014 and 2067.*

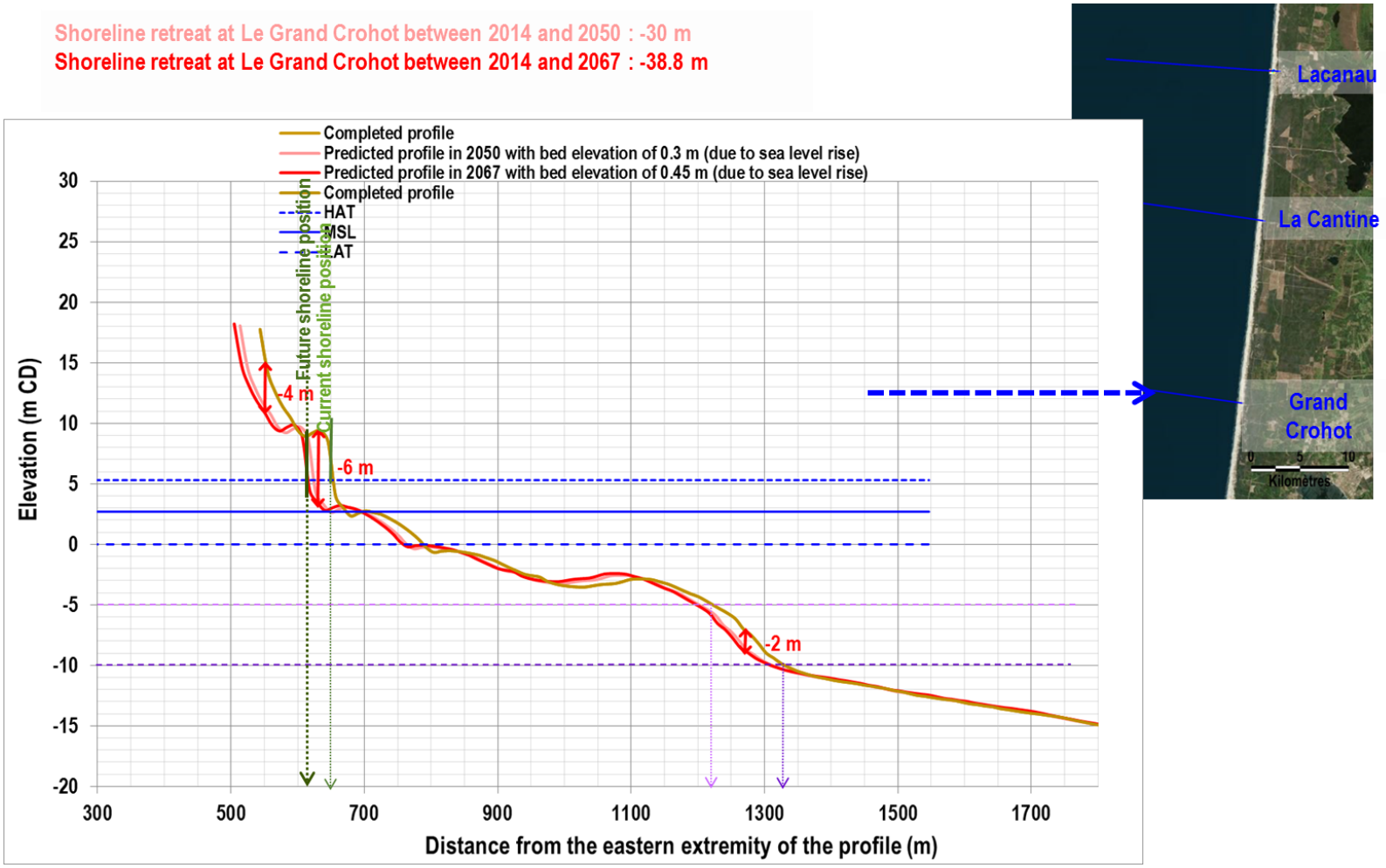

***Figure 32.** Appplication of the predicted shoreline retreat in 2050 and 2067 to Grand Crohot profile and observation of resulting vertical variations of the sea bed between 2014 and 2067.*

2.2.7.2. Long term evolution of the dune

Concerning the dune area, the assessment of the long term vertical variations of the ground is carried out based on the historical profiles surveyed by the ONF and provided by OCA for the needs of the present study.

In the vicinity of the 3 landfall locations, 6 profiles were regularly surveyed by the ONF, at the following dates: 2001, 2003, 2007, 2008, 2009, 2010, 2011, 2012, 2013, 2014, 2016.

Those dune profiles are located on figure below.

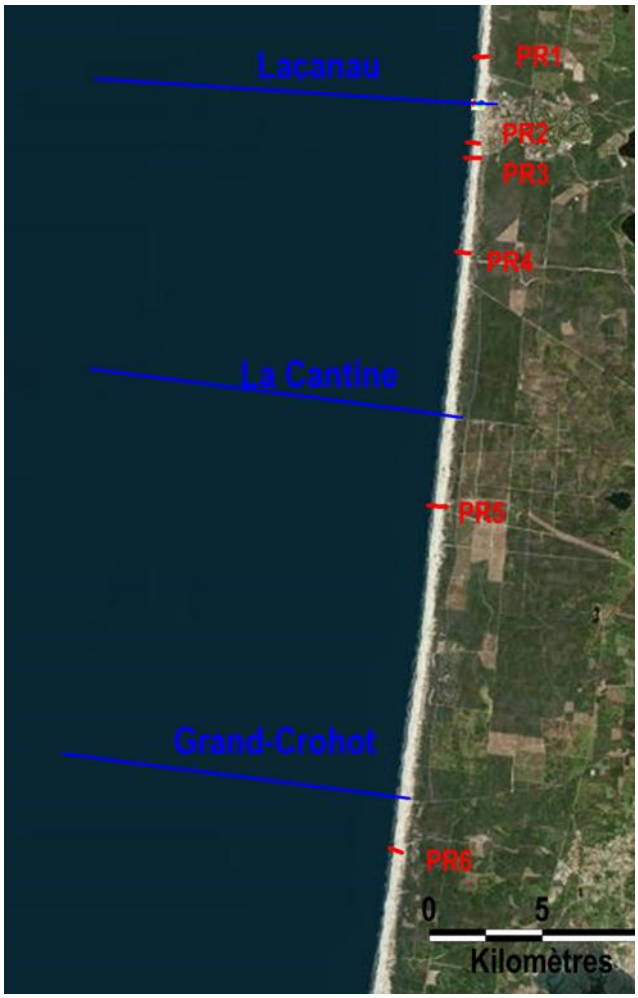

Figure 33. Location of the 6 dune profiles surveyed by ONF : PR1 to PR6 (provided by OCA).

Coordinates in UTM30 (WGS84) of the two extremities of each profile are given below :

PR 1 Eastern extremity [642 071.4 m; 4 986 699.4 m]

Western extremity [641 661.2 m; 4 986 674.2 m]

PR 2 Eastern extremity [641 855.9 m; 4 983 980.3 m]

Western extremity [641 482.5 m; 4 984 004.8 m]

PR4 Eastern extremity [641 631.5 m; 4 980 523.5 m]

Western extremity [641 225.5m; 4 980 554.3 m]

PR5 Eastern extremity [641 092.3 m; 4 972 548.5 m]

Western extremity [640 523.5 m; 4 972 565.6 m]

PR6 Eastern extremity [639 919.4 m; 4 961 630.0 m]

Western extremity [639 533.8 m; 4 961 768.6 m]

Profile by profile, historical dune evolutions are plotted in Figure 34, Figure 35, Figure 36, Figure 37, Figure 38.

The graphs show that vertical variations are the greatest (6 m for PR1, 4 m at PR4) above the HAT level. Below this elevation, maximal variations are in the same order of the vertical variation assessed at the higher part of the 3 characteristic profiles (1 to 2 m).

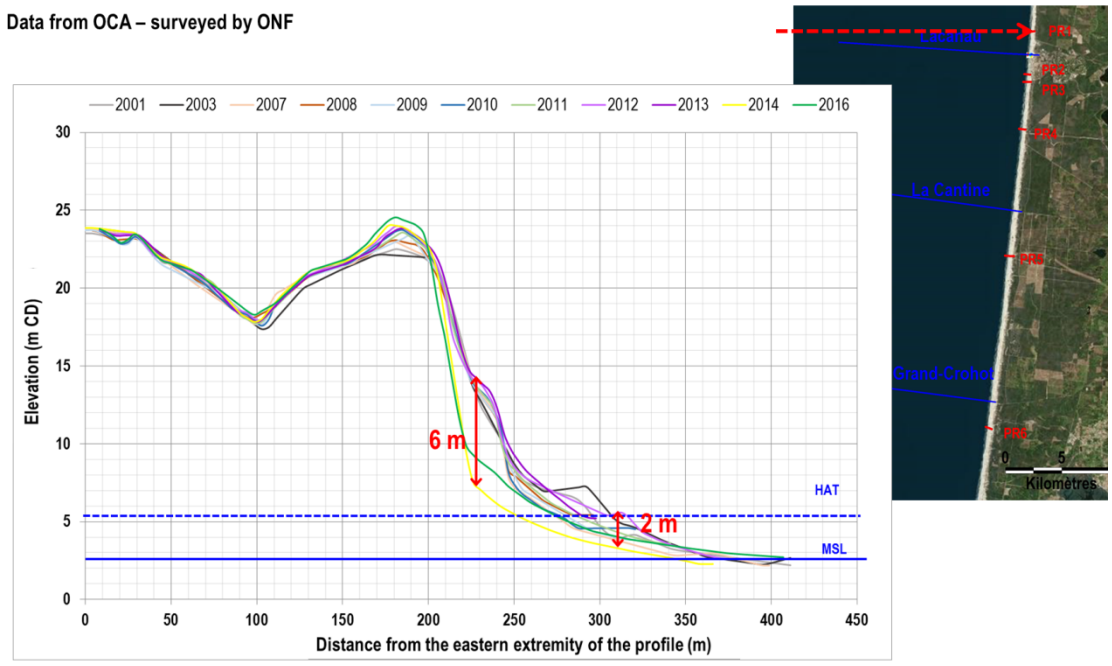

Figure 34. Historical evolutions of dune profile PR1

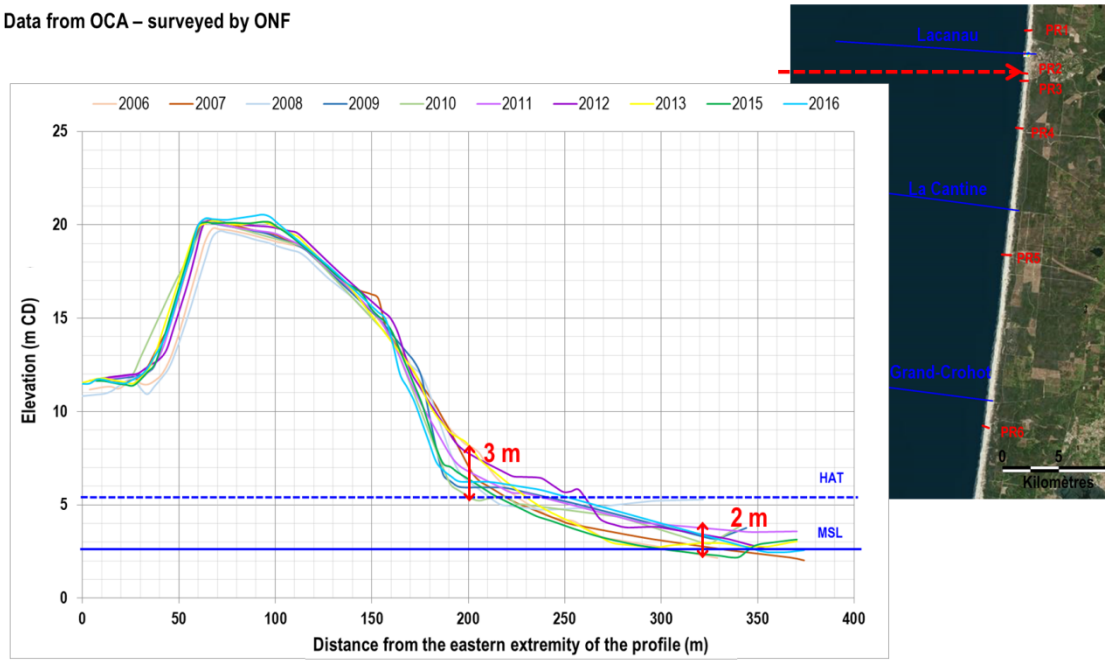

Figure 35. ***Historical evolutions of dune profile PR2***

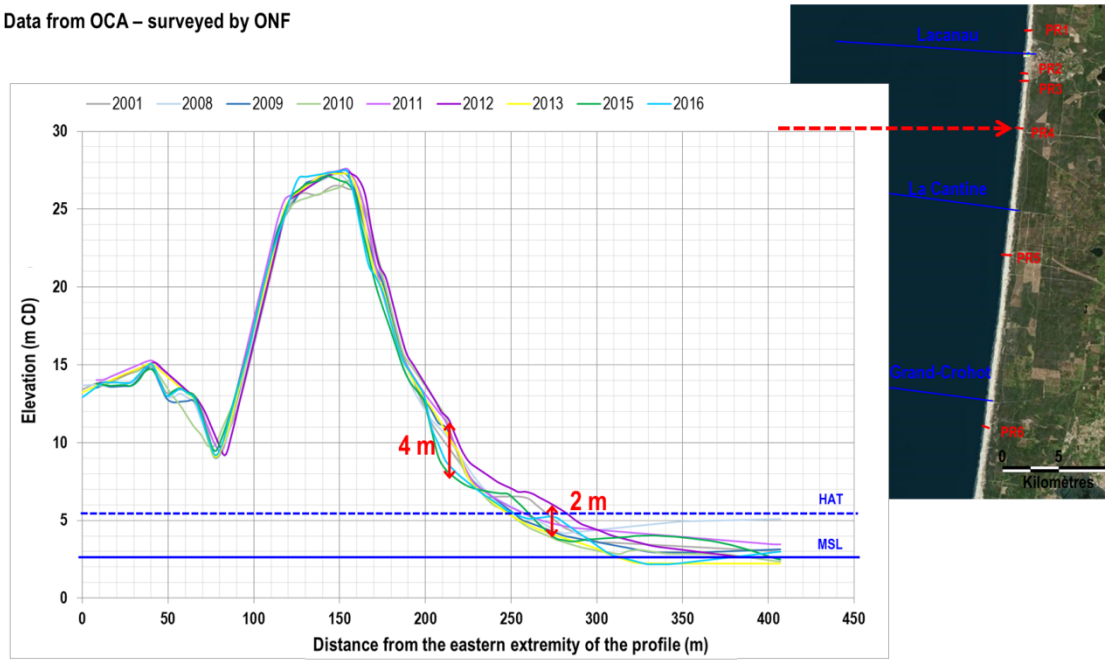

Figure 36. ***Historical evolutions of dune profile PR4***

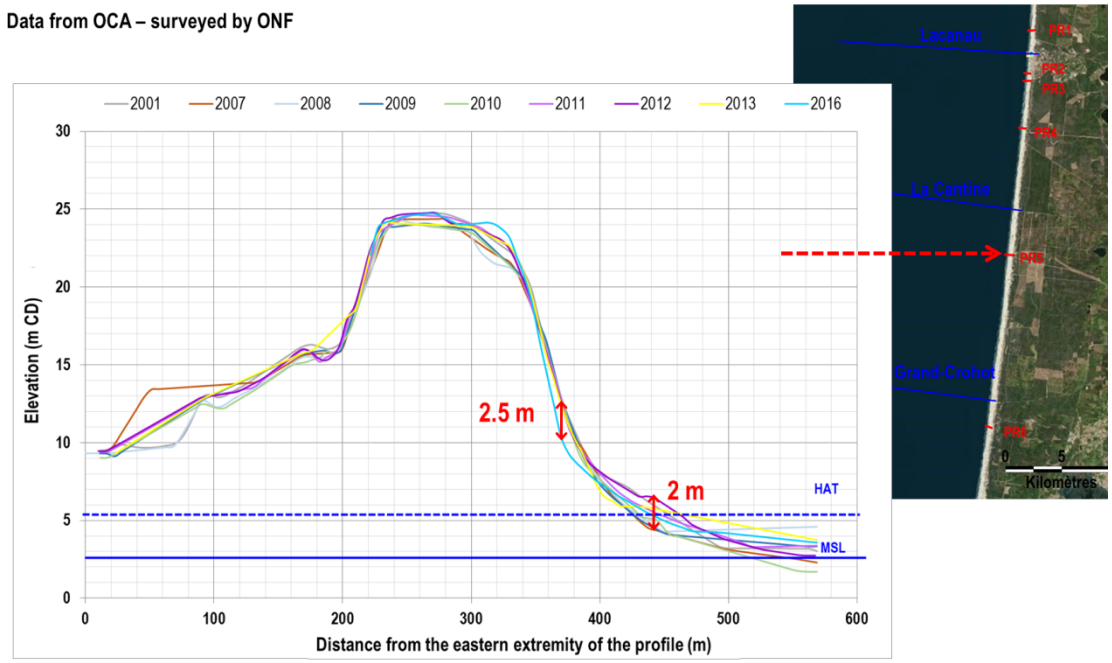

Figure 37. ***Historical evolutions of dune profile PR5***

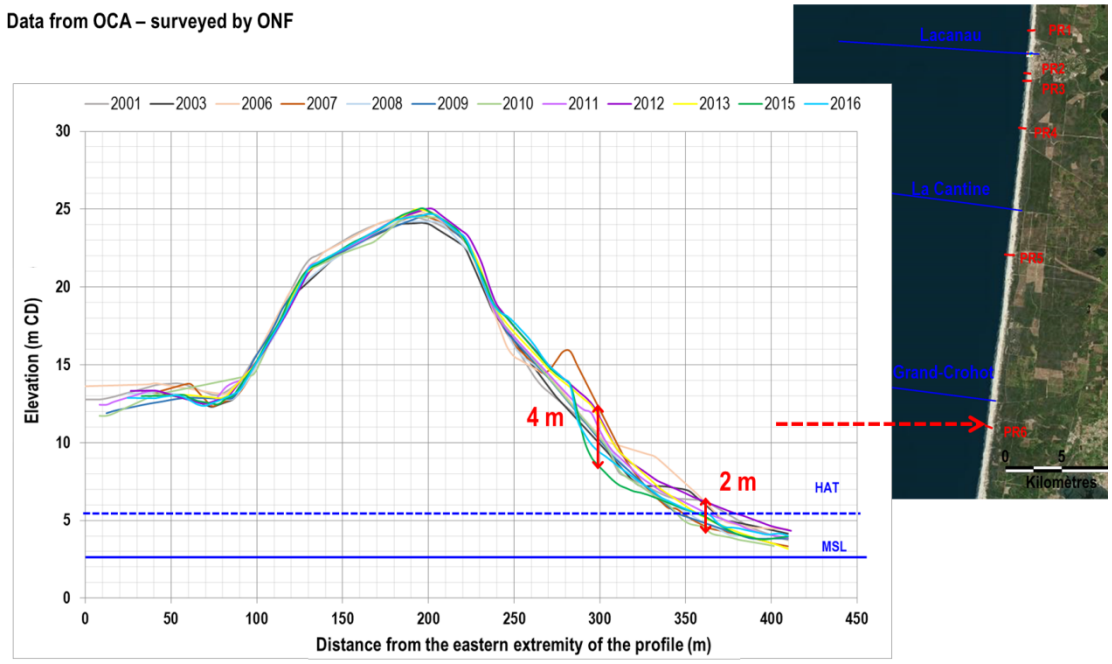

Figure 38. ***Historical evolutions of dune profile PR6***

2.2.8. Cross-shore shoreline evolution during storm events

In order to assess potential short term profile reshape above the closure depth due to storm conditions, the evolutions of the 3 topo-bathymetric profiles subjected to Hercule storm (January 2014) conditions are calculated using SBEACH model.

2.2.8.1. Closure depth calculation

The closure depth (or beach toe) which is defined as the offshore limit of significant seasonal profile variability, can also be assessed considering Hallermaier formula as following:

$$h_p = 2.28 * H_{s12} - 68.5 * \frac{(H_{s12})^2}{g * (T_s)^2}$$

where:

h_p, closure depth (m)

H_{s12}, significant wave height for 12h per year (m) = 5.6 to 6.40 m

Ts, associated significant period (s) = 11 to 15 s

g, acceleration of gravity (m^2/s)

Thus, assessment of closure depth in front of the landfall areas considering Hallermaier formulais about -11 to -13 m, which is in concordance with field observations (see description of surveyed cross-shore profiles in section 2.2.5.2) and with the estimate (from - 10m to -15m) made in 2005 by experts in a technical guide titled “Connaissance et gestion de l’érosion du littoral” (see [20]).

2.2.8.2. SBEACH modeling

SBEACH is a numerical modelling system for simulating the change in beach profile that is suitable for predicting the impact of storms on the coastline. It needs to be calibrated with respect to observed events.

It was developed in collaboration with:

- Department of Water Resources Research (TVRL), Lund Institute of Technology, Lund University, Sweden.
- Coastal Engineering Research Centre, US Army Waterways Experiment Station, Vicksburg, MS, USA. 04/02 MFN

Model functions

- Internal model for simulating random wave propagation, including the surf zone;
- The time-dependent variation in wave height and sea level (storms) can be defined;
- Calculation of beach and dune erosion from a semi-empirical formulation of the rate of longshore drift representing bar formation mechanisms;
- Description of the impact of structures (breakwater or rocky bed).

Model limitations

- No wave reflection on the structures
- Limited change in beach profile during storms (erosion)

- No prediction of longshore drift effects.
- It is noted that evolutions calculated by SBEACH do not take wind into account. As sandy dune system above 10 m CD is mainly shaped by winds, Sbeach software, which calculates profile evolution under storm waves, does not describe short term evolution of the dune area.

2.2.8.3. Storm condition

The storm event used in this study is the storm Hercule, on January 7th 2014, that led to serious retreat of the shoreline along the Aquitaine coast as documented in [15].

The following input parameters were used:

- Time series of significant height and peak period from Homere (point 7247) from 3/01/2014 to 10/01/2014 (see section 2.2.4.2);
- sea level = 6.6 m CD (surge level);
- Sensitivity test to grain size = 0.30 mm and 0.35 mm;

2.2.8.4. Modelling results

Sbeach results are used to assess the short term vertical evolutions below 10 m CD due to profile reshaping under Hercule storm conditions.

Shoreline retreat due to the storm is highest at Lacanau (about 30 m) and smallest at La Cantine (less than 10 m) and grand Crohot (almost nil).Sand is taken on the beach and moved offshore, leading to vertical variations (erosion above sea level, accretion below sea level) of 1 to 4 meters depending on the profile.

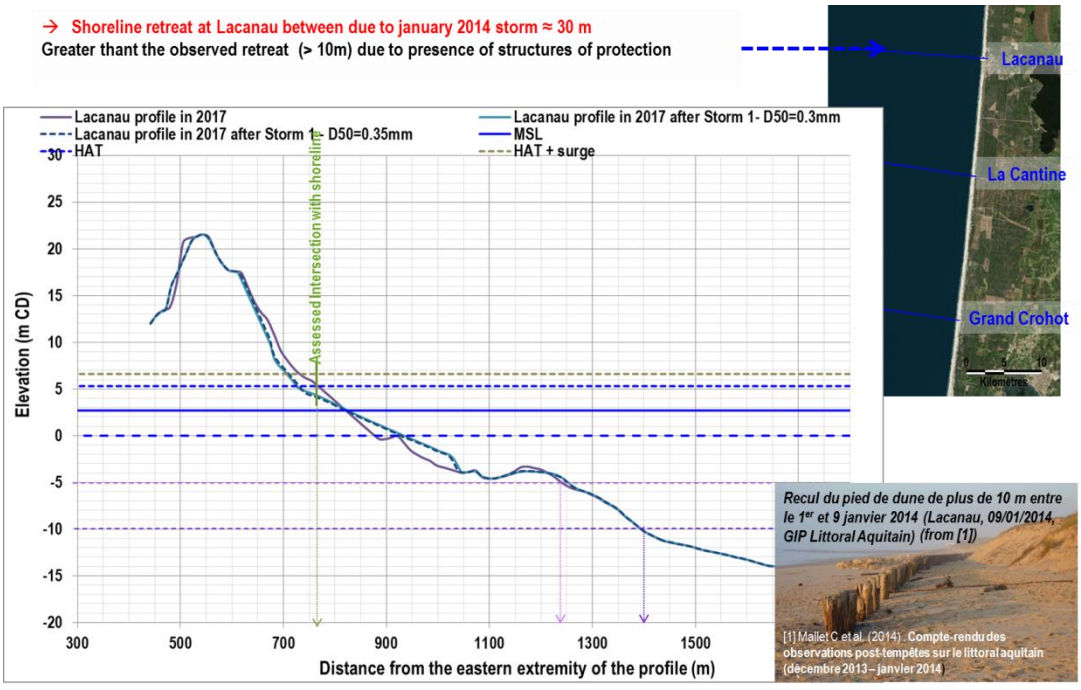

Figure 39. Cross-shore profile evolutions at Lacanau caused by storm Hercule

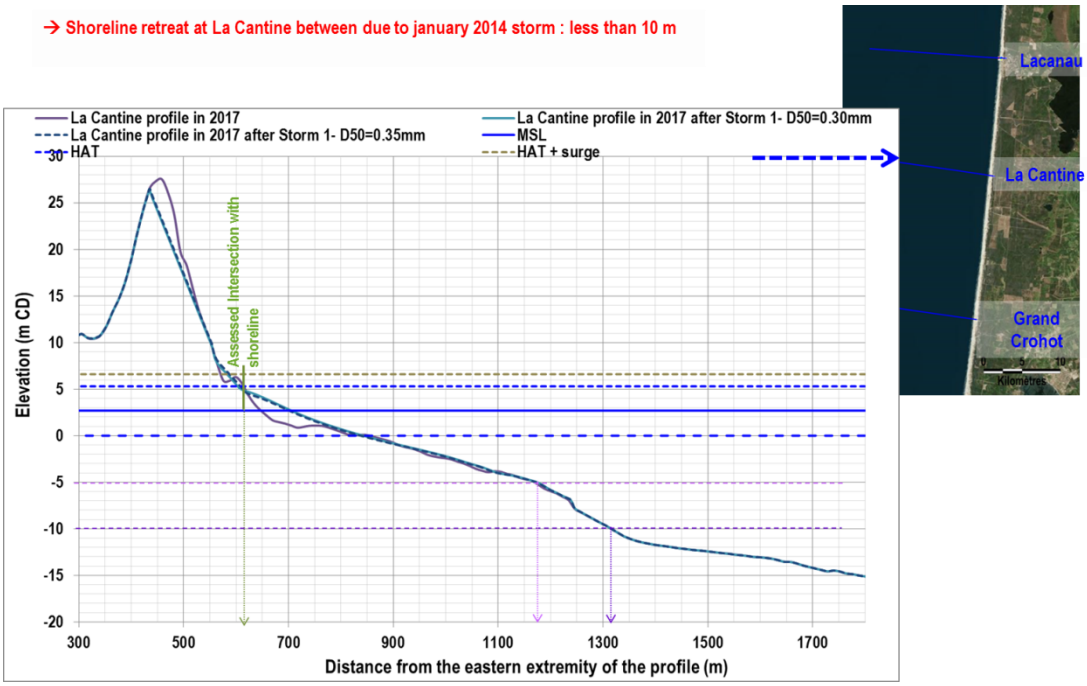

***Figure 40.* Cross-shore profile evolutions at La Cantine caused by Storm Hercule**

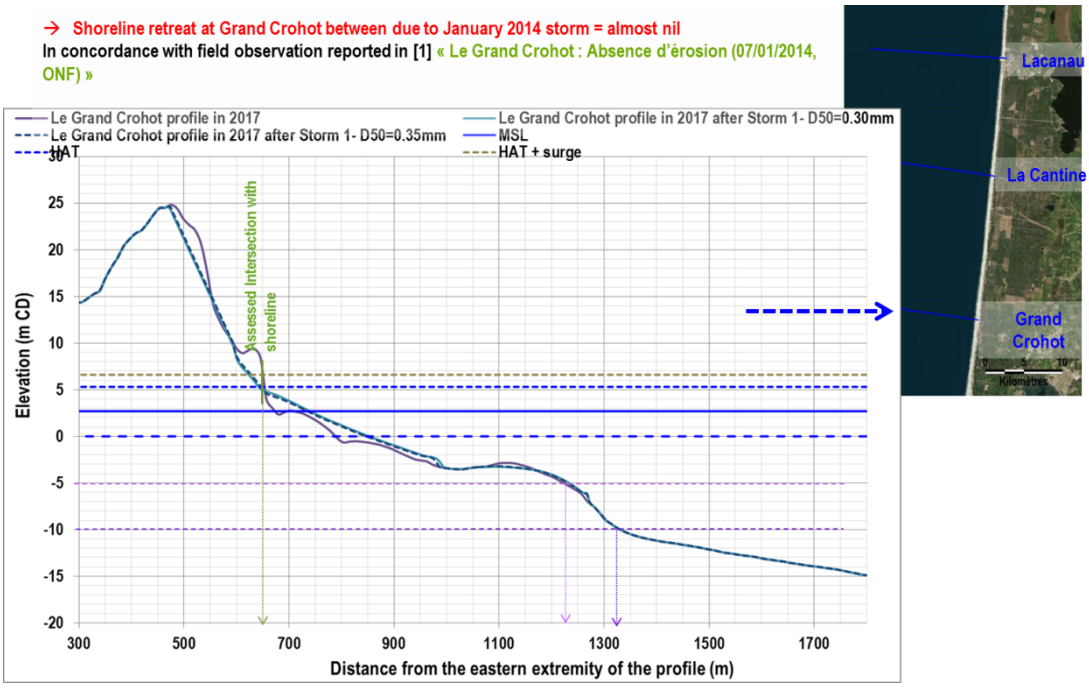

***Figure 41.* Cross-shore profile evolutions at Grand Crohot caused by storm Hercule**

2.3. CAPBRETON AREA

2.3.1. Location of the Capbreton canyon area

Capbreton Canyon is located in the Southeast of the Bay of Biscay and deeply incises the Aquitaine continental slope and shelf. It is a 300-km long meandering submarine structure that runs parallel to the North coast of Spain, before curving northwards and disappearing down the continental slope at a depth of -3500 meters.

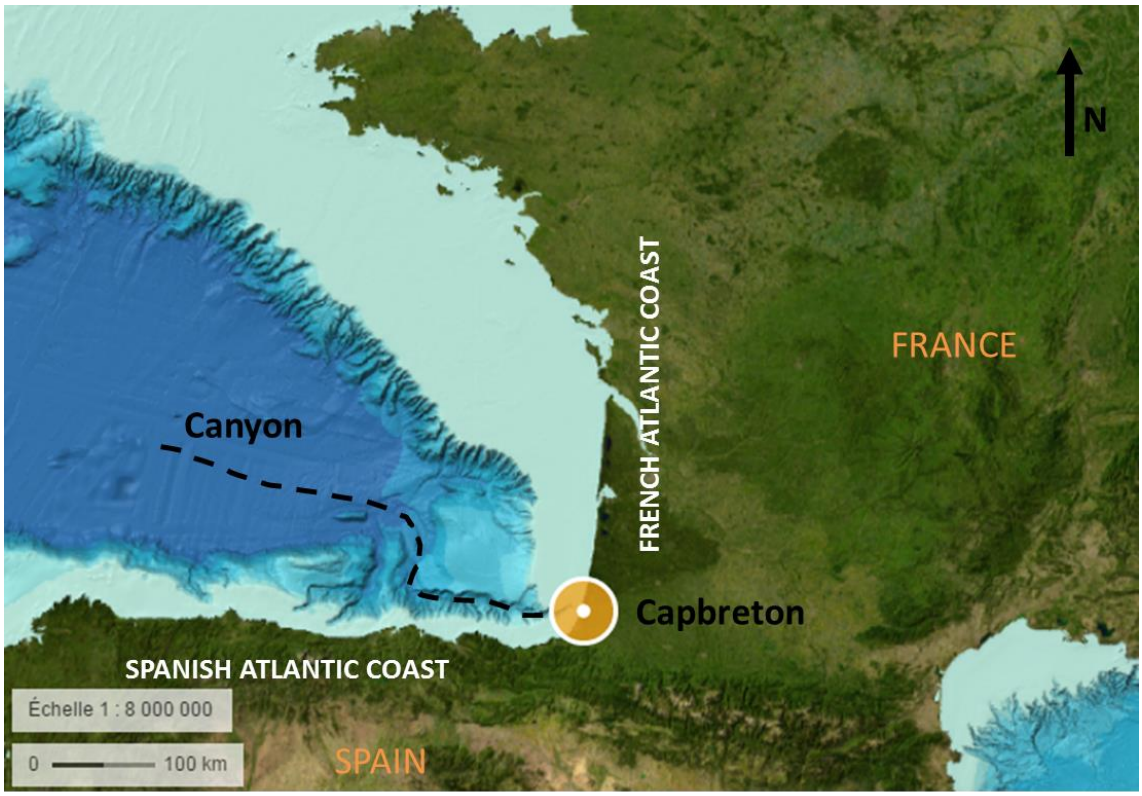

Figure 42. Capbreton canyon area

Lateral slopes along the canyon are steep, which is a problem for the cable to cross it. A first study led by Ifremer in 2012 [14] concluded that the better area for the cable to cross the canyon is its inshore part, presenting gentler slope in comparison with the deeper part of the canyon.

Consequently, the area between the canyon head and the shoreline is the focus of this specific study: it is located only 250 m off the coastline and ranges from a depth of -10 to -100 m CD.

2.3.2. Hydrodynamics forcing

2.3.2.1. Sea levels

Tidal level in Capbreton

Chart datum (0 CD) at Capbreton is located 2.09 m below the origin of the Nivellement Général de France system (0 NGF/ 0 IGN69) (from SHOM 2014).

Tidal sea levels at Capbreton are given by the SHOM and presented in the following table.

Table 8 - Tidal levels in front of Capbreton

Type of tide	HAT	MHWS	MSL	MLWS	LAT
	Highest astronomical tide	Mean High Water Spring	Mean Sea Level	Mean Low Water Spring	Lowest Astronomical Tide
Water level (m IGN 69)	2.7	2.21	0.32	-1.49	-2.06
Water level (m CD)	4.79	4.3	2.41	0.6	0.03

50-year sea level in Capbreton

According to CETMEF document [9], extreme sea level occurring with a 50 year return period reaches **3. 0 m NGF/ 5.09 m CD**.

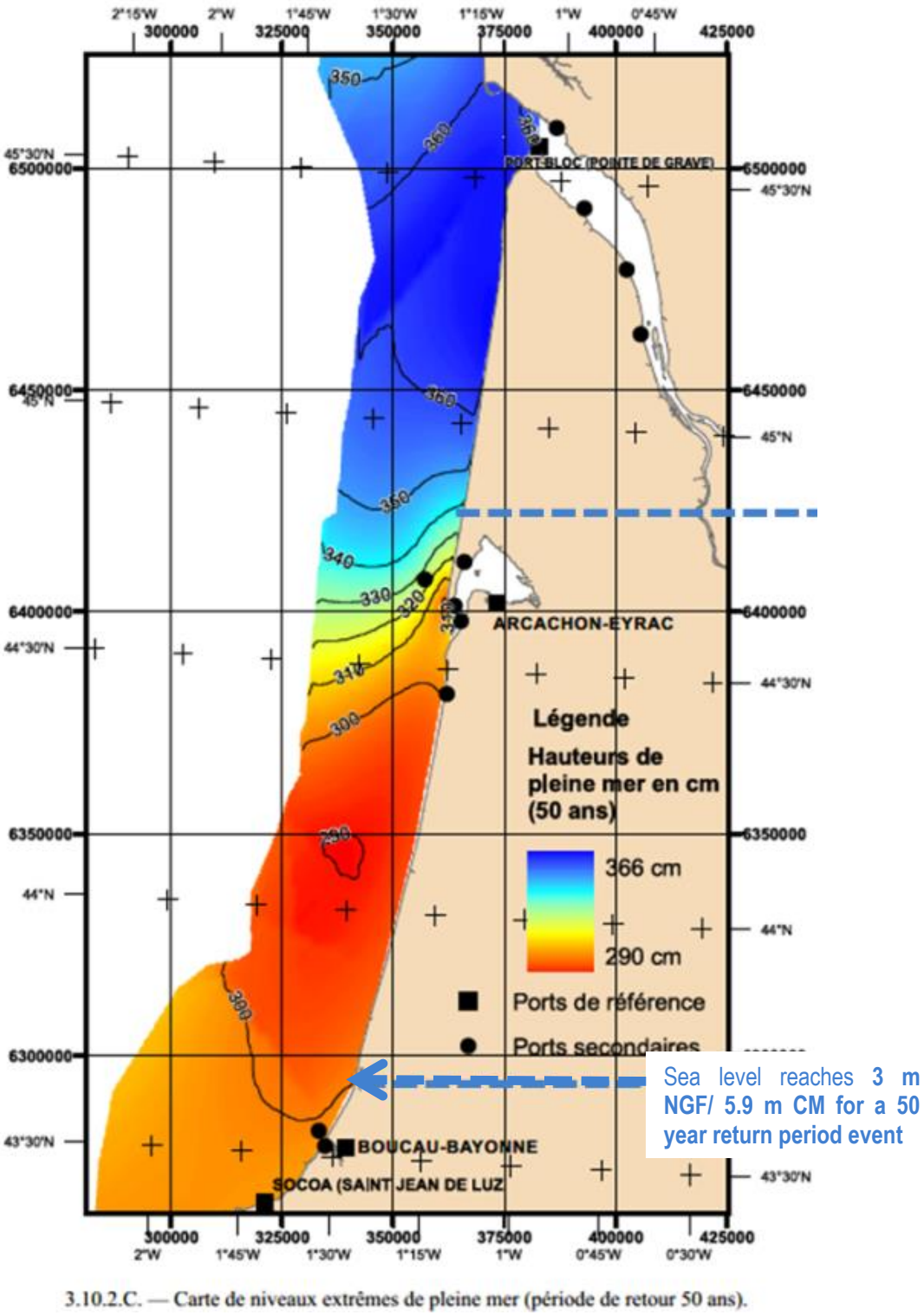

Figure 43. ***Map of the sea level reached with a 50 year return period (from CETMEF expertise [9])***

2.3.2.2. Operational and extreme wave conditions

According to the wave analysis carried out in [1] at the specific locations plotted in Figure 44 the **operational wave conditions** in front of Capbreton are the following:

- The **canyon** has an important effect on wave propagation through the phenomena of **reflection** and **refraction**. Waves approaching the canyon obliquely (mainly from the north-west) will tend to be reflected on the northern side of the canyon because the depth stops decreasing and suddenly increases again. The longer the period is, the more important the effect on wave propagation is. This creates **areas of over-agitation north of the canyon** and **areas of under-agitation south of the canyon**.
- North of the canyon (point S04), the wave climate is mainly westerly from November to April. Then, the direction turns slightly and the waves come from the West-North-West sector. The values of H_s and T_p evolve depending on the season; they are consistent with those offshore.
- At the head of the canyon (point S06), the waves are clearly directed by the canyon shape with a narrow rose around the direction N280°/N290° and the wave propagation phenomena at the canyon's border deflects part of the wave energy away from the canyons head especially in winter (wave with longer periods are more sensitive to the reflection/refraction processes) with H_s lower than 3.5 m all the time.
- South of the canyon (point S05), the impact of the canyon on the wave propagation is apparent (reflection and refraction phenomena). Unlike the 2 previous points, the waves approach from 2 different directions: the West and the North-West (especially in summer).

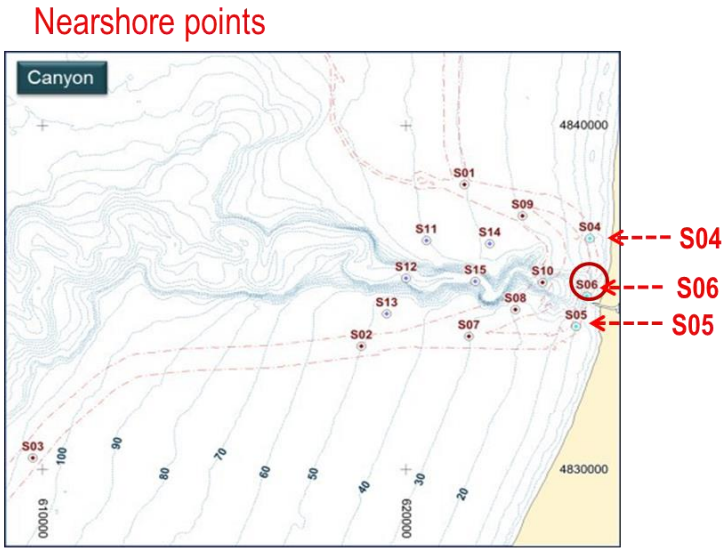

Figure 44. Locations of points where wave climate was analyzed, from [1]

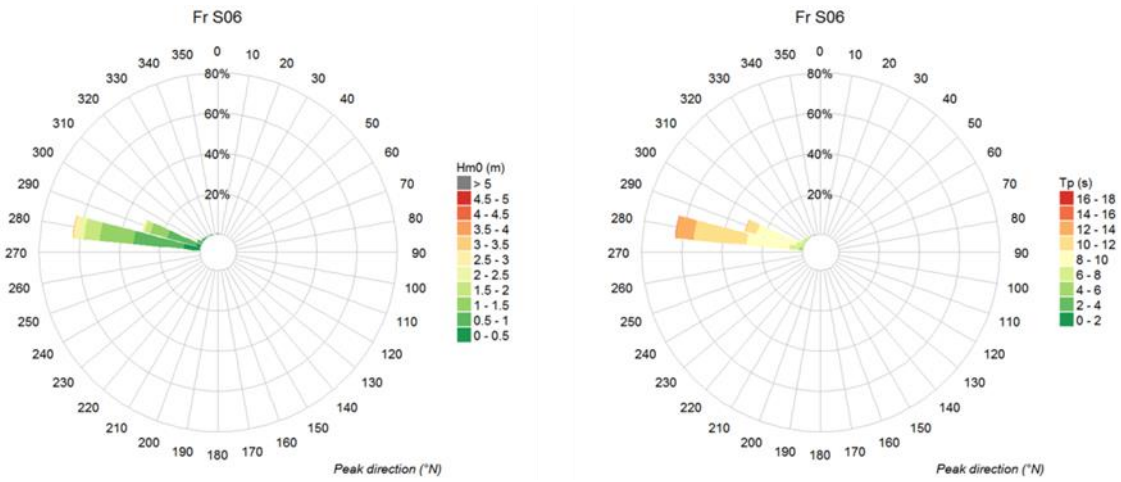

Figure 45. Annual wave rose – Point S06 – Coast - Canyon head

In [1], a study of the **extreme wave climate** was carried out at the same locations. As shown on Figure 46, at the nearshore point S06, 50-year significant wave height Hs is assessed to be about 5.16 m (mean value of the confidence interval) and its corresponding period is about Tp = 12 s

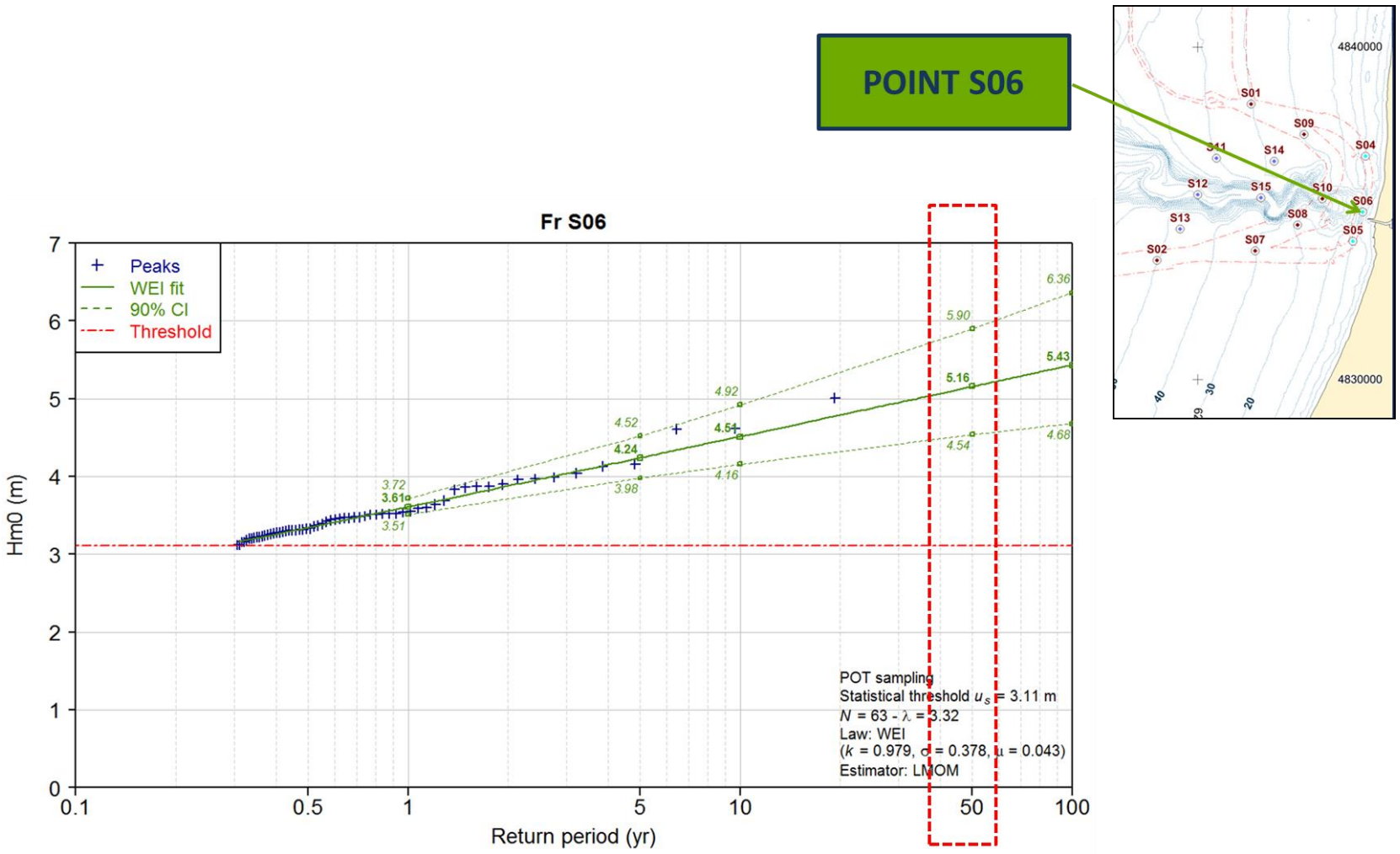

Figure 46. Point S06 – Extrapolation of storm peaks by a Weibull distribution, from [1], Appendix 5

2.3.3. Morphology of the area

The canyon is known to constitute a highly dynamic morphological regime. Sea bed levels are known to fluctuate significantly over short timescales, experiencing distinct phases of accretion, following by rapid erosion. The local hydro-sedimentary processes that shape the canyon head have been subject to numerous scientific studies, most notably by H. Gillet of the University of Bordeaux, who has contributed to the present report.

In [13], H. Gillet describes the canyon head, as follows:

"*The canyon head runs from 10 m to 100 m water depth respectively from it longshore rim to the gullet which connects it with the downstream meandering canyon. It forms a deep and wide amphitheatre opening towards the coast. This amphitheatre is 1200 m wide at the shallowest part (longshore rim).*

Its width decreases to 280 m down to the gullet. The slope of the surrounding inner shelf does not exceed 0.5°. At the head of the canyon, the longitudinal slope increases strongly with a 3.25° average for the first 2 kilometres. The slope reaches up to 10° on the first 100 m, just below the longshore rim.

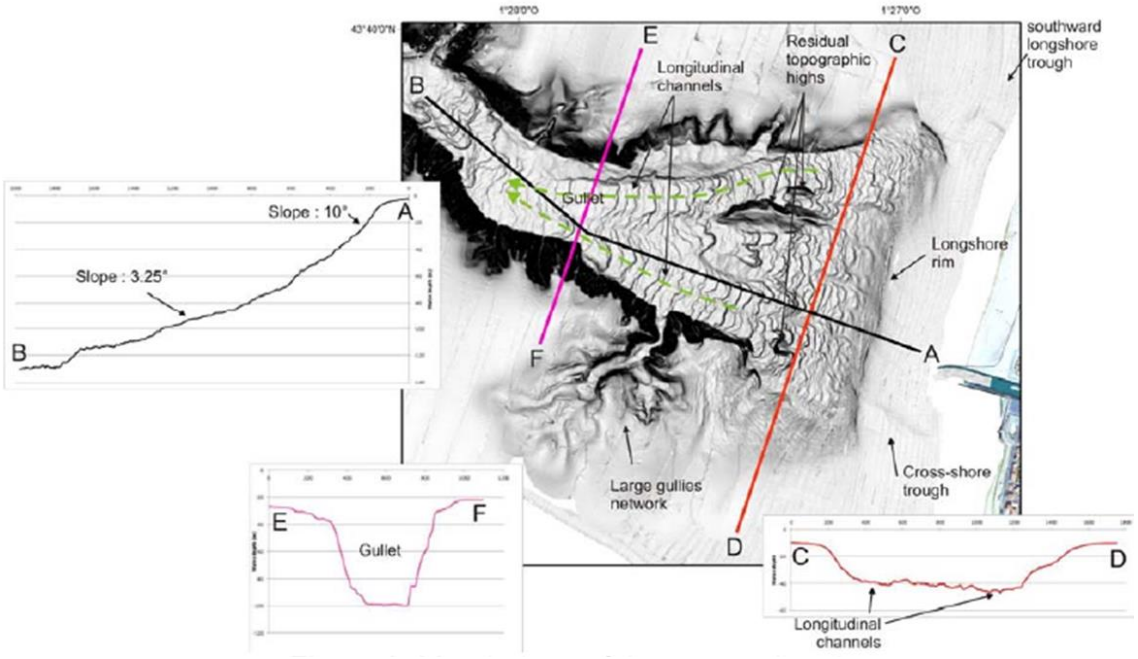

Figure 47. morphology of the canyon head, from [13]

The proximal longshore rim appears to be relatively straight. […]

The two flanks of the canyon head are asymmetric:

- *The north flank is relatively steep, with average slopes ranging from 12° to 25°. It is dissected by three small gullies about 60 m wide;*
- *The southern flank looks slightly gentler with average slopes ranging from 5° to 10°. However, the slope may reach here up to 40° for a few 10s m. This flank is severely downcut by a large northward gullies network.*

The floor of the canyon head is characterised by large and small amplitude morphologic features:

- *Among the high amplitude morphologic feature, we found a set of three longitudinal residual rocky topographic highs.* ***The tallest of all reaches 20 m high*** *above the surrounding seabed. Two 100 m wide longitudinal channels respectively border the northern and southern flanks of the canyon head. These two channels, average 5 to 10 m under the surrounding seabed, appear as potential sediments downward transfer conduits.*

- *The analysis of the 2012 high resolution bathymetric data reveals that the* ***floor of the head is scattered with small amplitude morphologic features****. Two major kinds of features can be described. The concave down canyon bedforms correspond to crescent shaped morphologic steep* [editor's note : barchan dune]*. These features range from 30 to 50 m wide. The corresponding steeps range* ***from 2 m to 8 m high****. "*

H.Gillet interprets these transversal sub-linear bed forms as submarine sand waves. However, further morphologic and hydrodynamic studies are needed to specify the origins of these seabed features.

2.3.4. Local sediment grain size characteristics

The distribution of the superficial sediment characteristics is mapped on the following figure.

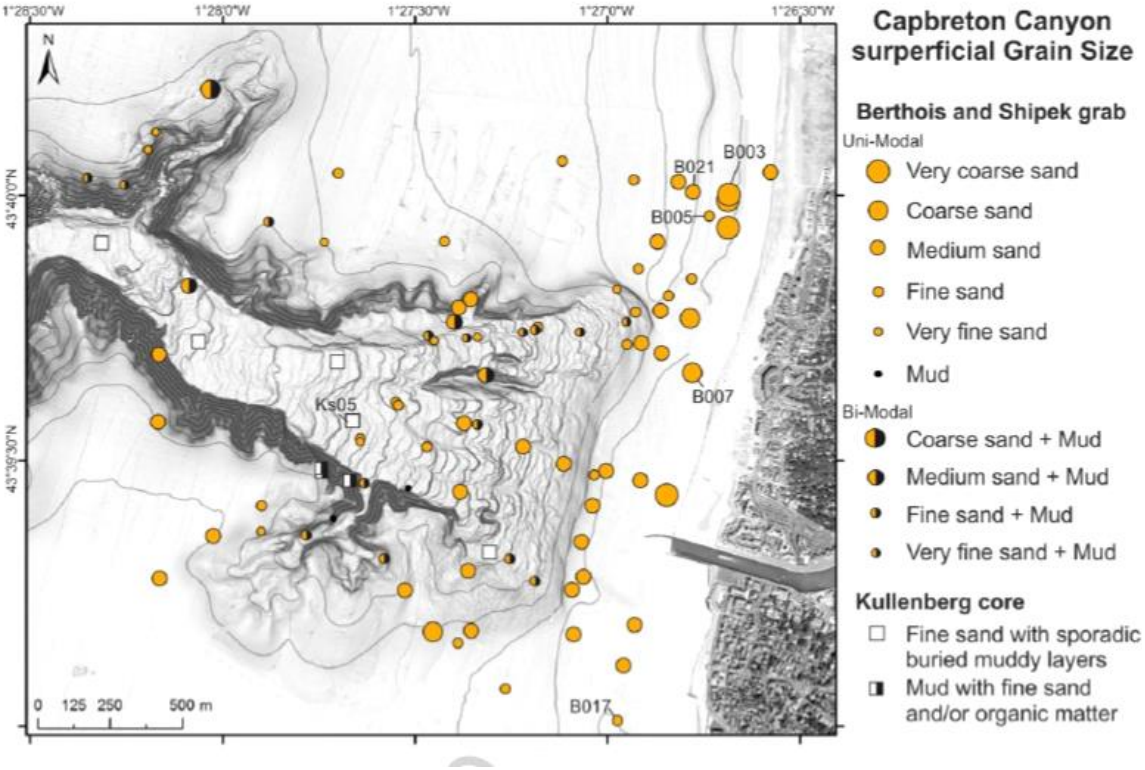

Figure 48. Surficial seabed sediment characteristics in Capbreton area [19]

2.3.5. Assessment of the maximal range of vertical variation of sea bed in canyon head area and adjacent coastal zone

This work is based on bathymetric data analysis.

2.3.5.1. Bathymetric data

- Topo-bathymetric surveys have been collected from the Capbreton Town Hall for the following dates: 2005, 2008, 2009 x2, 2013, 2014. They were realized by Casagec using GPS RTK (vertical accuracy +/- 2cm), coupled with a single beam sounder (+/- 2cm). Profiles were surveyed every 100 m.
- Bathymetric surveys carried out by EPOC laboratory (University of Bordeaux) in August 2009, June 2010 and June 2012 were also used. For GOUFHEAD survey (August 2009) the uncertainty is about 10 cm at Z =- 20 m CM, and 5 cm at Z=2 m CM. Considering the sea bed level range of the present survey (-40 m > Z > -2 m), the confidence interval is from 5 to 15 cm. For SEDYMAQ 2 & 3 missions (June 2010 and 2012): the uncertainty is about 0.2% of the water depth and about 5 cm at least. In the present study this leads to a confidence interval from 5 cm to 12 cm (as sea bed bathymetry is between - 8 m < Z < -60 m).
- Finally, the company I-SEA processed satellite images to derive bathymetric information. Images from SPOT 2, 4, 5, 6, Landsat 5, 8, Sentinel 2, Pléiades at the following dates were processed: August 1990, April 1995, April 2000, July 2003, August 2007, April 2010, October 2011, August 2013, June 2015, January 2016, March 2016, May 2016, August 2016, January 2017, April 2017.

  These bathymetric datasets have been produced without using any field ground truthing (as there were no simultaneous field/satellite pairs to calibrate the algorithm). Once produced, the bathymetric DEMs have been checked by a geomorphologist to control the range of depths and their coherence with reality and with the *in-situ* datasets available (Casagec / Epoc surveys). The mean vertical accuracy of satellite-derived bathymetry is of the order of 1 m. It should be known that the vertical accuracy decreases with increasing depth: vertical accuracy decomposes as follows: a mean vertical offset of 0.5 m plus 10-20% of water height. It means that in water depths of about 5 m, vertical accuracy is in the range of 1 – 1.5 m.

2.3.5.2. Processing of bathymetric data

The processing of the bathymetric data has been carried out by I-SEA, under the lead and collaboration of ARTELIA and Hervé Gillet from EPOC laboratory. The final report is available in **Appendix A** while the main results are presented below.

A series of 19 bathymetric surveys spanning a period of 27 years (1990 – 2017) were used to derive knowledge about nearshore beach dynamics and bottom stability along the Capbreton / Hossegor coastline.

A comprehensive understanding of shallow water beach morphodynamics capturing spatio-temporal sandbar variability and bottom change in depths ranging from +2 m up to -30 m relative to spring low tide level (zero of marine charts) is derived from the analysis of 5 cross-shore profiles mapped in Figure 50. Finally, lowest seabed level observed all along the profiles has been derived in Figure 51, giving at each location along the profiles, the minimum seabed level observed in the various datasets.

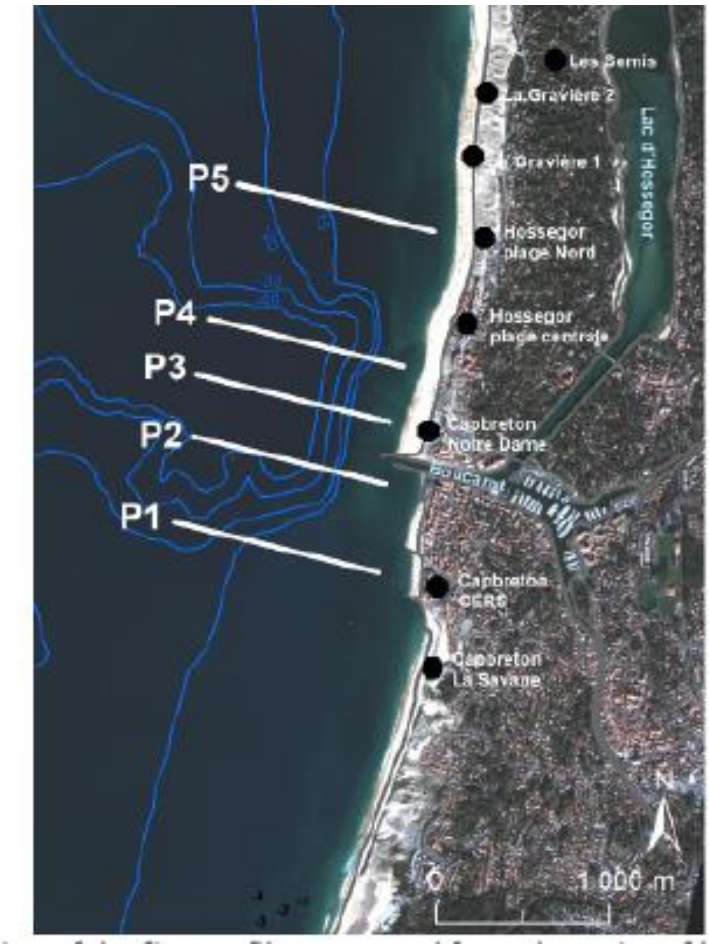

Figure 49. Location of the five profiles along which bathymetric data were extracted from the series of bathymetric DEM (ISEA study)

Coordinates in Lambert 93 of the two extremities of each profile are reminded below :

P1 : Eastern extremity [341 188.1 0m; 6 293 537.92 m]

Western extremity [340 010.03 m; 6 293 920.9m]

P2: Eastern extremity [341 262.7 m; 6 294 043.8 m]

Western extremity [340 157.5 m; 6 294 403.0 m]

P3: Eastern extremity [341 310.3 m; 6 294 394.7 m]

Western extremity [340 205.3 m; 6 294 756.5 m]

P4: Eastern extremity [341 412.4 m; 6 294 710.8 m]

Western extremity [340 304.5 m; 6 295 070.2 m]

P5: Eastern extremity [341 640.0 m; 6 295 470.9 m]

Western extremity [340 528.9 m; 6 295 833.5 m]

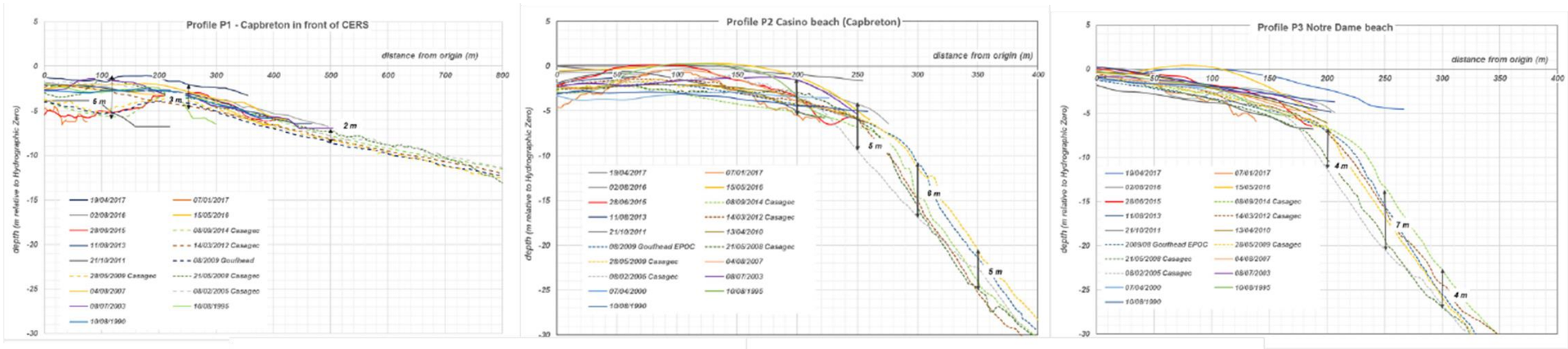

Figure 50. ***.Multi-temporal bathymetric profiles (19 dates) extracted from DEMs at 5 locations (P1 in front the Centre Européen de Rééducation Sportive de Capbreton, P2 Casino Beach south of Boucarot, P3 at the beach of Notre Dame, P4 at the central beach of Hossegor, P5 northern beach of Hossegor). Elevation reference level is expressed in m relative to Hydrographic Zero (HZ). The origin of the X axis is the same for all profiles and corresponds here to the beginning of the shortest profile***

The main results highlight the following statements:

- **Beach morphology is strongly affected by the location of the Capbreton canyon head**, showing typical regional sandbar morphology (intertidal ridge-and-runnel, crescentic outer sandbar) to disappear in front of canyon head, from Central Hossegor Beach (north) to Capbreton La Savane Beach (south).;

- The **vertical amplitude of annual bottom changes in front of canyon head is of the order of 5 m in very shallow waters** (intertidal beach + upper subtidal beach i.e. depths from +2 m to -5 m) attaining **8 m in higher depths** (-5 m to -30 m) due to the subtidal beach to be connected with the canyon head. The maximum vertical change observed over the area is 12 m at the north-east corner of the canyon in depths of 15-25 m.

- This high amplitude in bottom elevation change at such depths is very unusual, and it is suggested that **particular gravity mecanisms occur at the edge of the beach profile** where the slope becomes steeper driving large amount of sediments offshore into the canyon.

It is concluded that variations of seabed level in this area are cyclic and mostly due to migration of sand bars onshore/offshore with respect to wave conditions. Maximum vertical variations are important during a cycle, but no trend of long term evolution of seabed (erosion or / and accretion) has been highlighted so far.

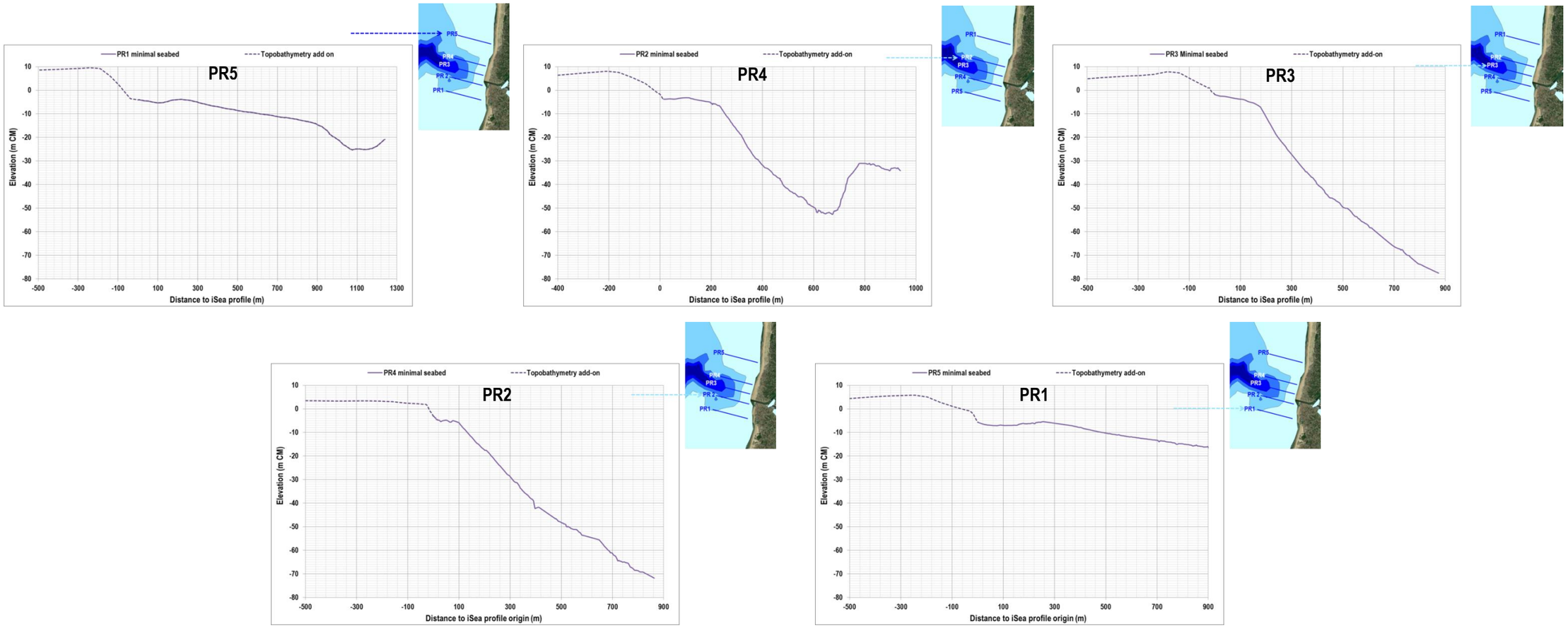

***Figure 51**. Interpreted lower bathymetry profiles PR1 PR2 PR3 PR4 PR5based on ISEA study result.*

2.3.6. Conclusions regarding the route crossing the canyon head

As stated before, **vertical amplitude of sea bed changes in front of canyon head is important for bathymetry above -30 m CD.** It can reach:

- **5 m in very shallow waters** (intertidal beach + upper subtidal beach i.e. depths from +2 m to -5 m CD)
- **8 m in greater depths** (-5 m to -30 m) due to interactions between the subtidal beach and the the canyon head.
- **A maximum 12 m vertical change is observed at the north-east corner of the canyon head** at depths of 15-25 m.

If the cable route is crossing this area, it can be expected that sometime during its lifespan, the cable will be buried under a sandbar, therefore 8 or 10 meters below the seabed surface. or exposed due to sand bar migration and consequential seabed erosion by 8 to 10 meters.

3. SEABED MOBILITY AND BED LEVEL CHANGE ALONG THE OFFSHORE MAIN ROUTE

3.1. INTRODUCTION

This section is dedicated to the study of the seabed mobility and potential vertical variation along the offshore route. The following figure presents the main offshore route (in red line), and its French and Spanish alternatives (in green and purple lines).

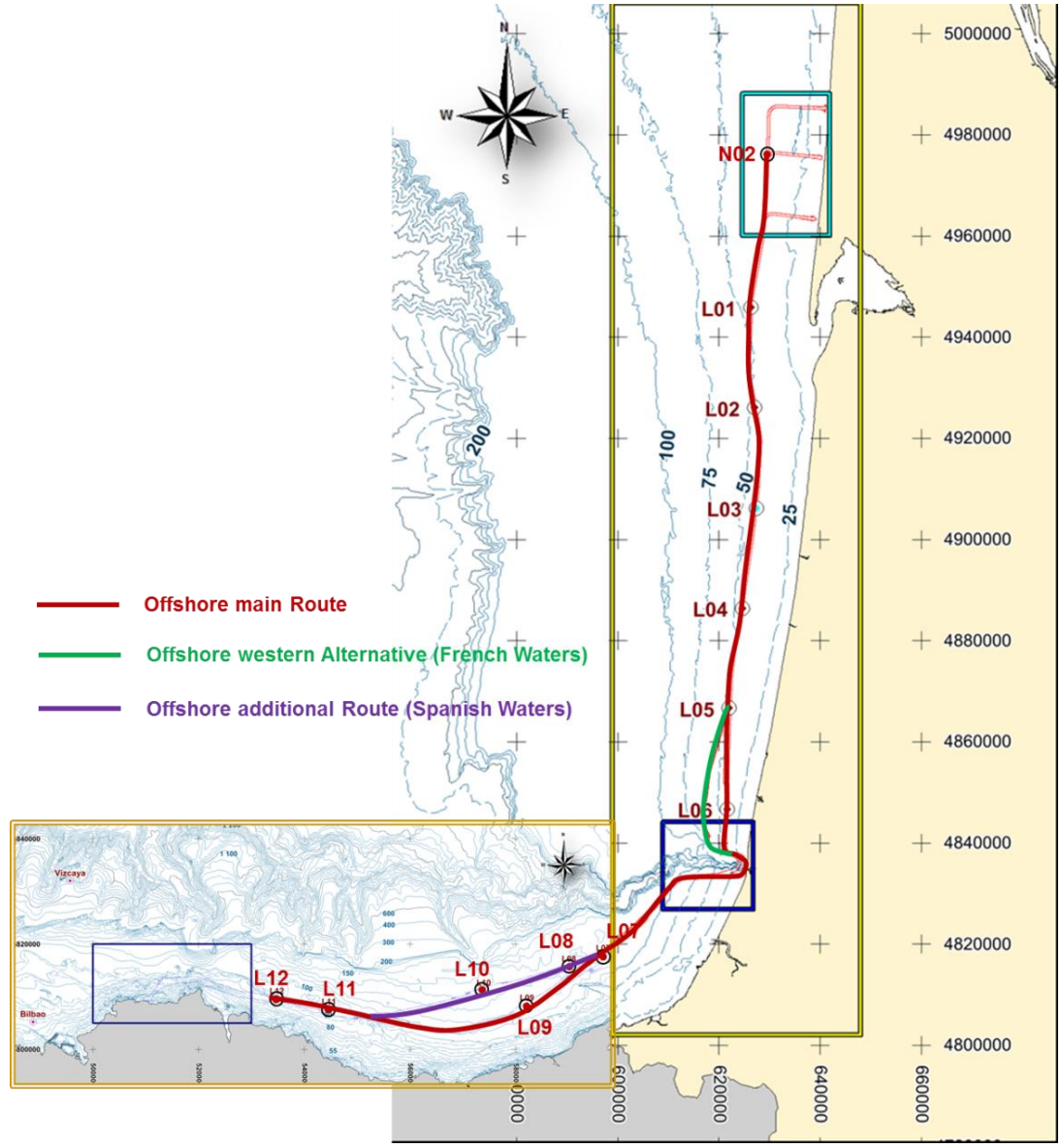

***Figure 52.** Presentation of the offshore main route and its two alternatives, and the 13 offshore points where currents and waves have been extracted from numerical studies*

In order to develop an understanding of the hydrosedimentary processes which operate along the proposed cable route and their influence on the morphological evolution of the seabed, the following assessments have been carried out:

- A general review of the seabed along the offshore cable route, based on the surveys carried out by MMT in 2016 and 2017: those results are recorded in the geophysical report [10] and the geotechnical report [16]. The outputs comprise a description of:
    - Sediment type and grainsize characteristics;
    - Thickness of surficial sediment layers;
    - Nature and size of sedimentary bedforms;
    - Water depth; and
    - Seabed slope.

  Note that this information provides the input conditions for the subsequent calculations of seabed potential mobility.

- An empirical assessment of seabed mobility in order to identify areas where the surficial sediment layers are mobilised by waves and/or tidal currents. This provides a first approximation of which sections of the route are ***potentially subject to bed level variation*** but it does not quantify the depth of sediment disturbance, or the extent of temporal bed change level.
-
- An assessment of potential bed level variability, based on the following information:
    - Sedimentary bedform characteristics derived from the survey data; and
    - Information on seabed variability and bedform migration rates obtained from scientific literature.

The assessments described above have been used to derive a holistic view of bed level variability along the cable route but are subject to the following assumptions and limitations:

- The empirical calculations of seabed mobility cannot be used to derive bed level change and it is not possible to determine the vertical extent of sediment disturbance using this approach;
- Given the water depth along the route, it can be assumed that for the most part, sediment disturbance is restricted to the upper layers of surficial sediment;
- In the absence of additional sources of bathymetry data with which to compare the most recent survey data, it is ***not possible to quantify*** the extent of bed level change, or the rate of bedforms migration along the whole route.
- In view of the above, it is assumed that in areas where there are no seabed features, bed level variability is negligible and there is no risk to cable protection;
- Where seabed features exist, the maximum extent of bed level change equates to the height difference between the crest and the trough of the feature;
- All observed features are assumed to be active and subject to potential migration

3.2. DESCRIPTION OF THE OFFSHORE MAIN CABLE ROUTE

3.2.1. Summary of the seabed along the main offshore route

Geophysical and geotechnical surveys carried out by MMT in 2016 and 2017 provide large amount of information on seabed characteristics along the main offshore route and its two alternatives in French and Spanish waters. Results of field surveys are summarized in a didactic representation the main information related to the following seabed characteristics:

- Granulometry (medium diameter) of superficial sediment;

- Type of sediments which compound the movable layer;
- Thickness of the movable layer;
- Strength over the movable layer;
- Water depth.

It is based on the bathymetric profile and slope of seabed mapped by MMT in [10], as shown in Figure 53 and includes the results of the vibrocore tests carried out at the numerous location presented in Figure 54.

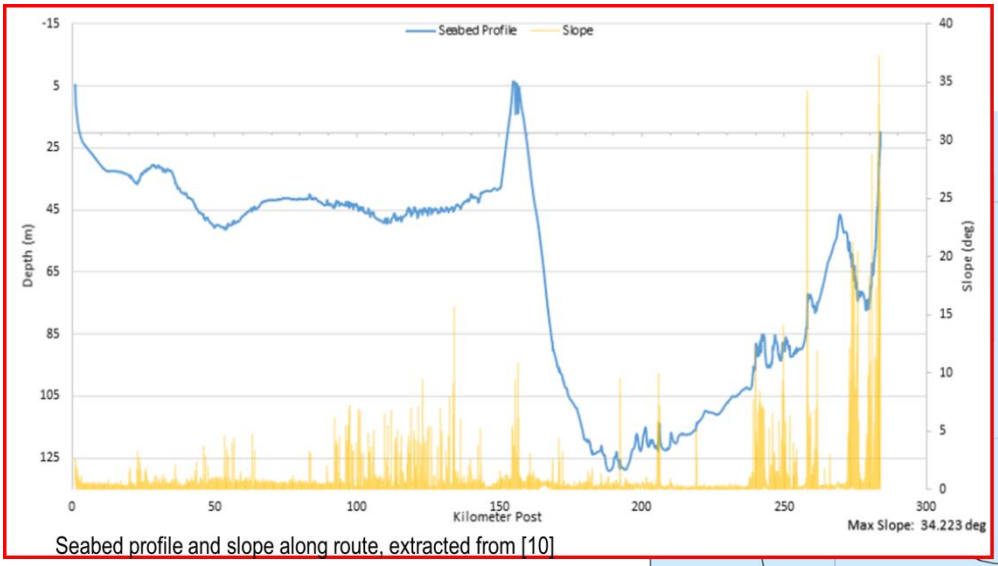

Figure 53. Bathymetric profile and seabed slope along the main offshore route, from [10]

The summarized graph is presented in Figure 55.

On the X-axis are reported the kilometric points from 0 (La Cantine landfall) to 283 (Bilbao Landfall). On the left vertical axis is reported the water depth below 0 CD. On the right vertical axis is reported the slope of the seabed in degrees. The horizontal sections give information on :

- The superficial granulometry (top horizontal section) :

  The mean diameter D_{50} deduced from vibrocore analysis carried out by PSL (Professional Soils Laboratory) are reported at the corresponding KP where vibrocore tests are done. As reminder, the particle size distribution curves done for each analyzed sediment sample are presented in [16], from p.225 to p.337

- Seabed forms and thickness of the movable sediment layer (intermediate horizontal section):

  Seabed forms identified along the route are reported according to their corresponding KP: type of the surficial form (ripples, dunes…) and range of dune dimensions if present. Thickness of the moveable sediment layer which overlays the Consolidated Seabed (CS), assessed by the field surveys, is also reported according to the corresponding KP.

- Type of granular material which compounds the movable seabed (lower horizontal section):

  Characterization of the granular material which compounds the movable sediment layer, provided by field surveys, is reported according to the corresponding KP. A color code identifies the type of granular material: in orange is represented a material made of sand and gravel, in yellow is represented a material mainly made of sand, in light green is represented a material mainly made of sand with clay, in darker green is represented a material mainly made of silt or clay.

The main offshore route is divided into 4 main sections referring to 4 geographic zones characterized by homogeneity of observed sea bed forms and assessed movable layer thickness.

Each section is divided itself in subsections referring to sub-zones characterized by an homogeneous type of granular material. A total of 12 subsections is identified.

Table 9 - Main route section and subsections.

Section	Subsections	Initial KP	Final KP	D50 (mm) of surficial layer	Metocean study time series output point
1	1	0	5.6	0.33 – 0.40	
	2	5.6	12.77	0.42 – 0.47	N02
	3	12.77	43	0.29 – 0.36	L01
2	4	43	88.45	0.29 – 1.2	L02, L03
	5	88.45	141.5	1.2	L04, L05, L06
3	6	141.5	163.3	0.18 – 0.32	
4	7	163.3	183	0.16 – 0.19	
	8	183	203	0.11	L07
	9	203	240	< 0.006	L08, L09, L10
	10	240	251		
	11	251	270	0.085 - 0.65	L11
	12	270	283	0.38 – 0.9	L12

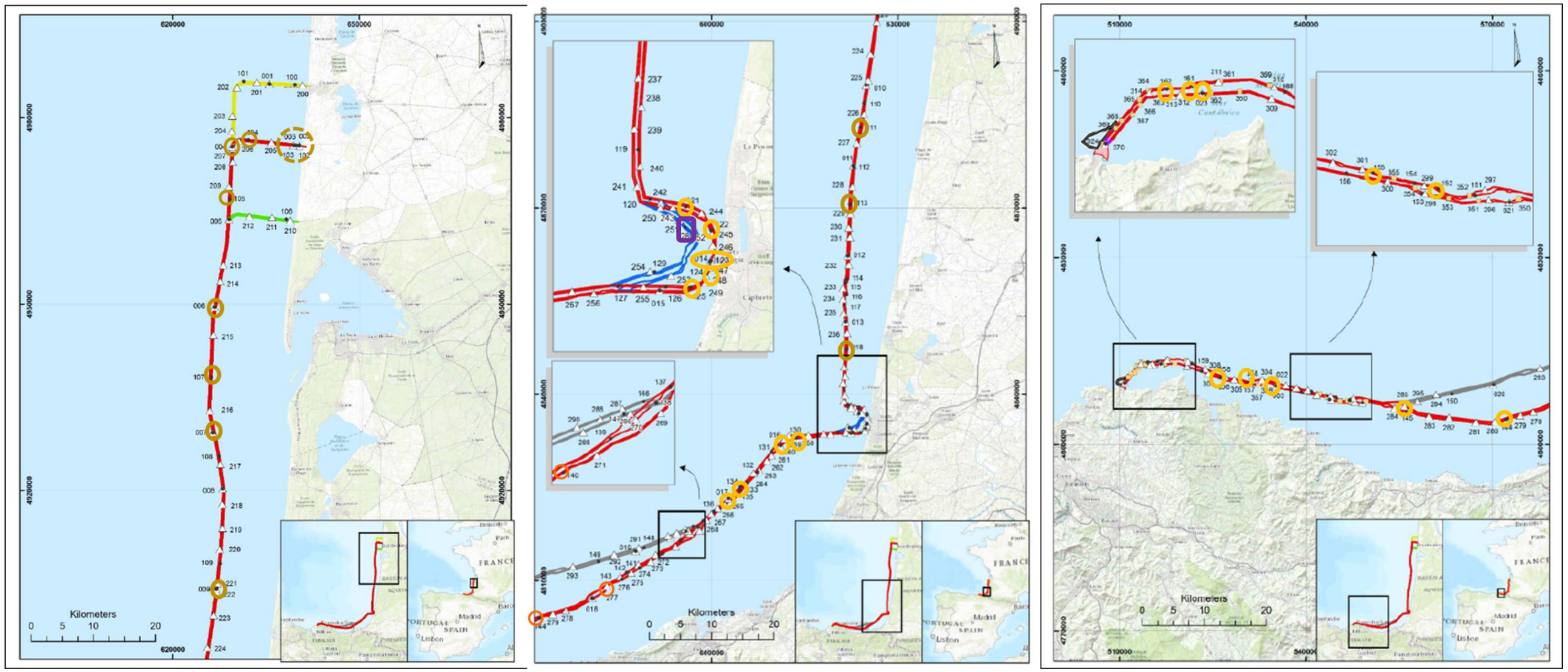

Figure 54. ***Locations (circled in brown or orange) of vibrocore tests carried out by MMT in 2016, from [16]***

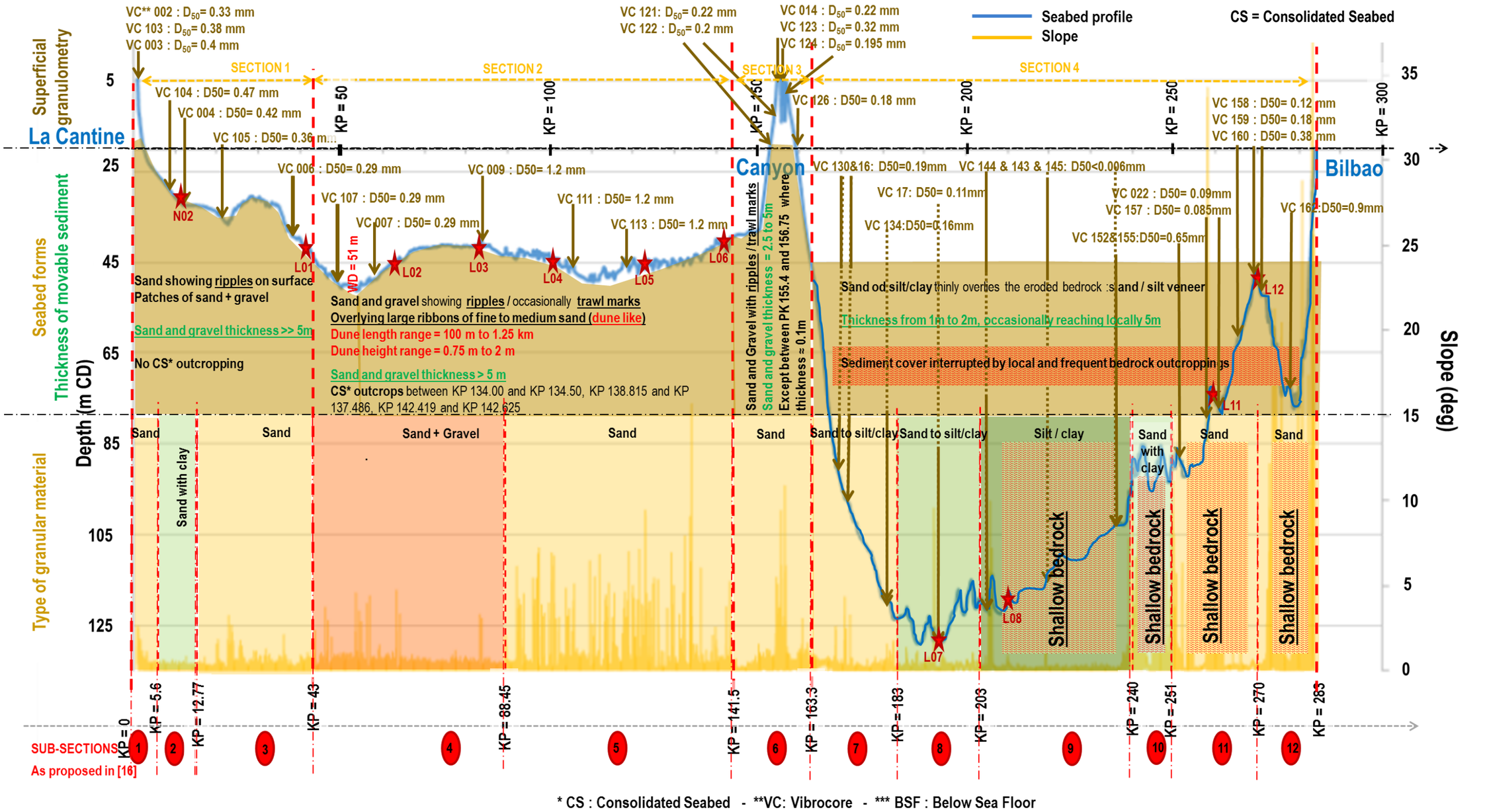

Figure 55. ***Synthetic representation of seabed characteristics along the main route (from main route profile mapped by MMT in [10])***

3.2.2. Description of seabed characteristics and bedforms in section 1, from KP 0 to 43

Seabed section 1 is mainly characterized by **sand ripples** on its surface.

Indeed, as shown on alignment charts, the recorded seabed bathymetry presents features with small height (of the order of the thickness of the chart line) and small wavelength, which is typical of sand ripples produced by waves and currents in loose sandy sediment.

Because the accuracy of the alignment charts does not allow us for concluding on the ripples' characteristics, we use the Yalin (1985) [22] characterization as follows : ripple height Δ_r =50 to 200 D_{50} and ripple length λ_r = 500 to 1000 D_{50} . Considering a mean grain diameter of sand of 0.35 mm, Δ_r =1.75 cm to 7cm, and λ_r = 17.5 cm to 35cm. As described in [10], within this first section the seabed:

- First relatively steep dips from -5.0 m CD to -11.5 m CD at KP 1.250
- then dips with reduced gradient to 23.5 m at KP 4.000 and 32.5 m at KP 12.500.
- then very gently dips to 34.0 m at KP 20.035
- and finally gently dips again with increasing KP reaching - 40 m CD between KP 39.000 and KP 40.220.

Movable sediment layer thickness (above the CS) is greater than 5 m.

3 subsections are identified.

Subsection 1

Material representative of subsection 1 is mainly sand. It is dense 0.60 m below seabed surface, very dense 1.52 m below seabed surface.

Subsection 2

Material representative of subsection 2 is sand with clay. Sand is slightly gravelly to gravelly, locally silty. Clay is medium to high strength and the granular material is medium dense to dense.

Subsection 3

Material representative of subsection 3 is sand. It is slightly gravelly to very gravelly, with gravel contents increasing with depth. Material becomes very dense at shallow depths from 0.78 m to 1.74 m. There is some extremely low strength clay at a single location, where clay is underlain by gravelly sand.

3.2.3. Description of seabed characteristics and bedforms in section 2, from KP 43 to 141.5

Seabed section 2 is characterized by **sand dunes, like sandy ribbons overlaying sand and gravel seabed** showing ripples and trawl marks (Figure 57). **The observed sand dune wavelengths vary from 100 m to 1.25 km and the observed dune heights vary from 0.75 m to 2 m.**

Shallow ridge features up to 1.5 m high are observed between KP 46.10 and KP 47.65.

Then overlying large 1 m to 2 m high ribbons of fine to medium sand cross the route at numerous locations defined by MMT in [10] p. 42 and 43.:

Within this second section:

- Seabed continues gently dipping to 50 m then gently undulates between around 50 and 51 m.
- Then stands predominantly at 50 m until KP 57.0., reaching - 42 m CD at KP 67.30
- Then it slightly undulates (1 m) with increasing KP,
- From KP 85.50 it very gently dips to -43 m CD with slight undulations to KP 100.25, where the slope slightly increases.
- Then the seabed continues to vary in response to the sediment overburden and maintaining a depth of -45 m CD. The seabed continues gently undulating (+/-1 m) from an average depth of 45.0 m until KP 136.35 where it begins to shoal very gently to 42.0 m at KP 140.200

In [10] is plotted the seabed slope along the offshore route. The graph corresponding to section 2 is highlighted on Figure 56.

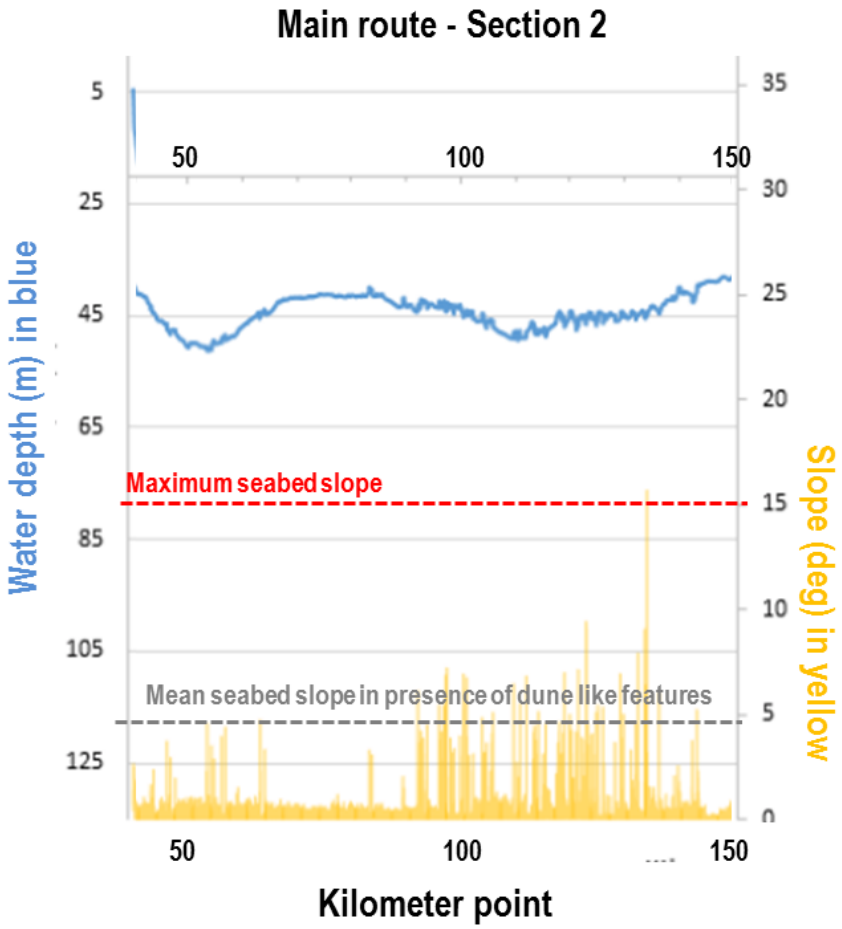

Figure 56. Seabed slope along section 2 of the main offshore route, from [10]

According to this graph, the maximum slope encountered in this section 2 (related to sand dunes) is about 16 deg. The average slope of the sedimentary features is about 5 deg.

Movable sediment layer thickness (above the CS) is mainly greater than 5 m, **but occasionally CS outcrops** between KP 134.00 and KP 134.50, KP 138.815 and KP 137.486, KP 142.419 and KP 142.625

2 subsections are identified:

Subsection 4 (from [16])

Material representative of subsection 4 is mainly sand and gravel. Material becomes finer with depth to slightly silty to silty, slightly gravelly sand. Isolated and thin sandy clay bands are observed at depth. Granular material is dense to very dense at shallow depths, 0.50 m below the seabed surface.

Subsection 5 (from [16])

Material representative of subsection 5 is sand. Locally surficial material is very gravelly to sandy gravel in upper layer. Occasional thin layers of sandy clay are observed. The material is very dense at shallow depths, <1.00m below de seabed surface, at the beginning of the subsection, then becoming deeper going south, >1.50 m below the seabed surface.

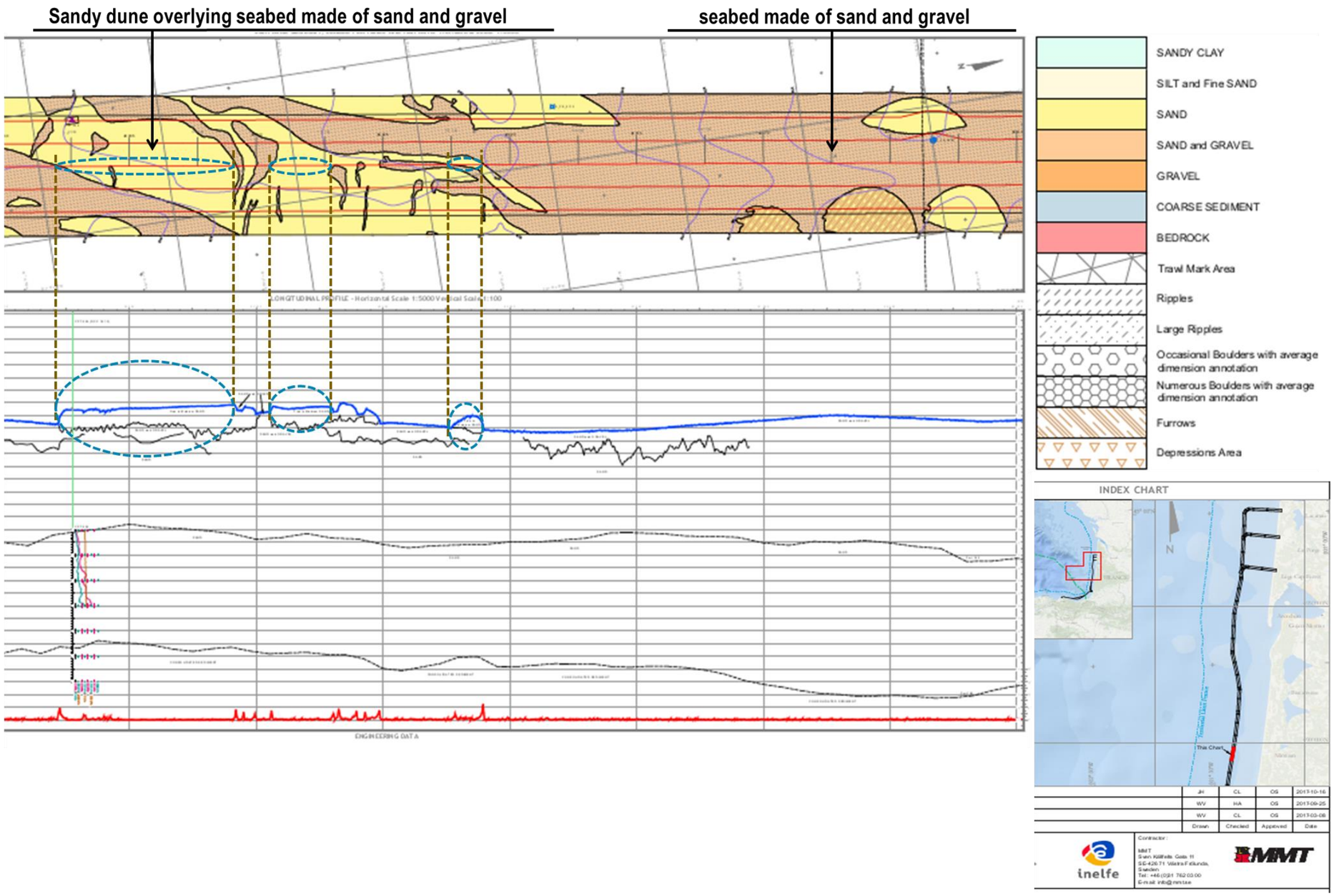

Figure 57. ***Illustration of sandy dunes overlying seabed made of sand and gravel in section 2, charts from [16]***

3.2.4. Description of seabed characteristics and bedforms in section 3, from KP 141.5 to 163.3

Seabed section 3 corresponds to the **Canyon area**. Sandy seabed shows ripples and trawl marks.

Within this third section:

- The relatively flat and featureless seabed continues to shoal with an increased slope until KP 154.30 where the seabed becomes rough. It reaches the top of the slope at -3.5 m CD at KP 154.70.
- It continues shallow at around 3 m until KP 155.50, at the edge of the canyon.
- Then between KP 155.5 and KP 156.75, on steep sides of the canyon, rough seabed alternatively dips to -14 m CD and then reaches - 3.5 m CD twice.
- Then relatively flat and featureless seabed slopes down with reasonable gradient to - 45 m

Movable sediment layer thickness (above the CS) is varying from 2.5 m to 5 m, except between PK 155.4 and 156.75 where thickness is very small (around 0.1 m)

1 subsection is identified:

Subsection 6 (from [16])

Material representative to subsection 6 is mainly sand. It is fine grained, dominated by slightly silty to silty slightly gravelly to gravelly sand. Local gravel bands are observed.

Consequently, considering a mean grain diameter of sand of 0.25 mm, ripples height is about Δ_r =1.25 cm to 5 cm, and ripples length λ_r = 12.5 cm to 25 cm, according to Yalin [22].

The material is very dense 2.00m below the seabed surface at the beginning of the sub section, then 1.50 m below the seabed surface going south.

3.2.5. Description of seabed characteristics and bedforms in section 4, from KP 163.3 to 283.3

Seabed section 4 is characterized by **sand or silty sand thinly overlying the eroded bedrock**: movable seabed is made of thin **sand or silt veneers**, frequently interrupted by bedrock outcroppings.

Within this fourth section:

- The seabed continues to slope down at same gradient until a depth of - 129 m CD at KP 188.20 ;
- Then the very rough seabed highly undulates between -122.2 m CD and -113.8 m CD between KP 195 and KP 210;
- Again the very rough seabed highly undulates between -100 m CD and - 85 m CD between KP 239 and KP 253;
- Sea bed reaches -45 m CD at KP 270, dips again to -70 m CD at KP 279 and rises at -20m CD at KP 283.

Movable sediment layer thickness (above the CS) is varying from 1m to 2m, occasionally reaching 5m locally.

Sediment cover is interrupted by local and frequent bedrock outcroppings.

The cumulative length of the outcroppings is about 20 km.

6 subsections are identified:

Subsection 7 (from [16])

Material representative of subsection 7 is mainly sand to silt/clay. Slightly gravelly silty to very silty sand overlays stiff and high strength silt/clay. Bands of sandy gravel are observed separating sand from underlying silt/clay. Clay is of intermediate to high plasticity. The granular material is generally dense, except in localised areas of very dense material

Subsection 8 (from [16])

Material representative fo subsection 8 is mainly sand to silt/clay. The fine grained material is both granular and cohesive within the section, made of slightly gravelly silty to very silty sand with silt and clay. When entirely cohesive, seabed has a low to very low strength, becoming higher with depth.

Subsection 9 (from [16])

Material representative of subsection 9 is mainly silt/clay. Seabed has an extremely low to very low strength. With depth, strength of material increases.

Subsection 10 (from [16])

Material representative of subsection 10 is mainly sand with clay. Silty gravelly sand contains gravel and cobbles. The movable sediment cover of the bedrock is poor.

Subsection 11 (from [16])

Material representative to subsection 11 is mainly sand. Granular sediment overlying bedrock is very loose to loose.

Subsection 12 (from [16])

Material representative to subsection 12 is mainly sand: slightly gravelly to gravelly sand with some gravel. Bedrock cover is generally good due to the presence of mudstone and interbedded sandstone and siltstone. Limestones are encountered at the end of the route section. Granular sediment overlying bedrock is loose to medium dense.

3.3. EMPIRICAL ASSESSMENT OF SEABED MOBILITY

As described in Section 3.1, empirical seabed mobility calculations have been carried out to determine the extent to which waves and/or tidal currents interact with the seabed along the proposed route and under which, if any wave and tidal conditions, the surficial seabed sediments are mobilized. This provides a first, qualitative approximation of which areas of the route may potentially be subject to changes in bed level over time, in order to narrow down the assessment to focus on the areas of greatest risk to cable security from natural processes.

The information and data used to inform this assessment include :

- Sediment grain size characteristics and water depth obtained from the survey data, as described in Section 3.2; and
- Wave and tidal information derived from the numerical modelling studies [1])

3.3.1. Notion of bed shear stress and threshold bed shear stress

For a fluid to begin transporting sediment that is currently at rest on seabed surface, the bed shear stress TAU exerted by the fluid must exceed the critical shear stress TAU_CR for the initiation of motion of grains at the seabed.

This basic criterion for motion can be written as: TAU ≥ TAU_CR.

TAU is related to the properties of the fluid (currents exerted on seabed due to tide, orbital velocity of waves, fluid density ρ_e …) whereas TAU_CR depends on the properties of sediment only (mean diameter D_{50}, sediment density ρ_s).

3.3.2. Calculation of bed shear stress along the main offshore route

To assess the capability of the granular sediment layer to move, calculations of bed shear stresses:

- due to the action of tides and winds (TAU_C);
- due to the combined action of tides, winds and waves (TAU_C+W or TAU_MAX);

are carried out over the year 2012, at the offshore locations N02 L01 L02 L03 L04 L05 L06 L09 and L11 (see Figure 52 for points locations).

Comparison with threshold bed shear stresses related to 3 types of grain is made at each location over 2012 and allows to assess times (in percent per year) of potential motion of seabed sediment along the route and thus, to qualify the potential mobility of the seabed along the offshore route.

The year 2012 has been chosen as representative of the site wave climate and allows us to compare the results with published work.

3.3.2.1. Critical shear stress

To take into account the variability of sand granulometry along the route, three grain sizes are considered. The following tables give, for each of the grain size, the critical bed shear stress.

Table 10 – Critical bed shear stress

Mean grain diameter (D50)	Critical bed shear stress (TAU_CR)
0.5 mm	0.25 N/m^2
0.25 mm	0.18 N/m^2
0.1 mm	0.16 N/m^2

3.3.2.2. Bed shear stress due to currents (TAU_C)

Calculations of time series of bed shear stress due to currents (TAU_C) over 2012, at the 11 offshore locations, are carried out from the simulation of hydrodynamics due to tide and wind (via numerical modeling presented in [1]).

Illustration of resulting field of bed shear stress due to tide and wind is given in Figure 58.

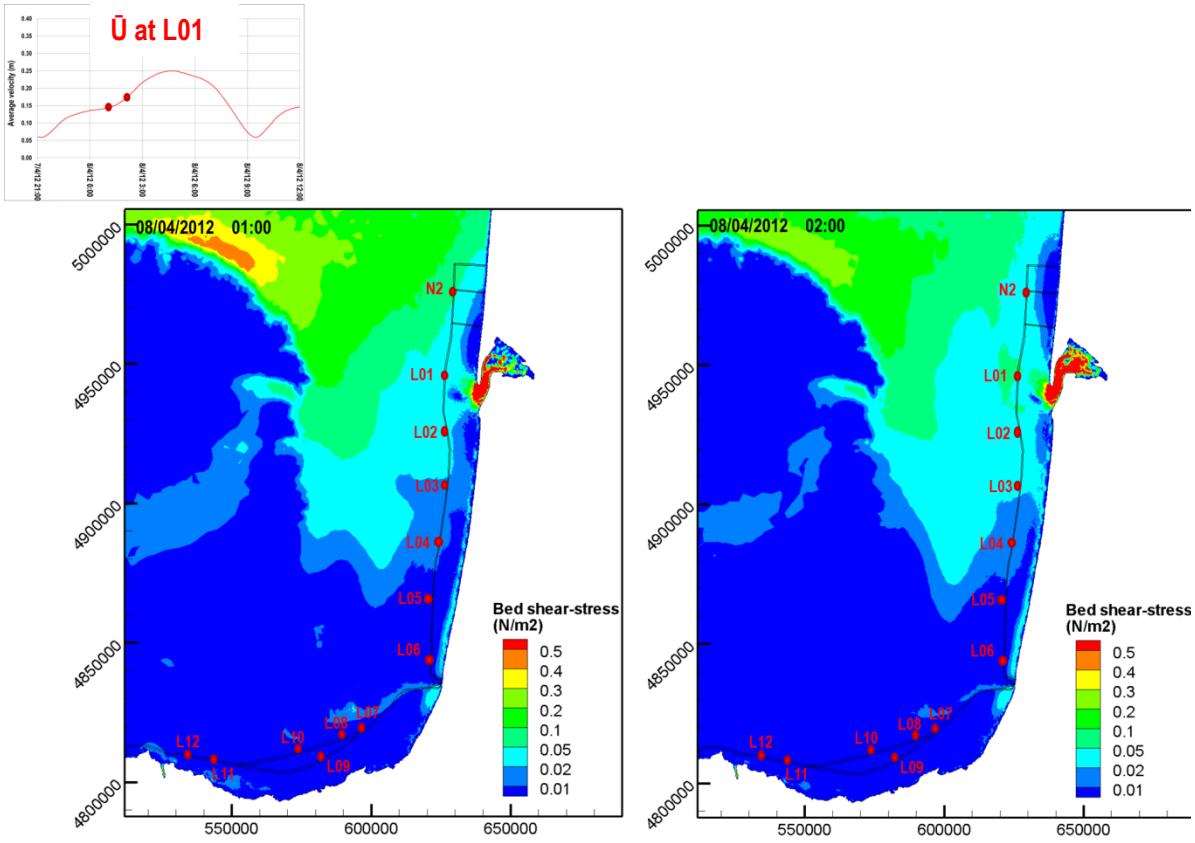

Figure 58. Instantaneous bed shear stress TAU_C at 8/4/2012 1:00 and 8/04/2012 2:00 mapped over the Biscay bay, and position of locations where time series of TAU_C are calculated over 2012

In Appendix B are presented maps of instantaneous TAU_C every hour from 7/04/2012 21:00 to 8/04/2012 8:00 (during a spring tide for which tidal currents are maximum)

According to these maps, even under maximum tidal currents, TAU_C remains small along the offshore route, not exceeding 0.1 N/m^2 in its northern part, and less than 0.01 N/m^2 in its southern part. It is not strong enough to exceed the critical bed shear stress (TAU_CR).

These results confirm that currents only do not succeed in mobilizing seabed sediments.

3.3.2.3. Bed shear stress due to wind, current and wave action (TAU_C+W and TAU_MAX)

Bed shear stress exerted on seabed is a combination of current and wave actions. Waves generate oscillatory bed shear stress; the bed shear stress due to the combination of currents and waves is considered through TAU_C+W and TAU_MAX as illustrated in the following figure.

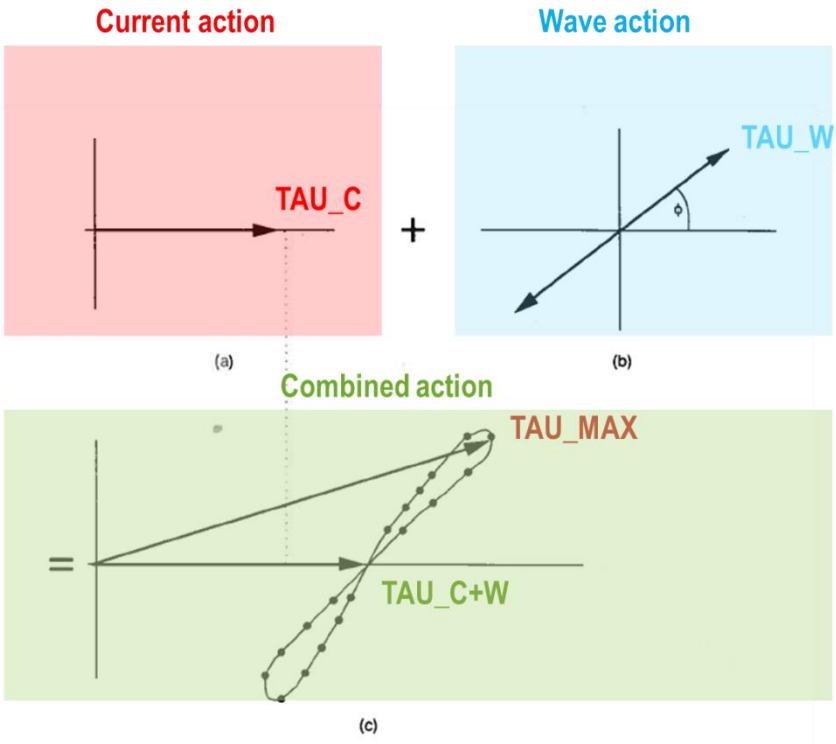

Figure 16. Schematic diagram of non-linear interaction of wave and current bed shear-stresses (reprinted from Soulsby et al. (1993), Coastal Engineering, 21, 41–69, by permission of Elsevier Science Publishers, BV)

Figure 59. Interpretation of TAU_MAX et TAU_C+W , from [18]

Total bed-shear stresses TAU_C+W and TAU_MAX are calculated as follows :

$TAU\_C+W = TAU\_C \times [1+1.2 \times (TAU\_W/(TAU\_C+TAU\_W)^{3.2}]$

$TAU\_MAX = [(TAU\_C+W + TAU\_W \times \cos\phi)^2 + (TAU\_W \times \sin\phi)^2]^{1/2}$

3.3.3. Assessment of potential seabed mobility along the offshore route

3.3.3.1. Comparison of bed shear stress with threshold bed shear stress

At each offshore location, the following parameters were plotted on a graph (Figure 60 for location N2, in APPENDIX C for other locations):

- Time series of TAU_C over 2012 (red line);
- Time series of TAU_C+W over 2012 (green line);
- Time series of TAU_MAX over 2012 (dashed dark red line);
- TAU_CR (D_{50} = 0.5 mm) (orange line) ;
- TAU_CR (D_{50} = 0.25 mm) (light orange line);
- TAU_CR (D_{50} = 0.1 mm) (yellow line).

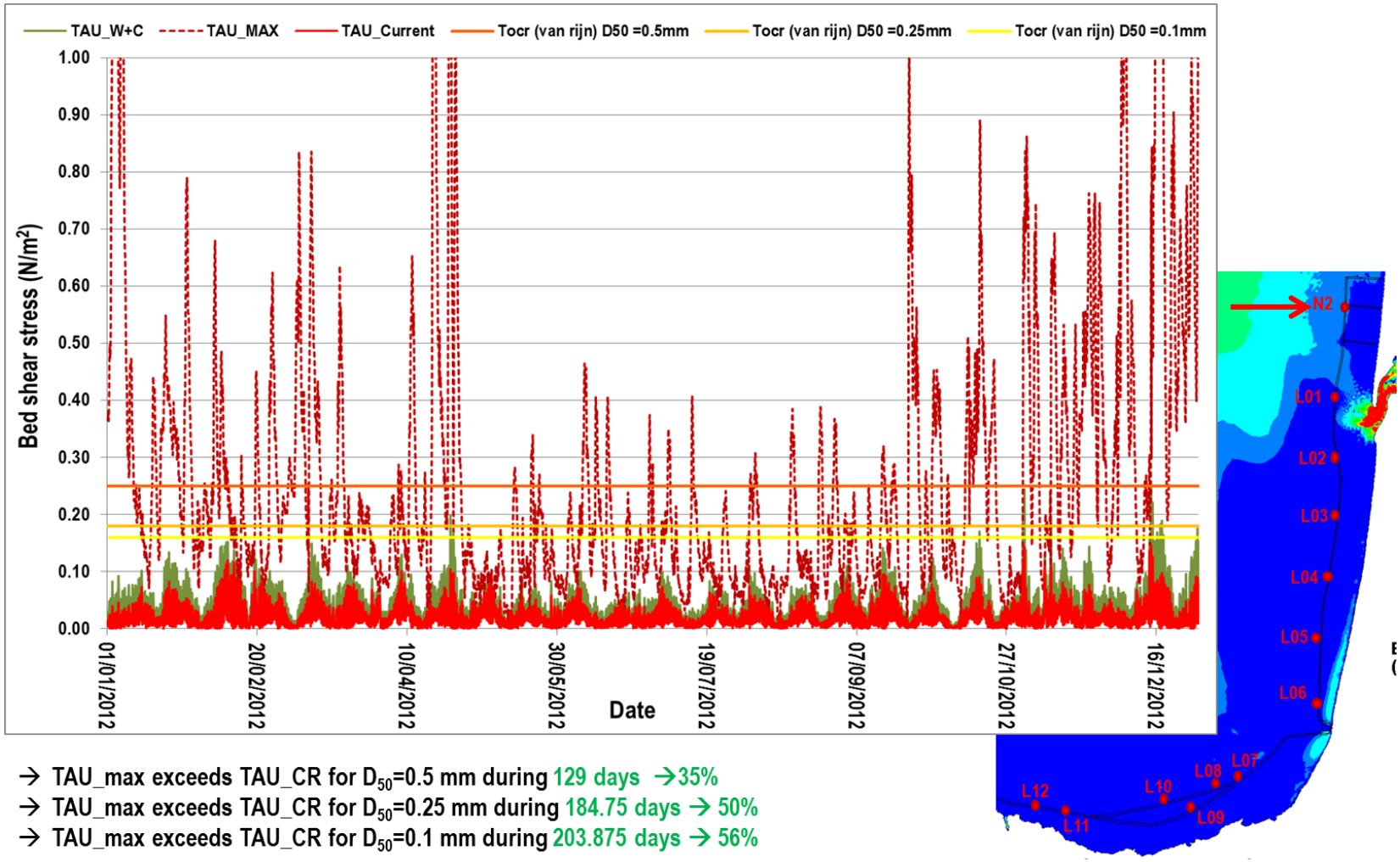

***Figure 60.** Plotted bed shear-stresses at N2 over 2012, to be compared to TAU_CR for grains of D_{50} = 0.5mm, of D_{50} = 0.25mm and of D_{50} = 0.1mm*

Duration for which TAU_MAX > TAU_CR is calculated over the year and provides the duration (in percent per year) of potential motion of seabed sediment along the route.

Table 11 – Yearly percentage of time where critical bed shear stress is exceeded for different assumptions of mean grain diameter – Main route

Location	D50 = 0.5 mm	D50 = 0.25 mm	D50 = 0.10 mm
N02	35 %	50 %	56 %
L01	18 %	28 %	32 %
L02	13 %	23 %	26.5 %
L03	20 %	30 %	34 %
L04	18 %	27.5 %	31.5 %
L05	17 %	26.5 %	30.5 %
L06	20 %	30 %	34 %
L09	0 %	0.1 %	0.65 %
L11	1.4 %	2.6 %	3.3 %

3.3.3.2. Conclusion in terms of potential seabed mobility along the offshore route

Graphs obviously show that potential of motion of seabed sediment is greater in Northern part of the route in particular at N02 (Figure 60) where 0.35 mm median diameter sediment can be moved 35% of the year and 0.1 mm median diameter sediment can be moved half the year.

Locations L03 to L06 experience quite similar potential of motion of seabed sediment: 0.35 mm mean diameter sediment can be moved about 20% of the year and 0.1 mm mean diameter sediment can be moved 30% to 35% of the year.

In the Southern part of the route, the potential is very weak, due to small current and wave conditions: at L09, 0.1mm median diameter seabed sediment can be moved less than 3 days.

These assessments are in concordance with calculation carried out by Mazières in 2014 and consistent with the observations of bed forms along sections 1 to 3.

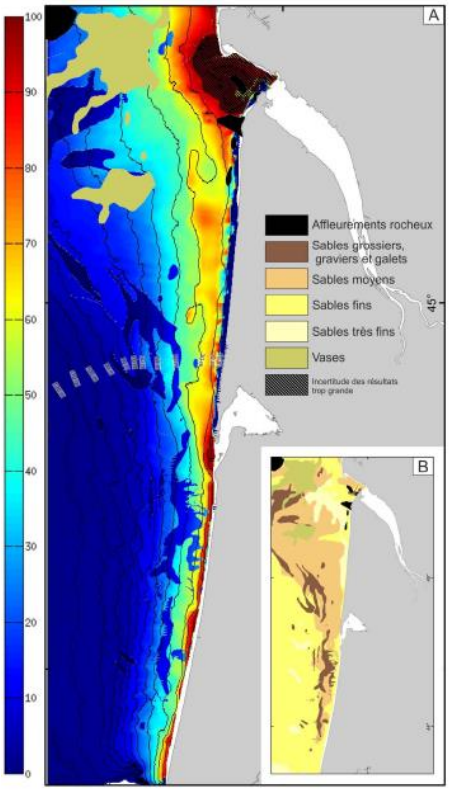

***Figure 61.* Yearly percentage of sediment mobility according to Mazières 2014**

3.4. ASSESSMENT OF INDUCED POTENTIAL BED LEVEL CHANGES ALONG THE OFFSHORE ROUTE BASED ON ANALYSIS OF SEDIMENTARY BEDFORMS

3.4.1. Major assumptions governing the assessment of the potential bed level changes

Based on the analysis of MMT geophysical and geotechnical surveys combined with calculation of bed shear stress due to wind, current and wave actions over a representative year**, the previous results conclude on potential of sediment mobility along the main route**.

In order to determine the extent of bed level change, an assessment of the sedimentary bedforms found in the cable route corridor has been carried out.

Specifically, the assessment has calculated the height of the features, on the assumption that the maximum bed level change equates to the difference between the crest and the trough of the features.

A more accurate and quantitative assessment of seabed level change is only possible *via* regular bathymetric monitoring of the areas characterized by potential mobility to record the short, mid and long term vertical seabed evolutions. This bathymetric monitoring could be completed with a physical model, or a complex CFD modelling calibrated on bathymetric measurements, but both of which are outside the scope of this study.

3.4.2. Analysis of the sand feature migration process - based on academic research works

3.4.2.1. Review of academic works covering section 2 of the offshore route

Concerning the seabed morphodynamics of section 2 (from KP 54.24 to 143.3) of the main cable route, many academic studies were carried out to investigate its typical sedimentary features (isolated sand dunes and sandy ribbons). These works are used hereafter to deepen the understanding of the morphodynamic processes.

From the 80^{ies}, seabed has been surveyed in front of “La Salie”, a studied area located on the inner Aquitaine shelf by water depths from 25 m to 60 m (see Figure 62). In its PhD thesis [19], A. Mazière makes reference to the research works led by Berné et al. (1986), Turcq et al. (1986), Cirac et al. (1997) summarized in Cirac et al. (1999).

Based on the following scientific missions FASEC (1984), GEODEP 3 (1989) , ITSAS 1 (1998), ECORS (2007), SEDYMAQ2 (2010), SEDIMAQ3 (2012) and PROTEUS DUNE (2013), a characterization of the sedimentary features characteristic of section 2 (isolated sand dunes and patchy sandy ribbons overlaying sand and gravel seabed) was done in terms of seabed form, sediment facies, predominant hydrodynamic forcing, induced morphodynamics and thickness of movable seabed effectively reworked under hydrodynamic forcing.

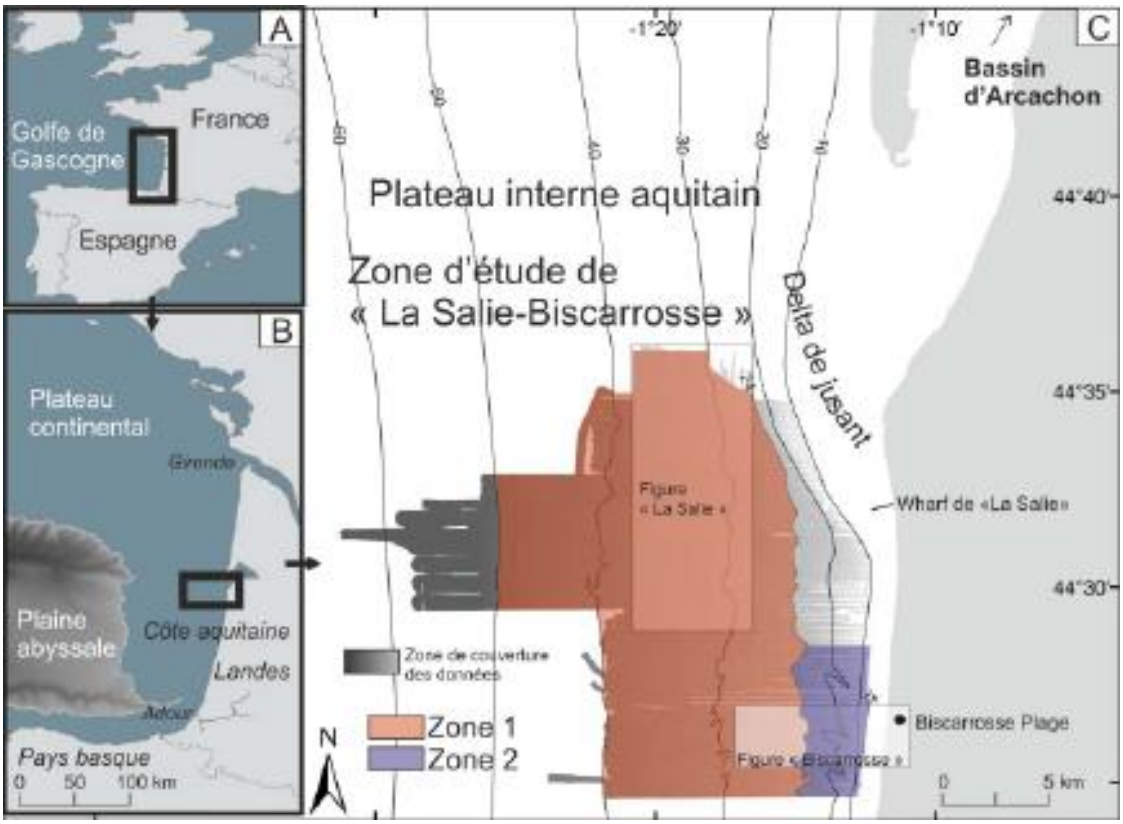

Figure 62. (A), (B) and (C) : Location of the study area of « La Salie-Biscarrosse », on the South Aquitaine inner shelf, and the secondary zone « La Salie » (zone 1) and « Biscarrosse » (zone 2) , from [19]

In 2000, Cirac [21] already confirmed that the predominant forcing within the area are waves and he identified the thin veneer (about 1–2 m) of sandy sediments overlying coarse-grained deposits. He described the surficial sand sheet as shaped into various bed forms corresponding to the contrasted physical processes operating at different water depths and time-scales. These identified

bed forms are: a) sand patches separated by depressions or 'furrows', b) large transverse dunes and c) large wave ripples.

3.4.2.2. Record of seabed mobility in section 2 by field surveys

Among the major results achieved by these academic studies, is the highlighting of the migration of sand dune-like features. Indeed, comparison of bathymetric data recorded in 2010 and 2012 showed submarine dune-like features migrating shoreward with **displacements ranging from 14 to 66 m over these two years** (see Figure 63).

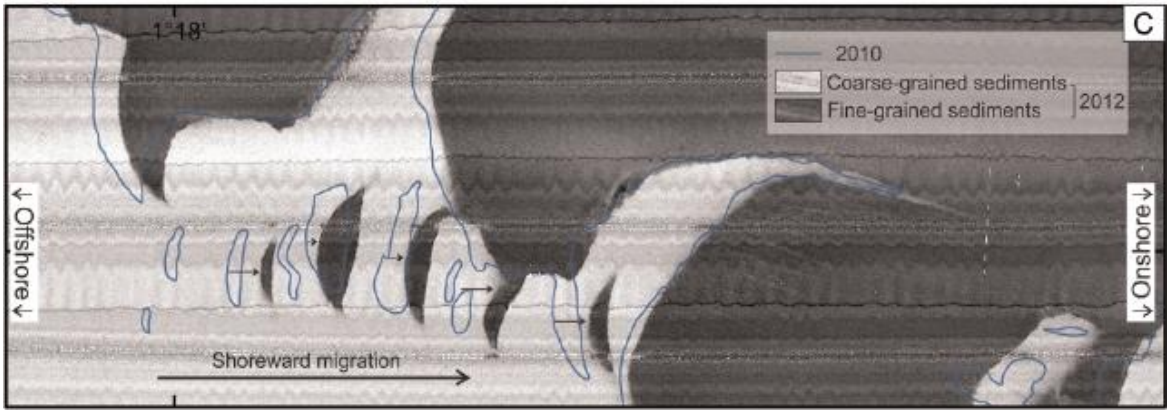

Figure 63.Highlighting of shoreward dune migration, from [19]

3.4.2.3. Sediment transport process involved in sand dunes migration

Moreover, in [21], Cirac informs on the processes that enable this bedform migration.

He shows that dune migration is possible thanks to the mobilization of the upper sediment layer during major storms. This means that bed forms do not translate as rigid bodies but progressively, through complex dynamics in the exposed upper layer (reworked layer). Eventually, the final shape remains globally the same, but translated.

An assessment of the thickness of reworked seabed layer is done in [21]. It depends on the water depth as plotted onFigure 63**.** As seabed features within section 2 of the main route are located at water depth from 40m to 50 m, it can be assessed that the effective thickness of reworked seabed layer is less than 60 cm along section 2 of the main offshore route.

Considering these academic results, we can assess that, thanks to the reworking of the 0.60 m-thick upper sediment layer of the sandy ribbons and isolated sand dunes characteristic of main route section 2, those seabed features migrate shoreward and globally keep their dimensions (height and wave length).

Therefore this migration of seabed features can bury or expose the cable over a vertical extent equivalent to their height.

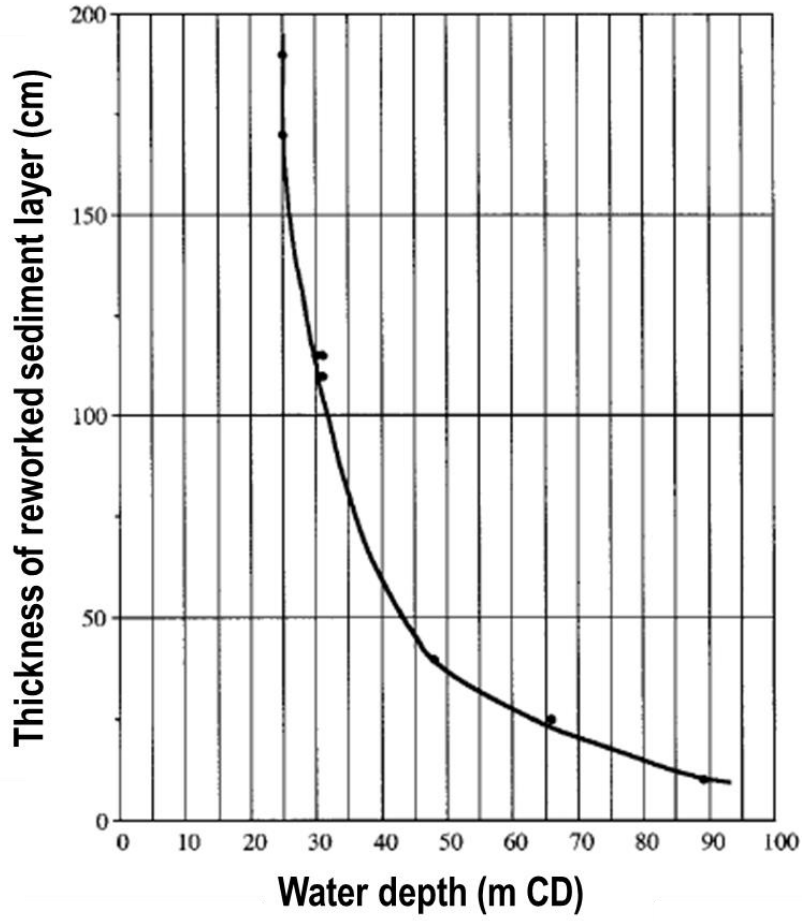

Figure 64. Assessment of the thickness of reworked sediment layer responsible for bedform migration, depending on water depth, from [21]

3.4.3. Summarized table of seabed mobility and potential bed level change along the main cable route

Results of bed shear stress calculations and analysis of academic works are put into perspective with the characteristics of each of the twelve subsections identified along the main route (MR), mainly the mean diameter, the existence of bed forms and the thickness of erodible layer as shown in Table 12.

From these analyses, sections 2 and 3 of the main route are most at risk from bed level change:

- about +/-2 m in section 2 due to sand dune migration at a rate of 7 to 33 m per year,
- about +/- 8 m to 10 m at the canyon head cyclically and mostly due to migration of sand bars onshore/offshore with respect to wave conditions (cf section 2.3).

Within these sections at high risk of bed level change, the rate of sand bar migration is sufficiently rapid for the features to move across the cable route during the proposed lifetime of the asset, and to bury or expose the cable of the equivalent of their height.

Table 12 – Subsections mobility along the Main Route

Section	Subsection	Metocean analysis point	Bed forms	Thickness of erodible layer	D50 (mm) of surficial layer	Seabed mobility (% of the year)	Seabed level change
MR 1	1	N02	Sand ripples Δr < 7 cm	Larger than 5 m	Sand, 0.29 – 0.40	From 35% to 50%	Maximum bed level change is likely to be of the order of 10 cm
	2	N02				About 35%	
	3	L01				About 18%	
MR 2	4	L02, L03	Sandy ribbons and isolated sand dune like bed forms with height of 2 meters	Larger than 5 m	Sand + Gravel, 0.29 – 1.2	From 13% to 30%	Maximum bed level change is likely to be around 2m, which is the height of the largest seabed features. These features migrate at a rate of 7 to 33m per year
	5	L04, L05, L06				< 20%	
MR 3	6		Sand ripples Δr < 5 cm	2.5 to 5 m	Sand, 0.18 – 0.32	Important rate of mobility	Formation and migration of sand ripples/ height of sand ripples < 5 cm outside the canyon head and seabed level changes of +/- 8 m to 10 m at canyon head
MR 4	7		No bed forms identified	From1 to 2 m, with local outcrops	Sand, silt and clay		Negligible bed level change
	8	L07					
	9	L08, L09, L10				<0.65%	
	10					No seabed mobility	
	11	L11			Sand, 0.09 to 0.9	Weak seabed mobility	Negligible bed level change
	12	L12				Weak seabed mobility	

4. SEABED MOBILITY AND BED LEVEL CHANGE ALONG THE HDD CANYON CROSSING ROUTE (HDCC)

4.1. INTRODUCTION

The HDD Canyon Crossing Route (noted HDCC in geophysical report [10]) is an alternative route crossing the canyon further offshore than the Main Route (MR).

In order to assess the sea bed stability and the maximum extent of the potential vertical variations along this alternative canyon crossing route, the following specific methodology has been implemented:

- Characterization of seabed nature and in situ movable sediment thickness based on the geophysical and geotechnical surveys;
- Assessment of potential mobility of surficial sediment based on calculation of bed shear stress due to wind, current and wave action provided by the met ocean study at S8 and S9 over 2012, following the same methodology as in 3.3.3
- Research of evidence for seabed mobility based on the geophysical and geotechnical surveys;
- Conclusion on the potential vertical variation of the movable seabed layer based on local calculated hydrodynamics and presence of in situ seabed forms.

4.2. LOCATION OF THE HDD CANYON CROSSING ROUTE

The HDD Canyon Crossing Route (noted HDCC in geophysical report [10]) is 8.595 km long. This alternative route crosses the canyon further offshore than the Main Route (MR) and is connected to the MR at KP 140.461 and KP 161.922. This location is illustrated on Figure 65.

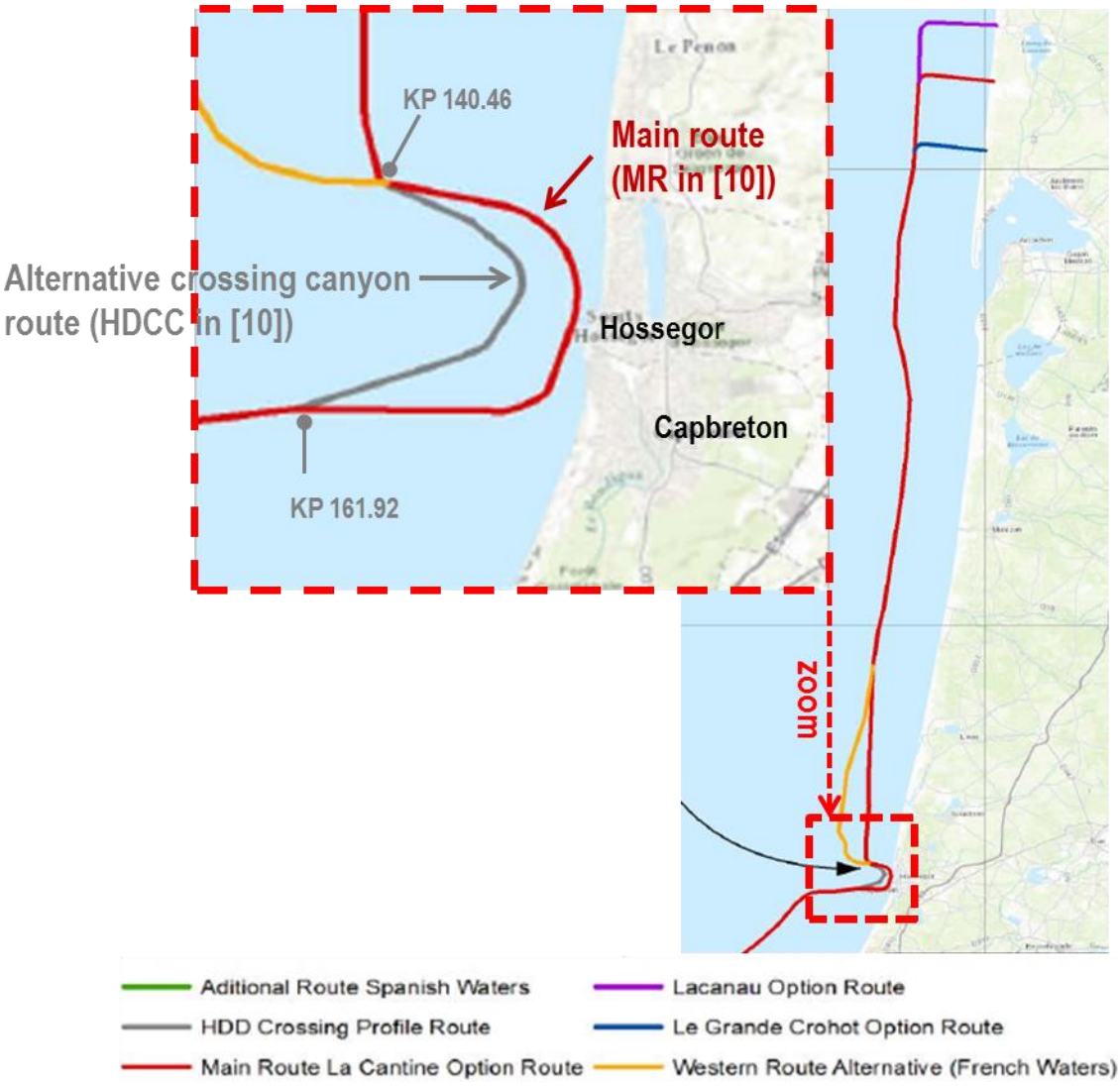

Figure 65.Location of the HDD canyon crossing route

4.3. GEOPHYSICAL AND BATHYMETRIC SURVEYS ALONG THE HDD CANYON CROSSING ROUTE

Due to the steep slopes of the canyon and abundance of fishing activity within the area, geophysical survey was carried out with hull mounted MBES and surface towed Sparker. It has to be noted that the MBES bathymetry resolution was relaxed to 1 m x 1m.

According to the bathymetry surveyed along the HDCC (presented on Figure 66), water depths (given in LAT) vary from 16.5 m (South edge of the canyon , KP 5.315) to 109.5 m. (canyon floor KP 4.396).

From KP 0.000 (northern extremity) to KP 3.432, water depth decreases from 37.7 m to 22.5 m.

Then it slightly increases to reach 25.0 m at KP 3.710 and 42.5 m at KP 4.100, the NE edge of the canyon.

From at KP 4.100, seabed steeply drops to reach the maximum depth of 109.5 m at KP 4.396.

From KP 4.420 to KP 4.480 seabed **rises very steeply** from -107.5 m CD to - 22.5 m CD.

The maximum slope of 59.1 deg is reached during this seabed rising: it is steeper than the maximum slope reached on the main route.

From the SW edge of the canyon at KP 4.815 , seabed rises with a reduced gradient to the elevation of -16.5 m CD at KP 5.315 then begins to gently drops again, reaching a depth of 40.2 m at KP 8.599 (southern extremity).

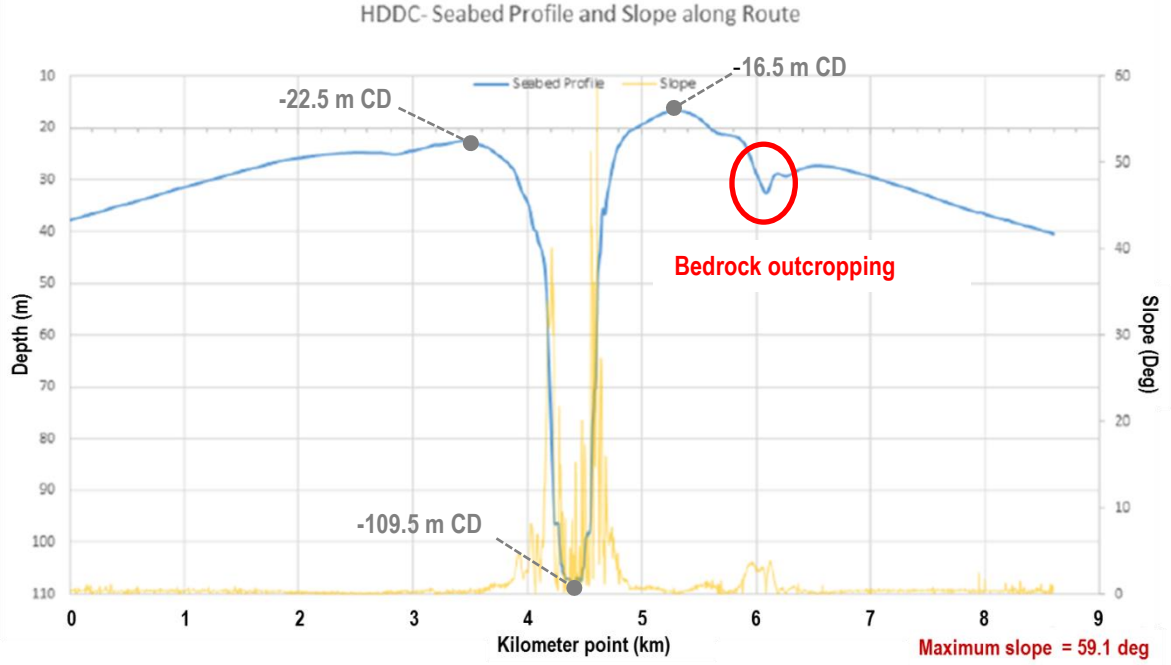

Figure 66. Surveyed bathymetry along the HDCC, from [10]

As showed on Figure 67 - A, between KP 5.5 and KP 6.4, a second canyon system encroaches on the survey corridor. Seabed drops by lateral steep slopes to -129 m CD. The route can avoid this second canyon if designed in the southern part of the surveyed corridor between the two KP mentioned before, by water depths of 25 m.

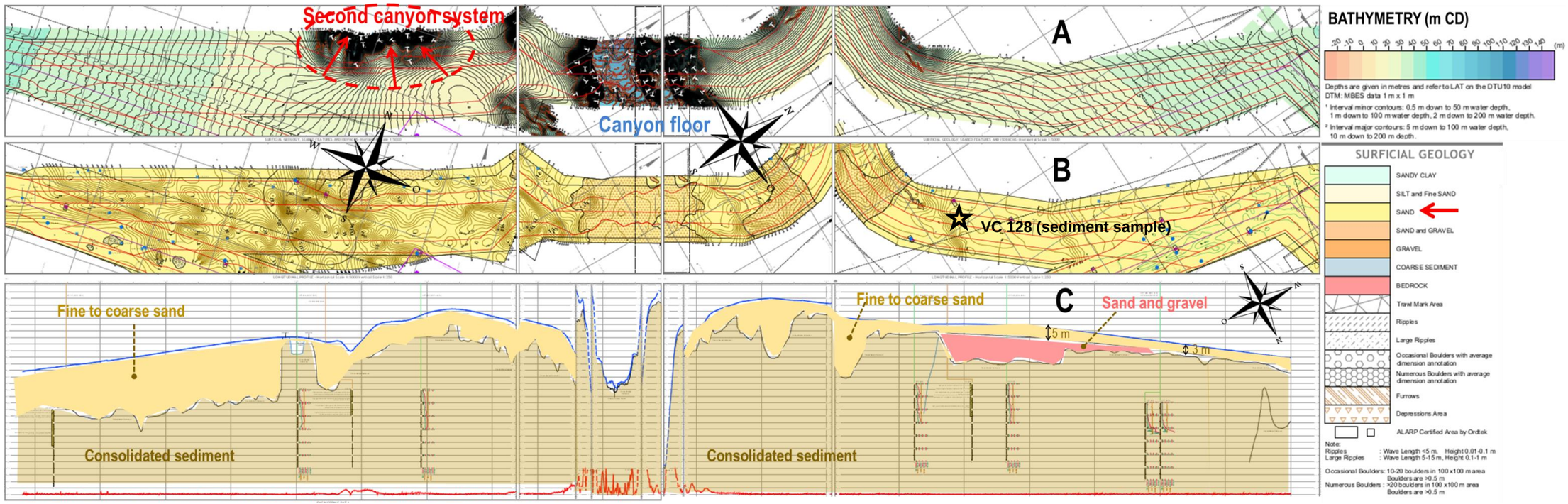

Figure 67. ***Bathymetric survey [A], nature of surficial sediment [B], thickness of movable sediment [C] along the HDCC corridor (from [10])***

4.4. NATURE OF THE SEABED

According to the survey results, the surficial geology is predominantly made of fine sand, as can be seen on Figure 67, B. Along the canyon floor, seabed is more likely to be gravelly sand to sandy gravel.

As shown on Figure 67, C and on Figure 68 , **thickness of sandy seabed over the Consolidated Seabed (CS) is generally greater than 3m**. **However from KP 6.383 to KP 6.606, the CS outcrops locally.**

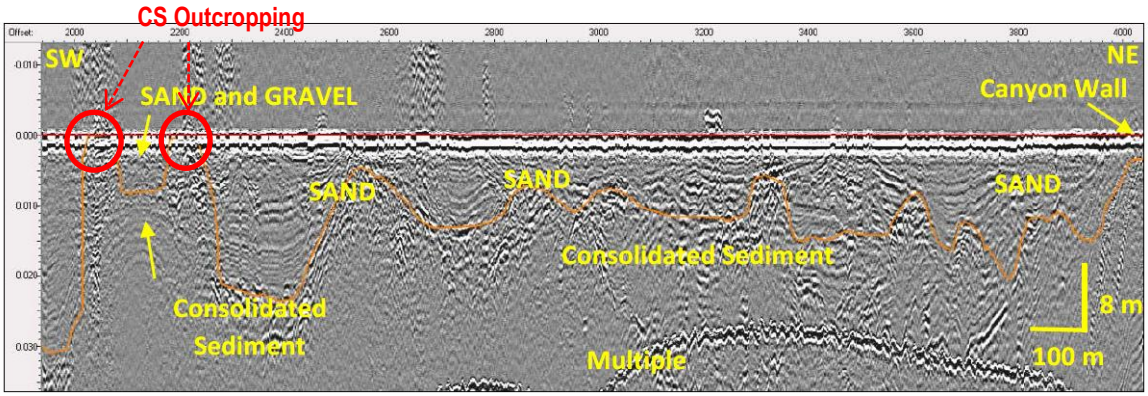

Figure 68. Sparker data image of seabed to SW of canyon system between KP 4.600 and KP 6.600, from [10]

4.5. GRAIN SIZE CHARACTERISTICS OF SEDIMENTS ALONG THE HDCC

Particle size distribution was carried out on a sediment sample collected at VC 128 (see Figure 67, B for its location).

Sediment at the upper layer (from 0.56 BSF to 0.94 m BSF) is mainly made of sand (99%) with 1% of silt. The median particle diameter is **D_{50} = 0.18 mm** (i.e. fine sand according to the Wentworth sediment classification).

The deeper layer (from 1.04m BSF to 2.0 m BSF) is mainly made of sand as well (99%), with 1% of silt too. The median particle diameter is D_{50} = 0.3 mm (i.e medium sand according to the Wentworth sediment classification).

4.6. LOCAL HYDRODYNAMICS

Analysis of met ocean conditions along the HDCC route was carried in [1] at points S08 and S09 (see Figure 69) in terms of currents due to tide and wind forcing, as well as in terms of wave conditions. Here are reminded the main results that are used further on to calculate the corresponding bed shear stress applied on seabed over a representative year (2012).

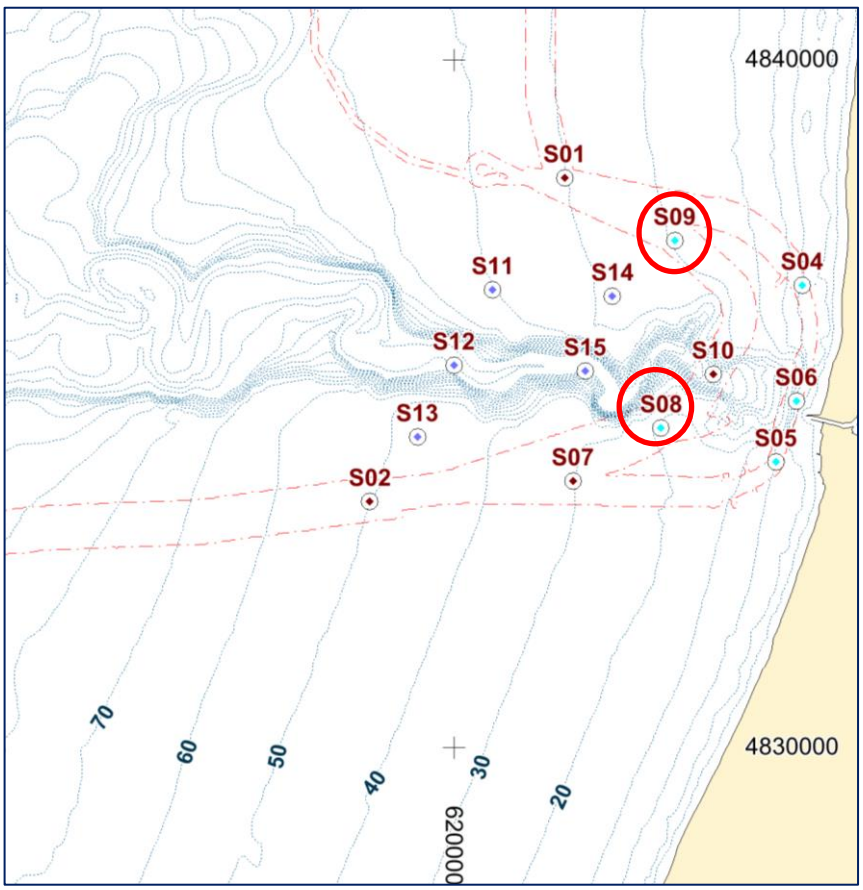

Figure 69. Locations of points where currents and wave climate were analyzed around the canyon head, identification of S08 and S09, from [1]

4.6.1. Tidal currents

According to the met ocean study [1], around the canyon, the total current directions are directed alternately towards North and South for the 5 points (point S04, S05, S06, S08 and S09). The weakest total current appears at the head of the canyon (point S06) where the intensity is lower than 0.3 m/s near surface and 0.25 m/s above the sea bottom. The flow coming from the west is deviated by the canyon features towards the south; thus **the total current is stronger to the south of the canyon (point S08) where it can be higher than 0.35 m/s**.

4.6.2. Usual wave conditions

According to the met ocean study, the canyon has an important effect on wave propagation through the phenomena of reflection and refraction. Waves approaching the canyon obliquely (mainly from the north-west) will tend to be reflected on the northern side of the canyon because the depth stops decreasing and suddenly increases again. The longer the period is, the more important the effect on wave propagation is. This creates areas of over-agitation north of the canyon and areas of under-agitation south of the canyon.

North of the canyon (point S09), the wave climate is mainly westerly from November to April. Then, the direction turns slightly and the waves come from the West-North-West sector.

South of the canyon (point S08), waves come clearly from 2 different directions: the West and the North-West (especially in summer).

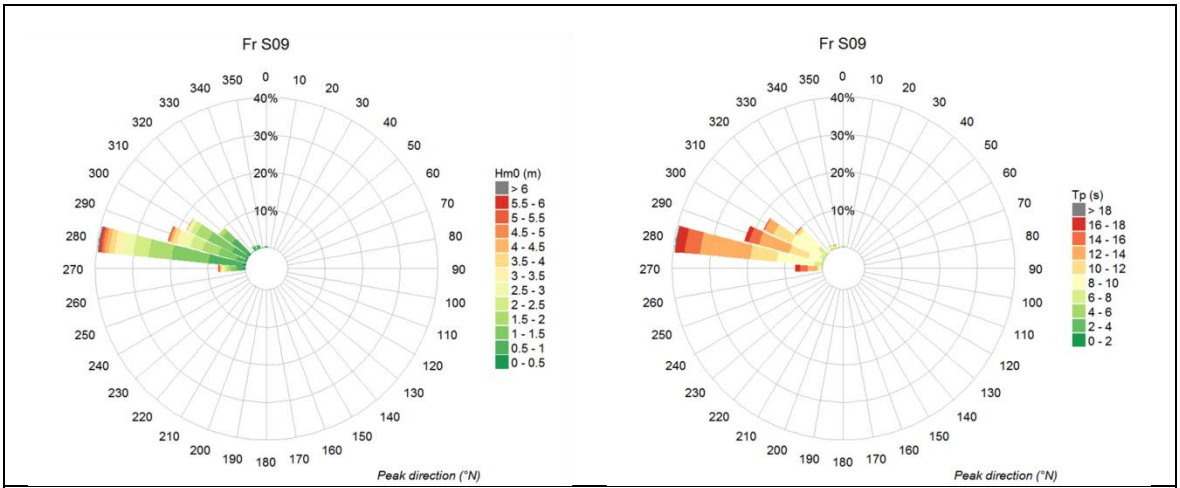

Figure 70. Annual wave rose – Point S09 (North of the Canyon) – HDCC route

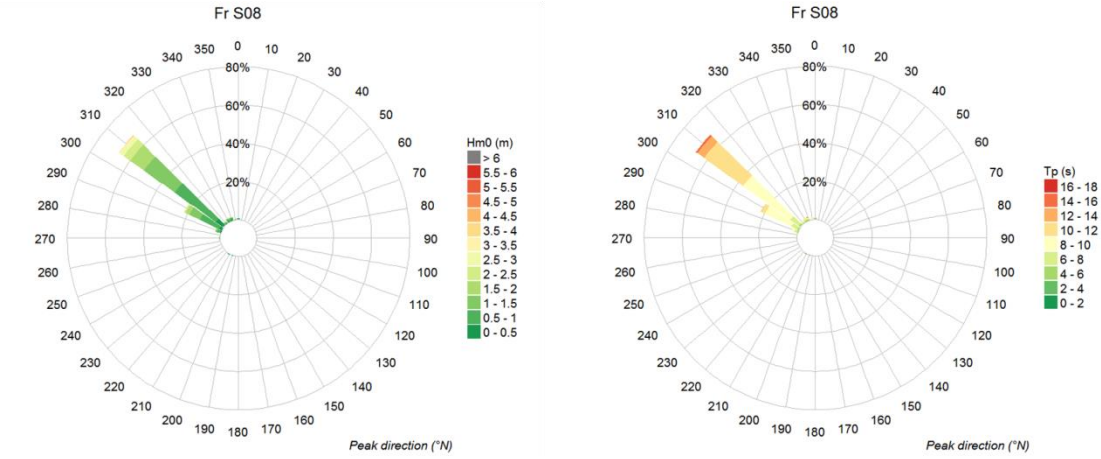

Figure 71. Annual wave rose – Point S08 (South of the canyon) – HDCC route

4.7. EMPIRICAL ASSESSMENT OF SEABED MOBILITY ALONG THE HDCC ROUTE

4.7.1. Calculation of bed shear stress along the HDDC route

To assess the potential mobility of the surficial sediment calculations of bed shear stresses on the canyon's sides:

- due to the action of tides and winds (TAU_C);
- due to the combined action of tides, winds and waves (TAU_C+W or TAU_MAX);

are carried out over the year 2012 at locations S08 and S09.

Comparison with critical bed shear stresses associated to 3 types of grain is made and allows to assess times (in percent per year) of potential motion of seabed sediment along the HDCC route.

The following table reminds, for each of the grain size, the critical bed shear stress.

Table 13 – Critical bed shear stress

Mean grain diameter (D50)	Critical bed shear stress (TAU_CR)
0.1 mm	0.16 N/m^2
0.25 mm	0.18 N/m^2
0.5 mm	0.25 N/m^2

4.7.2. Assessment of potential seabed mobility along the HDCC route

At S08 and S09, the following parameters were plotted on a graph (Figure 95):

- Time series of TAU_C over 2012 (red line);
- Time series of TAU_C+W over 2012 (green line);
- Time series of TAU_MAX over 2012 (dashed dark red line);
- TAU_CR (D_{50} = 0.5 mm) (orange line) ;
- TAU_CR (D_{50} = 0.25 mm) (light orange line);
- TAU_CR (D50 = 0.1mm) (yellow line)

Table 14 – Yearly percentage of time where critical bed shear stress is exceeded for different assumptions of mean grain diameter for sediment along the HDCC route

Location	D50 = 0.1 mm	D50 = 0.25mm	D50 = 0.5 mm
S09	59%	54%	40%
S08	83.3%	80%	69%

Along the HDCC route (apart from the canyon floor), wave action (TAU_MAX) is strong: it can put surficial fine to medium sand in suspension and rework the surficial layer of seabed from 40% to 59% of the year at the northern side of the canyon (S09) (see Figure 72) and even more at the southern side of the canyon (S08) from 69 to 83% (see Figure 73 where the depth is shallower

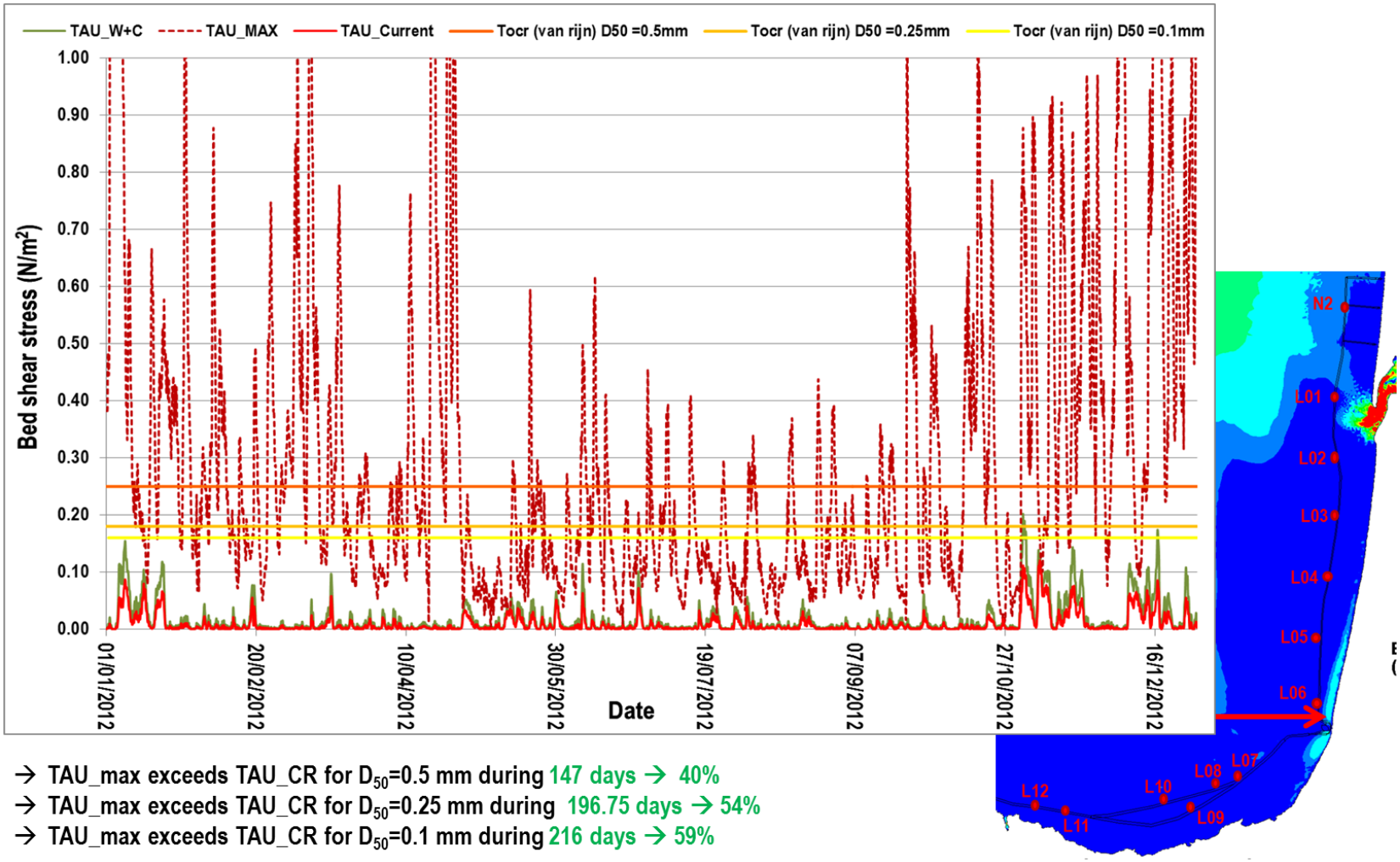

***Figure 72.** Plotted bed shear-stresses at S09 over 2012, to be compared to TAU_CR for grains of D_{50} = 0.1mm, D_{50} = 0.25 mm, D_{50} = 0.5 mm*

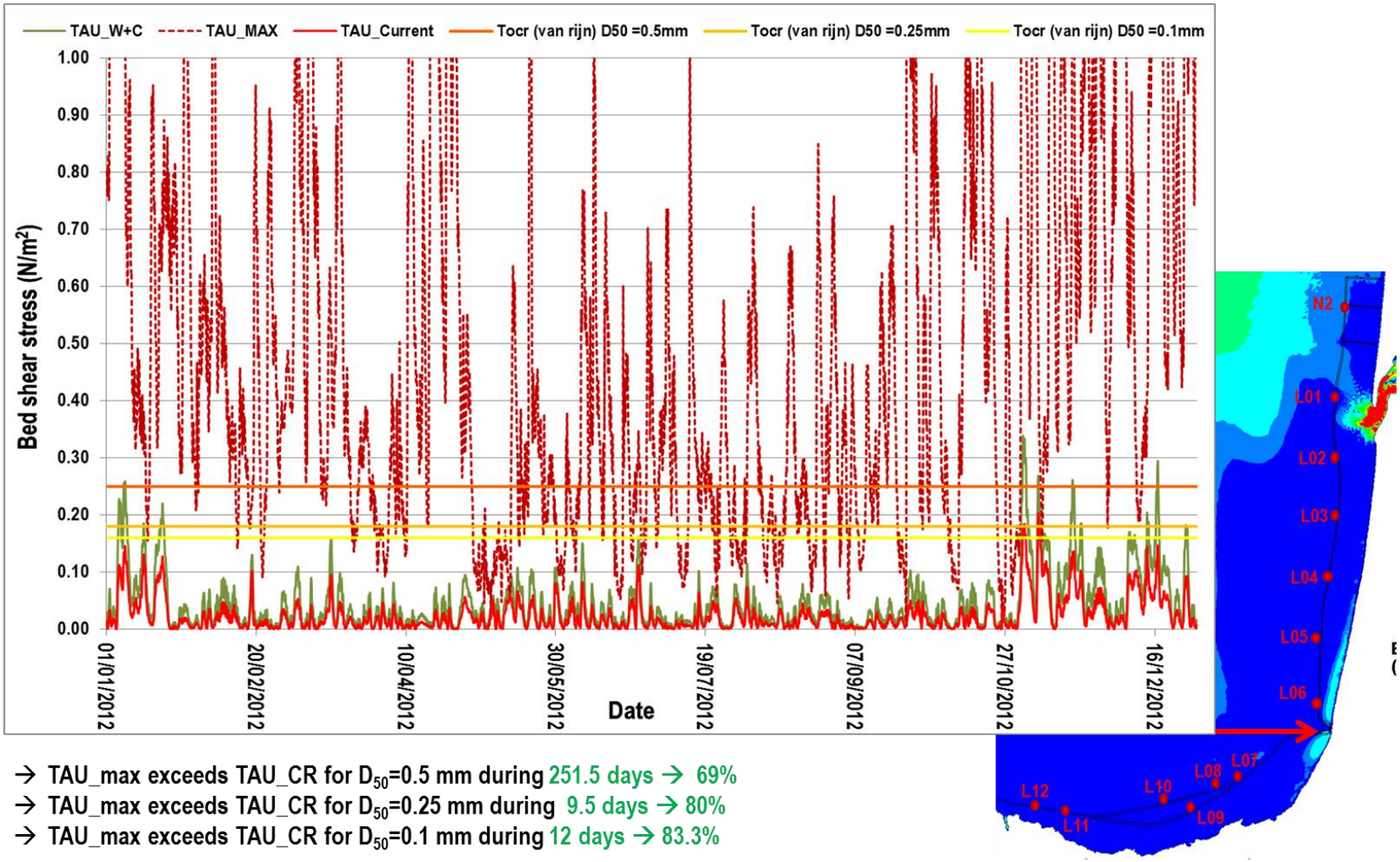

Figure 73. ***Plotted bed shear-stresses at S08 over 2012, to be compared to TAU_CR for grains of D_{50} = 0.1mm, D_{50} = 0.25 mm, D_{50} = 0.5 mm***

4.8. EVIDENCE OF EFFECTIVE SEABED MOBILITY ALONG THE HDCC ROUTE

According to pictures of the seabed presented in [10], no seabed feature is identified. However, between KP 4.013 and KP 4.656, sediment slumping/slides are evident on the canyon floor as shown on Figure 74.

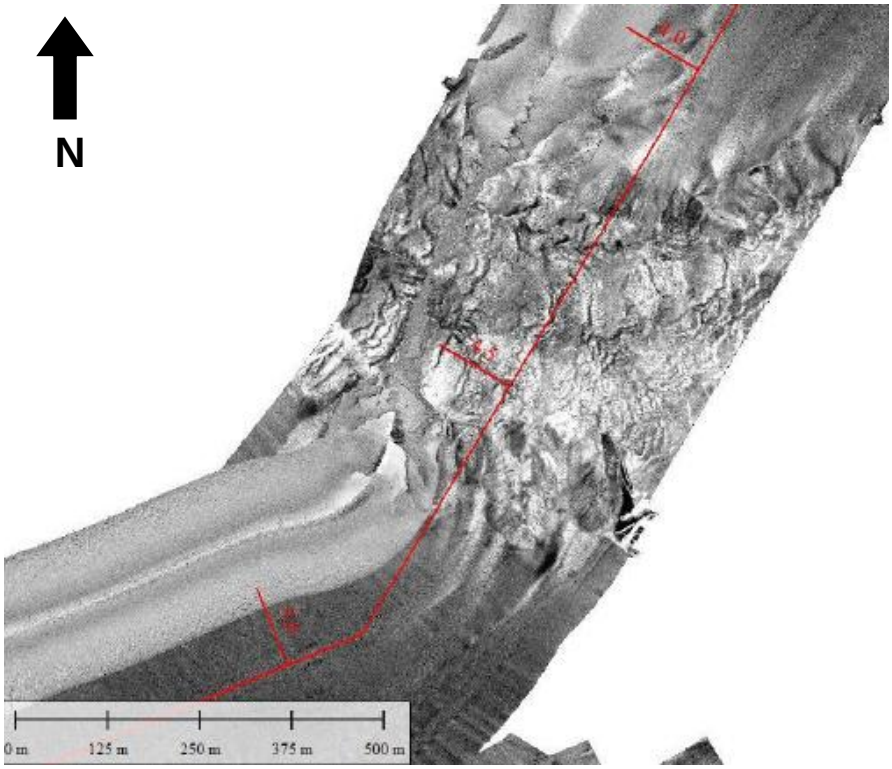

Figure 74. Image of MBES Backscatter from KP 3.75 to KP 5.25 - HDCC route, from [10]

This picture provides the evidence of seabed mobility that could possibly bury or excavate the cable. However, in absence of historical bathymetric survey along the corridor, it is not possible to assess the potential seabed level change due to these slumps.

4.9. SUMMARIZED TABLE OF SEABED MOBILITY AND BED LEVEL CHANGE ALONG THE HDCC ROUTE

Previous results have to be put into perspective with the characteristics of the HDCC route mainly the mean diameter, the existence of bed forms and the thickness of erodible layer as shown in the following table.

Table 15 – Potential mobility along the HDCC route

Section	Metocean analysis point	Bed forms	Thickness of erodible layer	D50 (mm) at surficial layer	Seabed mobility (% of a year)	seabed level change
KP 0 to KP 3.432	**S09**	No evidence of bedforms	**Mostly greater than 3m**	Fine to medium sand, **D_{50} = 0.18 mm**	High potential of seabed mobility due to local wave climate on canyon sides , from 40 to 59%	No evidence of seabed level change. Lack of data to conclude
KP 3.432 to KP 5.315	**Canyon walls and canyon floor**	**Steep slopes** at canyon walls (reaching 59 deg) **Sediment slump/ slides**	**No sediment along canyon wall and where the CS outcrops**	Gravelly sand at canyon floor	No mobility due to hydraulic forcingon the canyon walls and canyon floor	Evidence of **slumping seabed** in vicinity of the canyon walls
KP 5.315 to KP 8.599	**S08**	No evidence of bedforms. Two local CS outcropping	**Mostly greater than 3 m** Except between KP 6.383 to KP 6.606 when CS outcrops	Fine to medium sand, **D_{50} = 0.18 mm**	High potential of seabed mobility due to local wave climate on canyon sides , from 69 to 83%.	No evidence of seabed level change. Lack of data to conclude.

The previous analyses do not allow us to conclude on the seabed level change along the HDCC route on each side of the canyon. Indeed, seabed material can be mobilised through hydraulic forcing but no evidence of such seabed mobility (such as bedforms) is observed. Differential bathymetric data are needed to provide quantitative information.

What is important to note is the slumping/slides, observed along the canyon walls, that have to be linked with the flushing of sediments observed at the canyon's head (see section 2.3.5.2), mechanisms typical of submarine canyons.

5. SEABED MOBILITY AND BED LEVEL CHANGE ALONG THE ALTERNATIVE SPANISH ROUTE (ARSW)

5.1. INTRODUCTION

The Additional Route in Spanish Waters (noted ARSW in geophysical report [10]) is a northern alternative to the Main Route in its Spanish part.

In order to assess the sea bed stability and the maximum extent of the potential vertical variations along this alternative Spanish route, the following specific methodology has been implemented:

- Characterization of seabed nature and in situ movable sediment thickness based on the geophysical and geotechnical surveys;
- Assessment of potential mobility of surficial sediment based on calculation of bed shear stress due to wind, current and wave action provided by the met ocean study at L08 and L10 over 2012, following the same methodology as in 3.3.3
- Research of evidence for seabed mobility based on the geophysical and geotechnical surveys;
- Conclusion on the potential vertical variation of the movable seabed layer based on local calculated hydrodynamics and presence of in situ seabed forms.

5.2. LOCATION OF THE ALTERNATIVE SPANISH ROUTE

The ARSW Route is 47.68 km long. This alternative route is connected to the main route at KP 190.603 and KP 240.940. This location is illustrated on Figure 75.

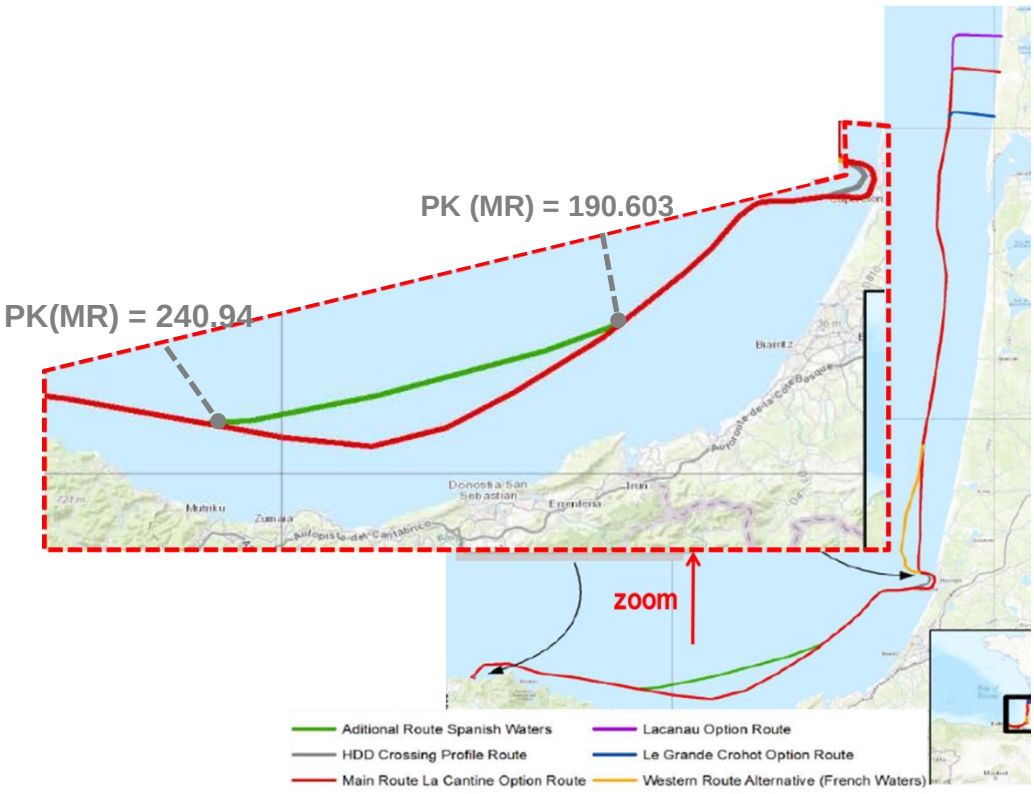

Figure 75. Location of the ARSW

5.3. GEOPHYSICAL AND BATHYMETRIC SURVEYS ALONG THE ARSW

The route was surveyed by the M/V Franklin, a fully equipped vessel for seabed survey in water depths between 10 to 2000 m...

According to the bathymetry surveyed along the alternative Spanish route (presented on Figure 76), the route starts by water depth of 124.6 m and goes deeper (134.3 m water depth at KP 7.240) **with undulations (high of features +/-2 m).**

Then it rises, first very gently then with increasing gradient (slope of 1 deg), to reach water depth of 125 m at KP 9.8 before dropping again to 133.2 m at KP 11.641.

From KP 13.326 to KP 14.975, seabed very gently rises again to an elevation of - 127.6 CD m and drops once more to - 133.6 m CD at KP 14.975.

From KP 14.975 the seabed gently rises to -127.5 m CD at KP 16.069 to drop once again to - 131.5 m CD at KP 17.000.

From KP 17.889 **seabed dips with undulations** to the elevation of - 134.2 m CD at KP 22.281 and reaches - 135.2 m CD at KP 27.542 showing **irregular undulating profile**.

From KP 27.542, seabed gently rises with very slight undulations to the elevation of - 104.2 m CD at KP 45.826 where it steeply rises (slope of 5.8 deg) to a **peak of bedrock reaching - 97.6 m CD at KP 46.040**.

Then it steeply dips to - 102 m CD at KP 46.335 to finally rise again to – 90 m CD at KP 47.690, where the alternative route joins the MR.

The maximum slope of 8.56 deg is reached at KP 25.5.

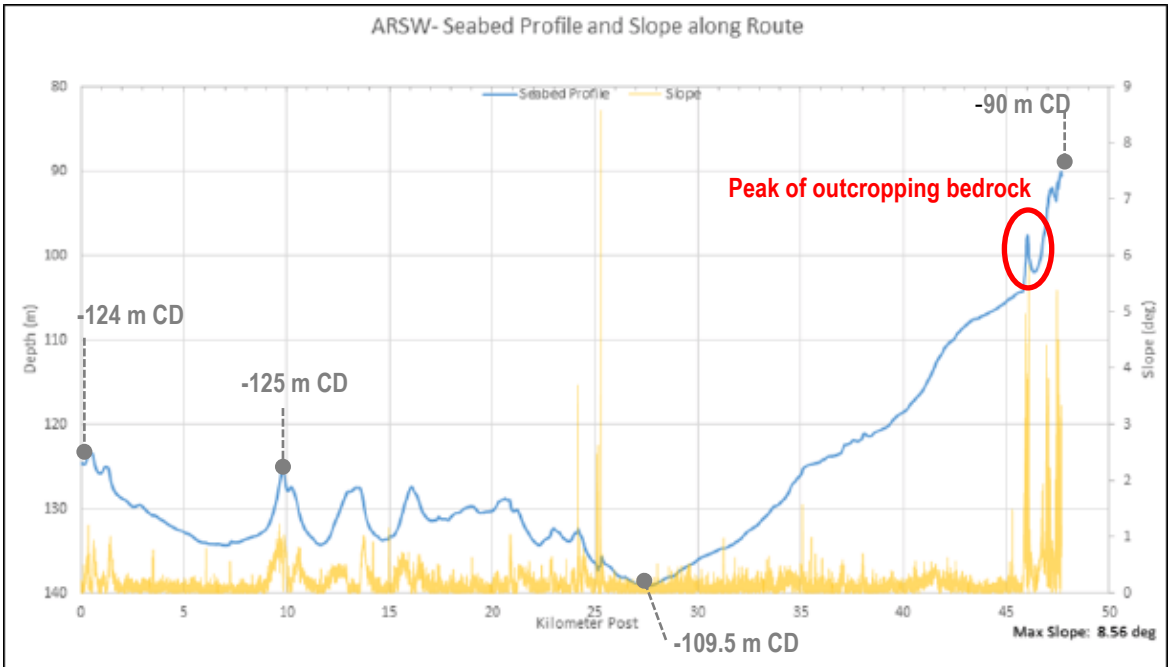

***Figure 76.* Surveyed bathymetry along the ARSW, from [10]**

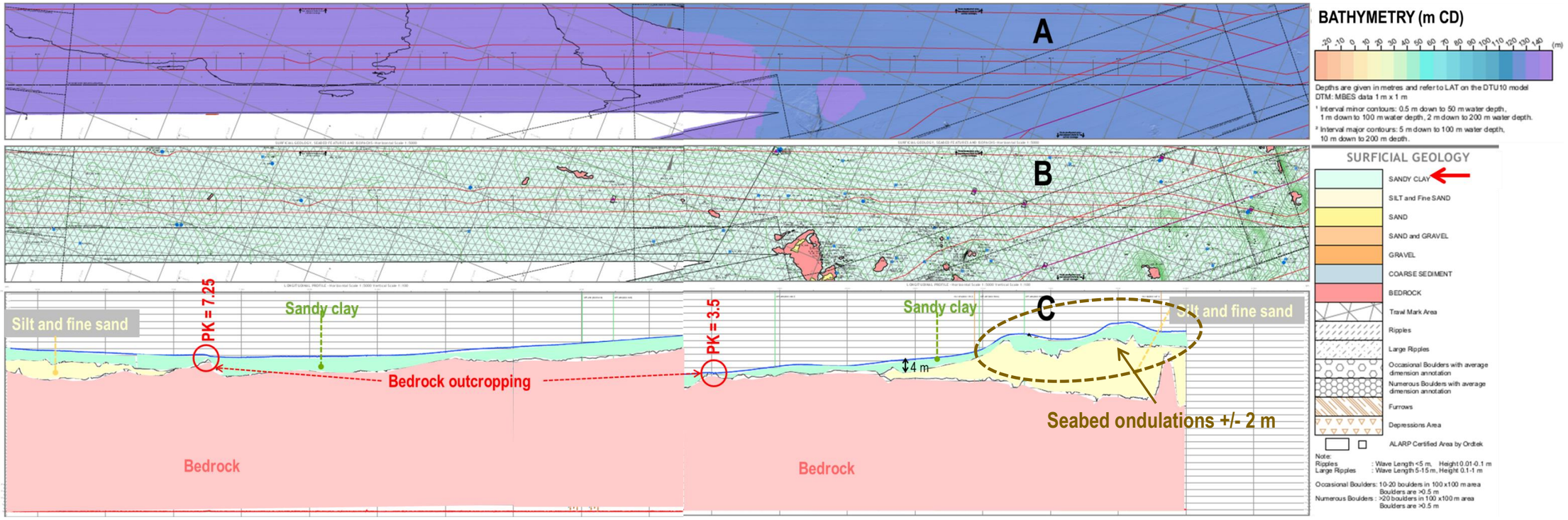

Figure 77. ***Bathymetric survey [A], nature of surficial sediment [B], thickness of movable sediment [C] along the ARSW corridor from PK 0 to PK 8.5 (from [10])***

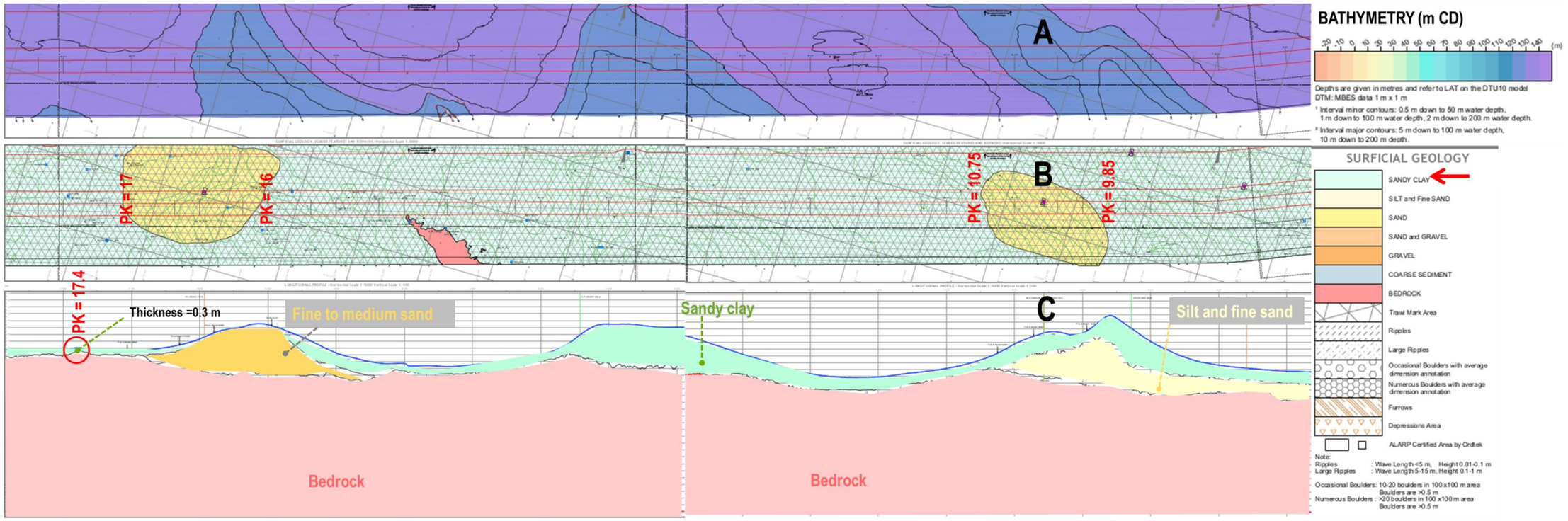

Figure 78. ***Bathymetric survey [A], nature of surficial sediment [B], thickness of movable sediment [C] along the ARSW corridor from PK 8.5 to PK 17.5 (from [10])***

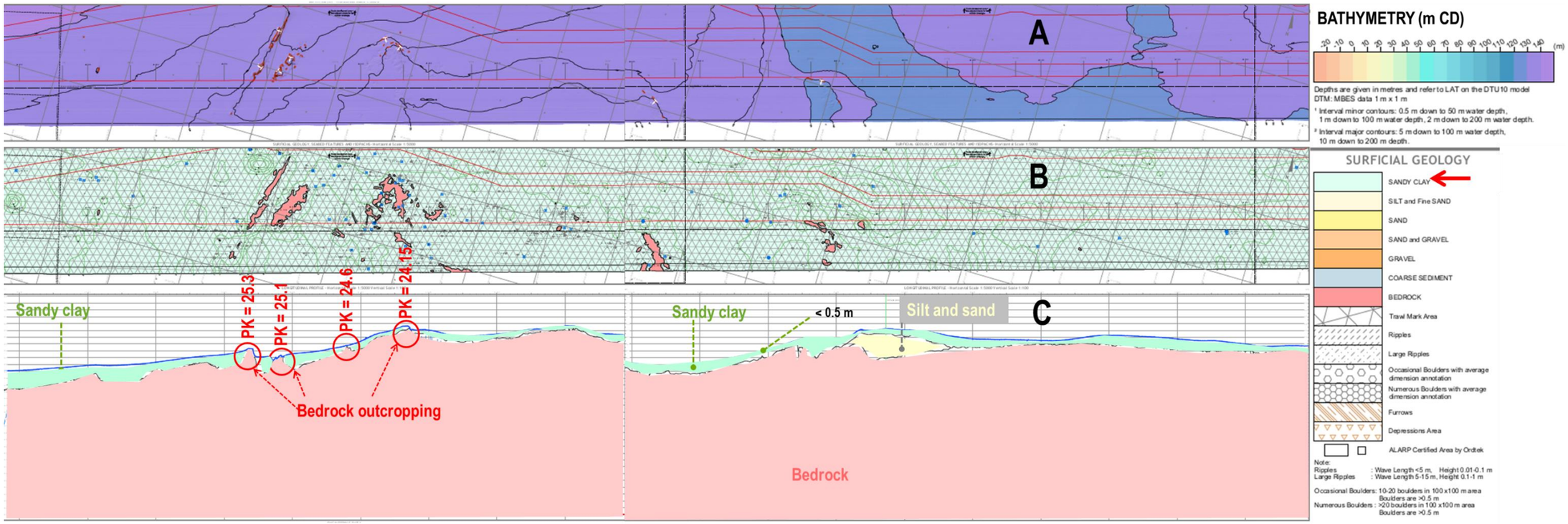

Figure 79. ***Bathymetric survey [A], nature of surficial sediment [B], thickness of movable sediment [C] along the ARSW corridor from PK 17.5 to PK 27 (from [10])***

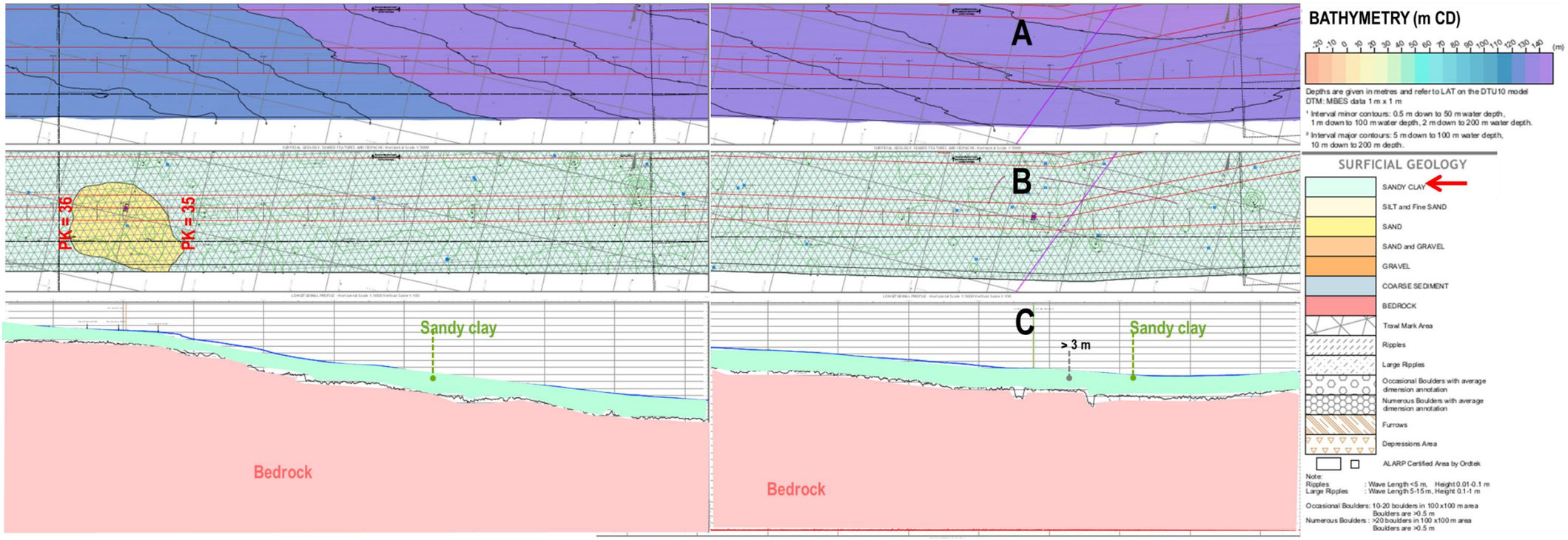

Figure 80. ***Bathymetric survey [A], nature of surficial sediment [B], thickness of movable sediment [C] along the ARSW corridor from PK 27 to PK 36 (from [10])***

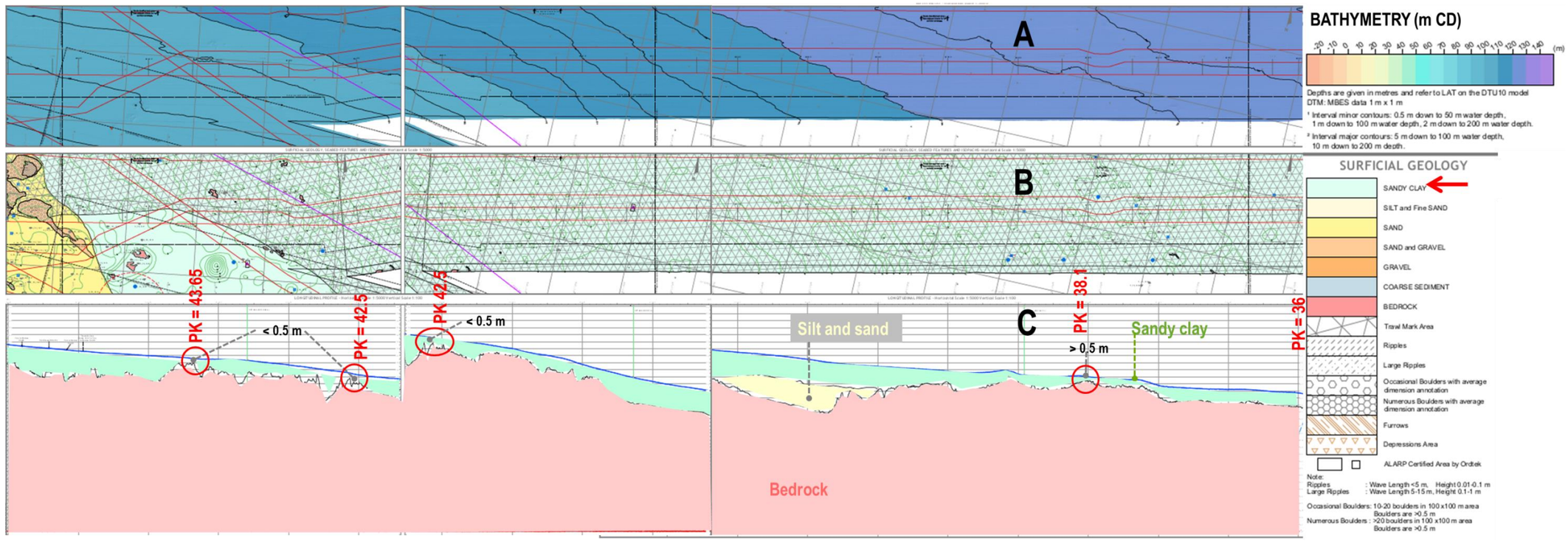

Figure 81. ***Bathymetric survey [A], nature of surficial sediment [B], thickness of movable sediment [C] along the ARSW corridor from PK 36 to PK 45 (from [10])***

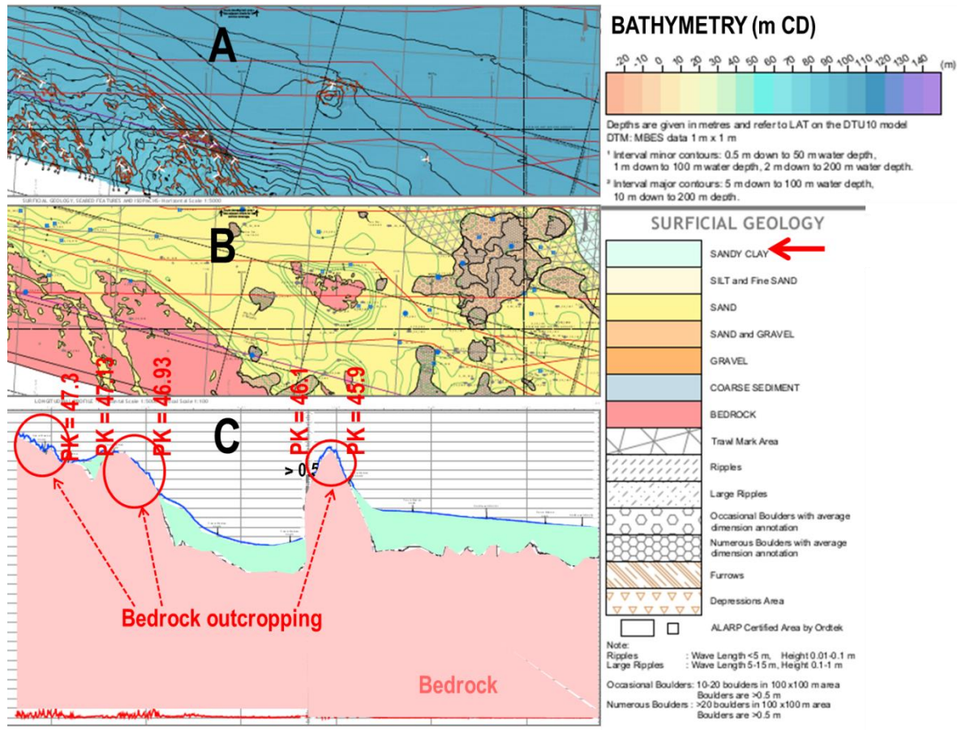

Figure 82. ***Bathymetric survey [A], nature of surficial sediment [B], thickness of movable sediment [C] along the ARSW corridor from PK 45 to the end of the route (from [10])***

5.4. NATURE OF THE SEABED

According to the survey results, the surficial geology is predominantly made of sandy clay, as can be seen on Figure 77 B, Figure 78 B, Figure 79 B, Figure 80 B, and Figure 81 B.

As shown on part C of those figures, the **thickness of surficial sandy clay layer over the bedrock varies from few meters to few centimeters, with several bedrock outcroppings at: PK = 3.5, PK = 7.25, PK = 24.15, PK = 24.6, PK = 25.1, PK = 25.3, from PK = 45.9 to PK =46.1, from PK =46.93 to PK =47.13, and from PK = 47.3.**

It almost outcrops (thickness of sandy clay layer < 0.5 m) at PK =17.4, PK =38.7, PK =42.5, PK =43.65.

5.5. GRAIN SIZE CHARACTERISTICS OF SEDIMENTS ALONG THE ARSW

Particle size distribution was carried out on sediment samples collected at:

- VC 138: 32% of fine, D_{50} = 0.18 mm
- VC 146: 28% of fine, D_{50} = 0.15 mm
- VC147A: 9% of fine, D_{50} = 0.25 mm
- VC 019: 26% of fine, D_{50} = 0.16 mm
- VC 149: 0% of fine, D_{50} = 0.19 mm
- VC 150: 58% of fine, D_{50} < 0.063 mm

These results are typical of fine sand with more or less important part of silt.

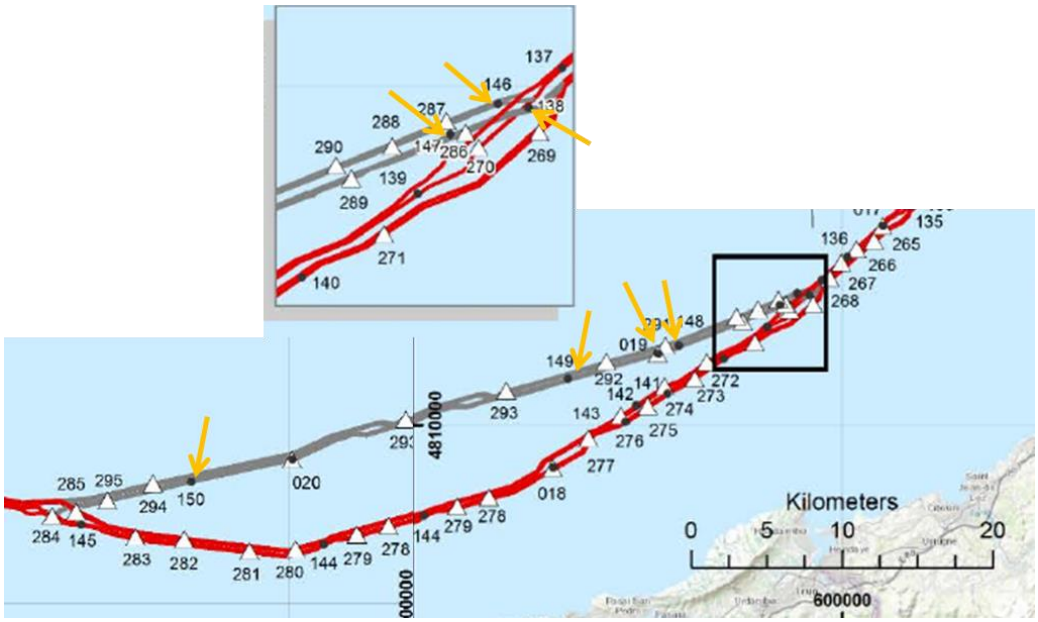

Figure 83. Locations of sediment samples analysed along the ARSW, from [16]

5.6. LOCAL HYDRODYNAMICS

Extraction of metocean conditions (waves and currents) along the ARSW was carried at points L08 and L10 from the metocean study [1] (see Figure 84). Time series of wave and current parameters over the representative year 2012 were used for the seabed mobility analysis.

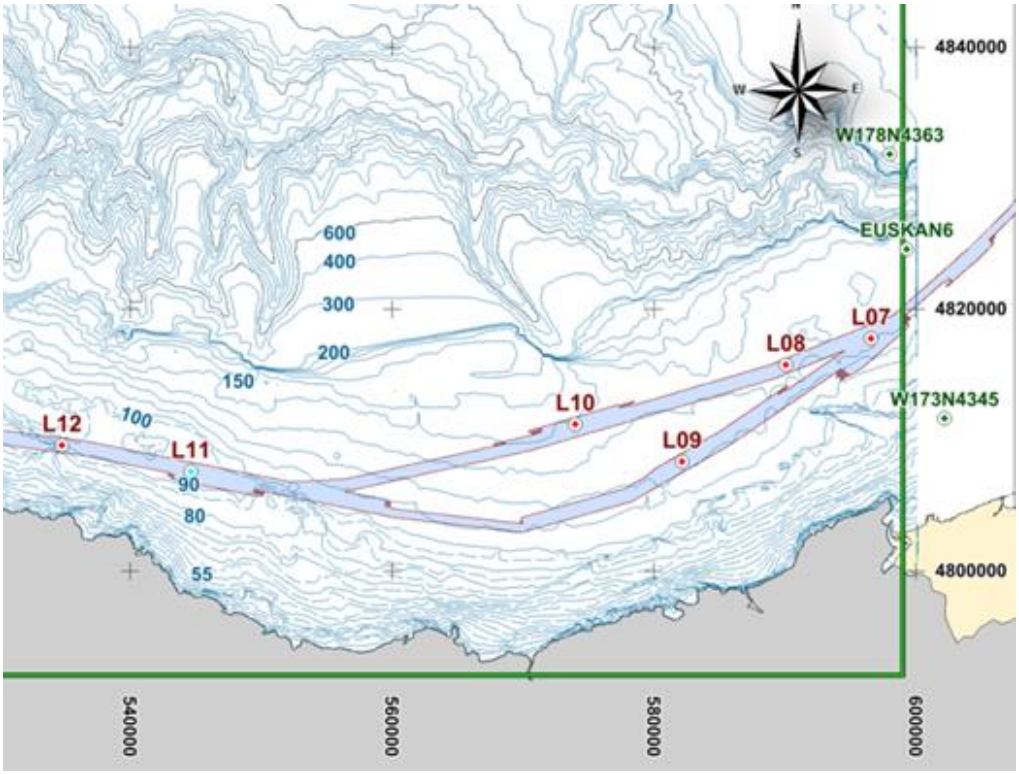

Figure 84. Locations of points L08 and L10 where time series of waves and currents were extracted from [1]

5.7. EMPIRICAL ASSESSMENT OF POTENTIAL SEABED MOBILITY ALONG THE ARSW

5.7.1. Calculation of bed shear stress along the ARSW

To assess the potential mobility of the surficial sediment calculations of bed shear stresses:

- due to the action of tides and winds (TAU_C);
- due to the combined action of tides, winds and waves (TAU_C+W or TAU_MAX);

are carried out over the year 2012 at locations L08 and L10.

Comparison with critical bed shear stresses associated to 3 types of grain is made and allows to assess times (in percent per year) of potential motion of seabed sediment along the ARSW route.

The following table reminds, for each of the grain size, the critical bed shear stress.

Table 16 – Critical bed shear stress

Mean grain diameter (D50)	Critical bed shear stress (TAU_CR)
0.1 mm	0.16 N/m^2
0.25 mm	0.18 N/m^2
0.5 mm	0.25 N/m^2

5.7.2. Assessment of potential seabed mobility along the Spanish alternative route

At L08 and L10, the following parameters were plotted on a graph (Figure 95):

- Time series of TAU_C over 2012 (red line);
- Time series of TAU_C+W over 2012 (green line);
- Time series of TAU_MAX over 2012 (dashed dark red line);
- TAU_CR (D_{50} = 0.5 mm) (orange line) ;
- TAU_CR (D_{50} = 0.25 mm) (light orange line);
- TAU_CR (D50 = 0.1mm) (yellow line)

Table 17 – Yearly percentage of time where critical bed shear stress is exceeded for different assumptions of mean grain diameter for sediment along the ARSW route

Location	D50 = 0.1 mm	D50 = 0.25mm	D50 = 0.5 mm
L08	0.4%	0.17%	0%
L10	0.3%	0.13%	0%

Along the ARSW, wave action (TAU_MAX) is very low: it can put surficial fine sand in suspension and rework the surficial layer of seabed only 0.4% of the year at L08 (see Figure 85) and even less (0.3%) at L10 (see Figure 86). These low values are due to the large water depths along the ARSW (between 90 and 135 m water depths).

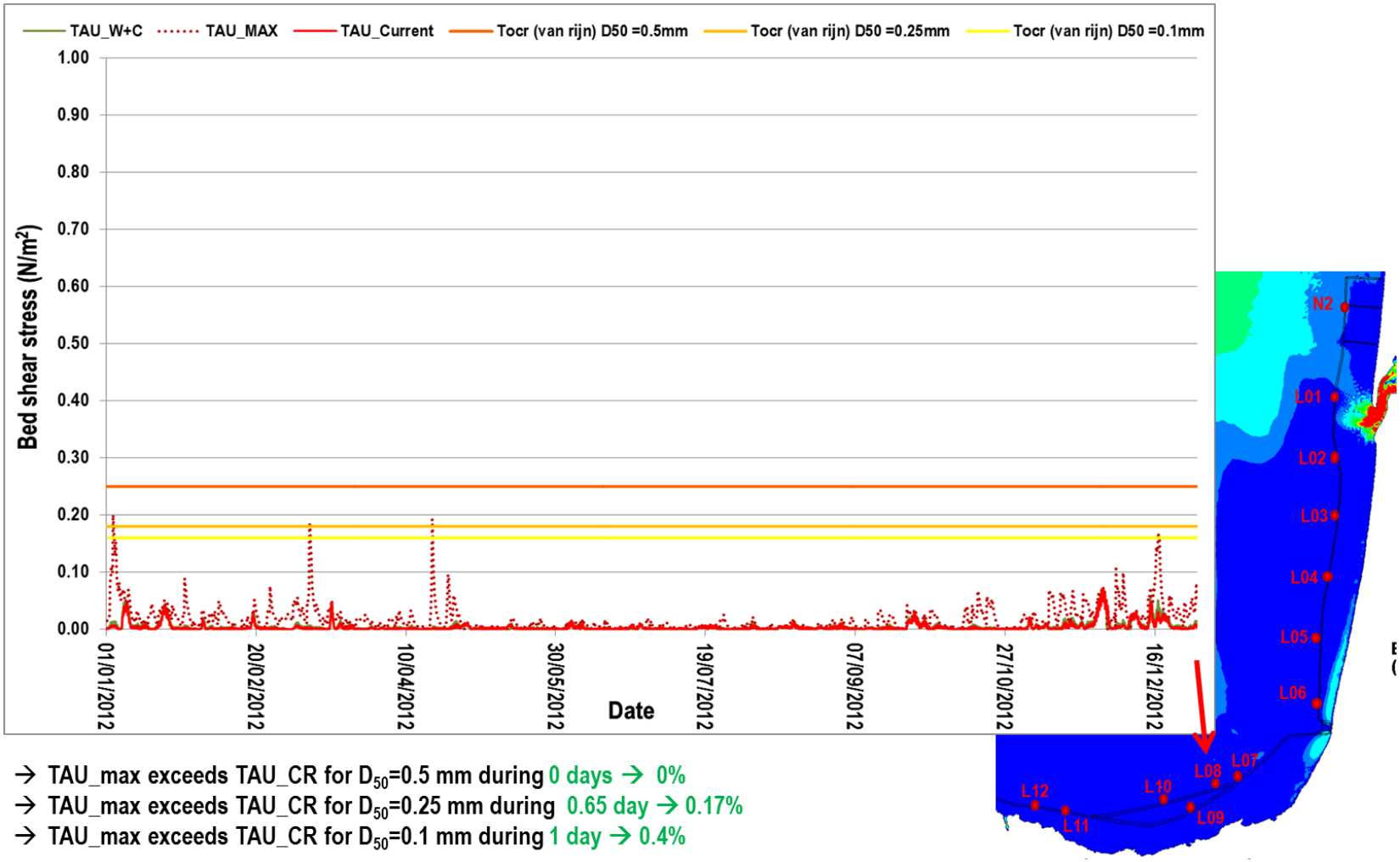

Figure 85. ***Plotted bed shear-stresses at L08 over 2012, to be compared to TAU_CR for grains of D_{50} = 0.1mm, D_{50} = 0.25 mm, D_{50} = 0.5 mm***

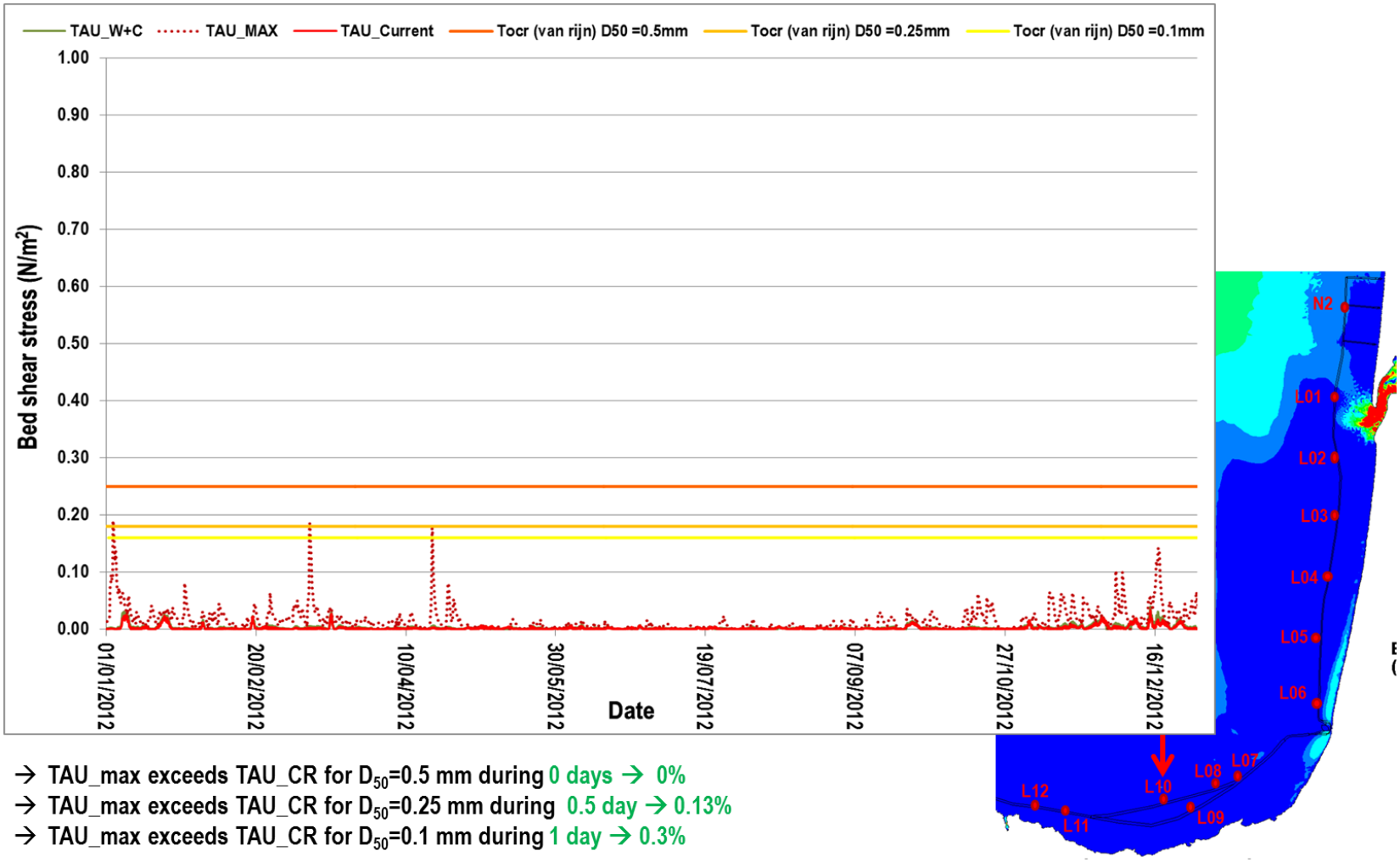

Figure 86. ***Plotted bed shear-stresses at L10 over 2012, to be compared to TAU_CR for grains of D_{50} = 0.1mm, D_{50} = 0.25 mm, D_{50} = 0.5 mm***

5.8. EVIDENCE OF EFFECTIVE SEABED MOBILITY ALONG THE ARSW

No evidence of seabed feature is given by the survey except:

- Undulations of the seabed at the beginning of the route, showing height of crest of + 2 m;
- Trawl marks all along the route;
- Several seabed outcroppings.

Considering the low potential of mobility at L08, we conclude that the undulations located at the beginning of the route hardly migrate. **More investigations based on historical bathymetry of the area are needed to provide more accurate conclusions**.

.

5.9. SUMMARIZED TABLE OF SEABED MOBILITY AND BED LEVEL CHANGE ALONG THE ARSW

Previous results are put into perspective with the characteristics of the ARSW mainly the mean diameter, the existence of bed forms and the thickness of erodible layer as shown in the following table.

Table 18 – Potential mobility along the ARSW

Section	Metocean analysis point	Bed forms	Thickness of erodible layer	D50 (mm) at surficial layer	Seabed mobility (% of a year)	seabed level change
ARSW	L08, L10	Bedrock outcropping Evidence of **trawl marks**	Relatively thin cover of surficial sediments over bedrock may not allow sufficient depth of burial for the proposed cable.	Fine sand , Sandy clay D50 < 0.2 mm	Very low potential of seabed mobility (< 0.4%)	Negligible bed level change.

The results show that the ARSW has a very thin layer of surficial sediments and that these sediments are not likely to be moved by the hydraulic conditions mainly due to the deep water depths.

The major constraint along this route is the relatively thin cover of surficial sediments over the bedrock that may not provide sufficient depth of burial for the proposed cable.

6. SEABED MOBILITY AND BED LEVEL CHANGE AT SPANISH LANDFALL

6.1. INTRODUCTION

The Spanish part of the offshore route ends at KP 283.3 and shoals from 30 m to the Spanish landfall site located close to Bilbao.

In order to assess the sea bed level variability and the maximum extent of the potential vertical variations at this Spanish coastal area, the following specific methodology has been implemented:

- Characterization of seabed nature and in situ movable sediment thickness based on the geophysical and geotechnical surveys;
- Conclusion on the potential vertical variation of the movable seabed layer depending on local hydrodynamics calculated for a representative year.

6.2. LOCATION OF THE SPANISH LANDFALL

The Spanish landfall is located in front of the Lemoiz nuclear plant built on the coastline (see Figure 87), 20 km NNE from Bilbao.

Figure 87.Location of the Spanish landfall site

6.3. GEOPHYSICAL SURVEY

Geophysical survey along the Spanish landfall was surveyed between the 25th of September and the 07th of November 2016.

It was conducted by two different vessels and overlapped the end of the main route survey area.

The two different vessels are the following:

- the M/V Geo Focus undertook the nearshore survey, thanks to a pole-mounted Innomar system that included a side scan sonar (SSS) and a sub-bottom profiler (SBP), plus a magnetometer towed from the aft deck and a multibeam echo sounder (MBES) was hull-mounted ;.
- The shallow water survey in Nearshore Spain was surveyed by Plasticbeam using MBES and a GoPro Camera

Due to the presence of dangerous shoaling bedrock nearshore, the survey lines were made offset from and across the landfall route. There is no KP data base to which to refer in the following descriptions. As reminder, the main route ends at KP: 283.278. Spanish landfall survey begins at this KP to reach the coastline.

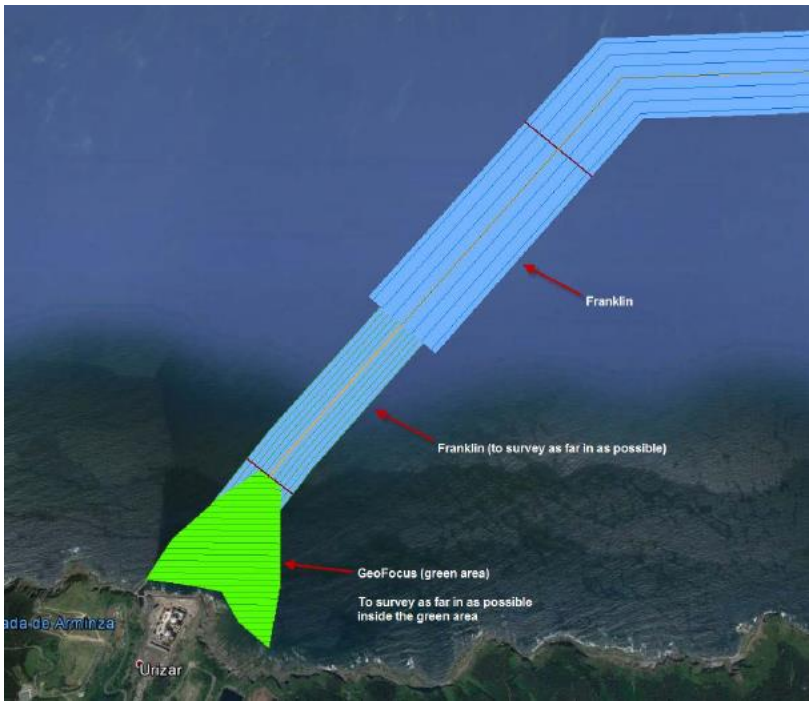

Figure 88.Surveys carried out along the Spanish landfall area

6.4. BATHYMETRY

According to the surveyed bathymetry at the Spanish landfall site (presented on Figure 89), water depths vary from 23.2 m in the Northwest to 1.6 m in the Southwest.

As shown in [10], the seabed along the Spanish landfall route is rough, as illustrated on Figure 90 .

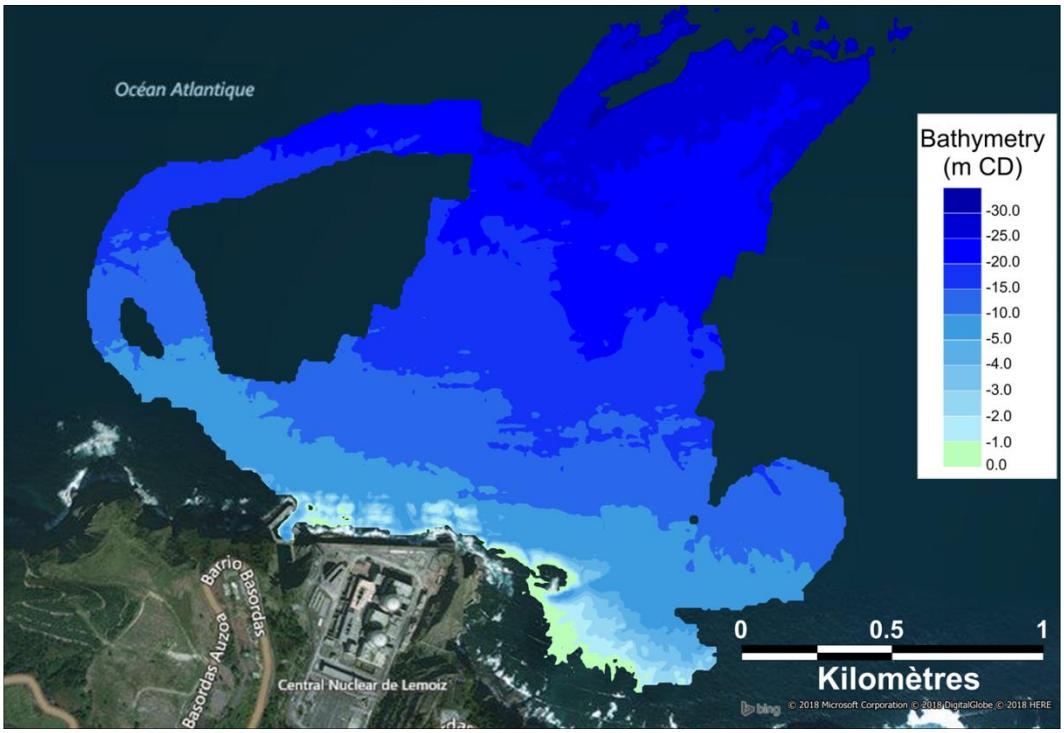

***Figure 89.** Bathymetry of Spanish landfall site, from ARTELIA*

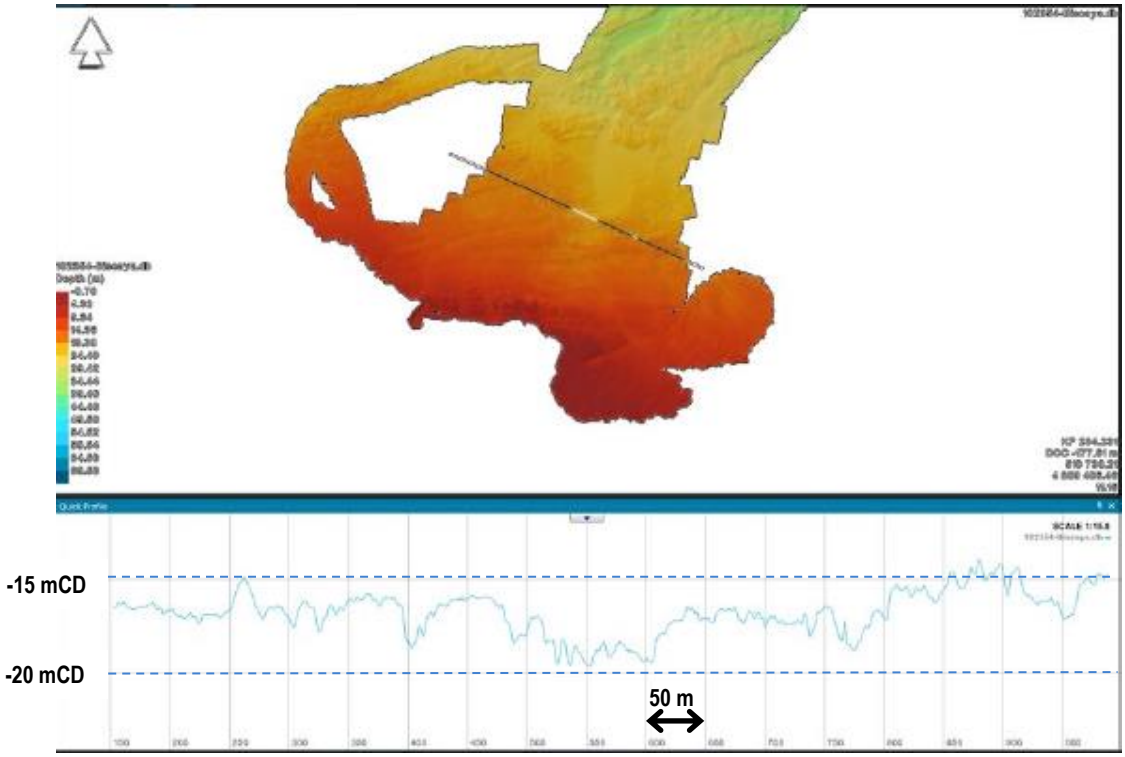

***Figure 90.** Bathymetric profile along a section crossing the landfall route, from [10]*

6.5. NATURE OF THE SEABED

According to the survey results, the surficial geology is predominantly bedrock.

However a patchy veneer of sand and gravel has been identified. This isolated sandy pouch is located at water depth of 20 m - 25 m CD, and is 220 m long and 160 m wide. Its thickness varies, reaching a maximum of 2.5 m.

Investigations on this sandy veneer were carried out in [10] along two transects plotted on Figure 91. They showed that sandy veneer thickness is greater along the Northern transect (reaching 2.5m) than along the Southern transect where the maximum thickness of the movable sediment layer reaches 2 m (see Figure 92).

Sand and gravel deposit (in pouch) shows ripples with wavelength from 0.5m to 1.5 m and height about 0.2 m. They are orientated WSW to ENE.

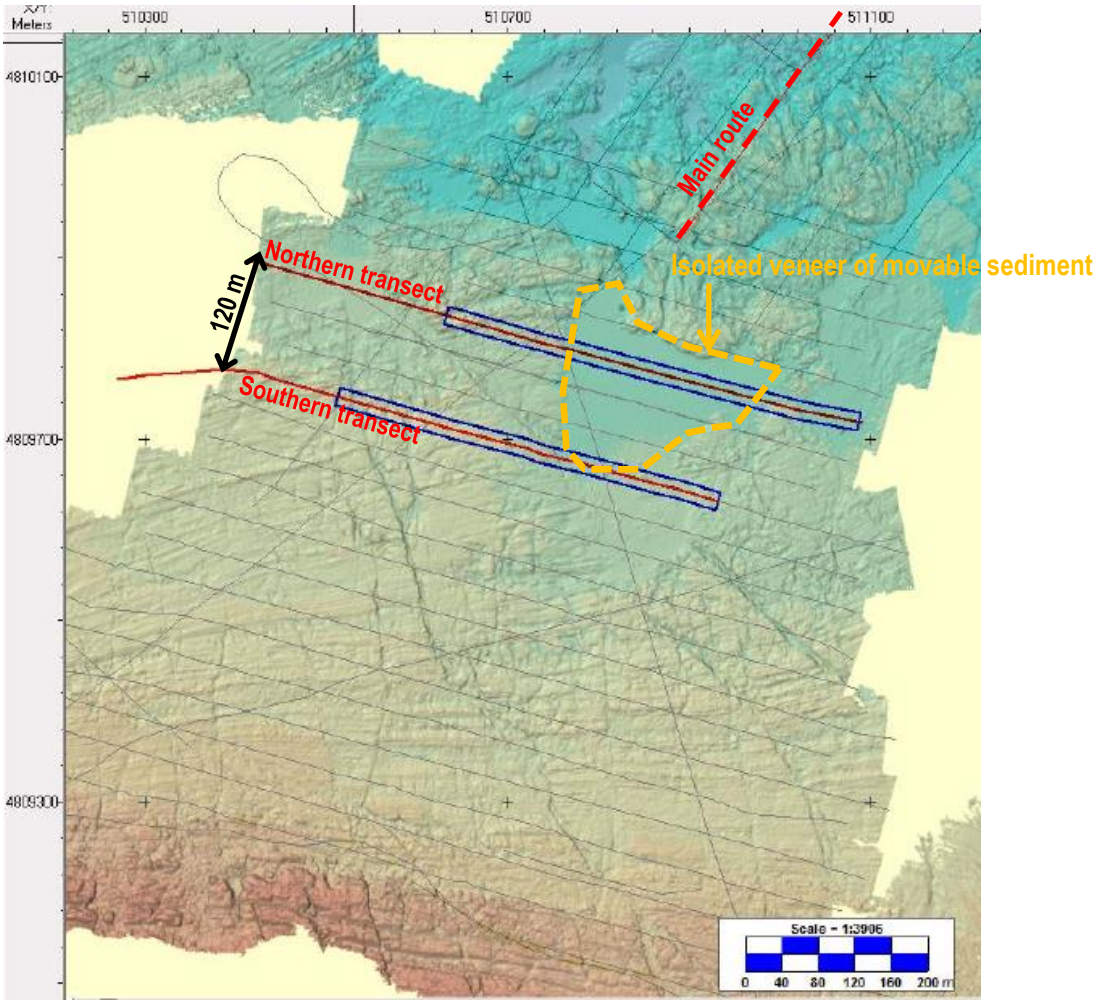

Figure 91. Shaded relief of Spanish landfall site, location of sandy pouch and of the two investigated transects, from [10]°

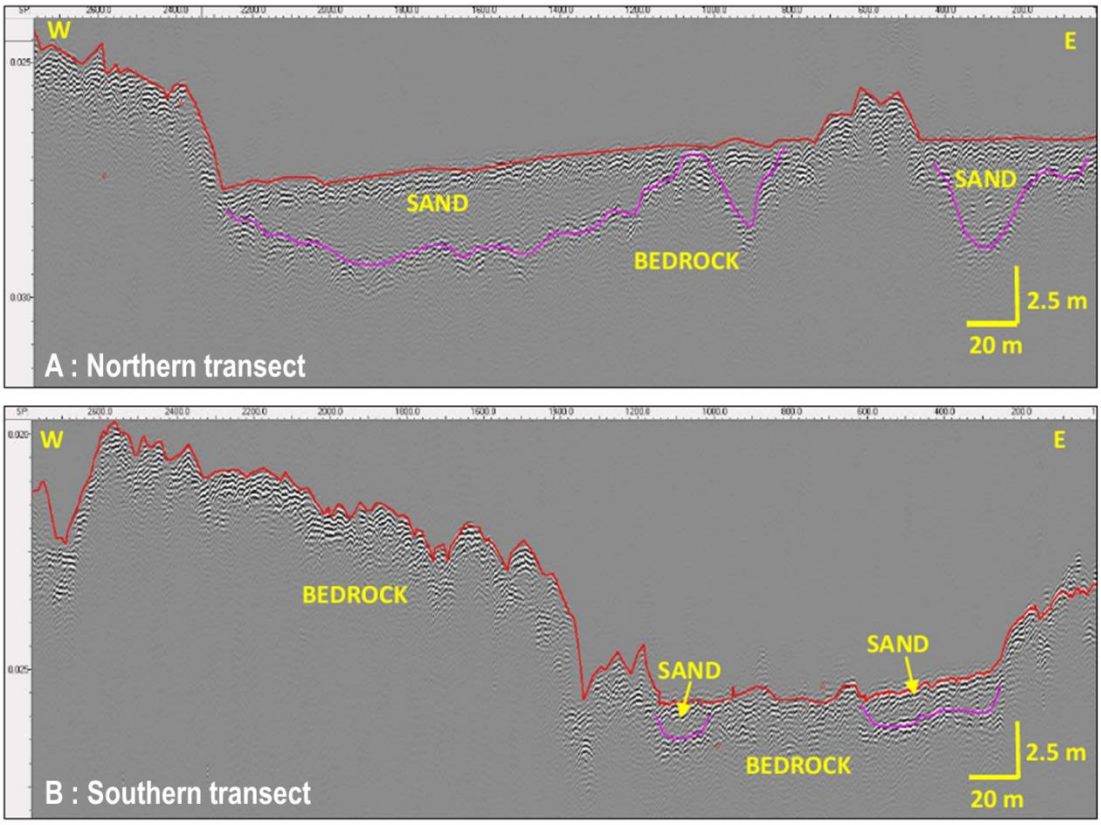

Figure 92. Seabed relief of Spanish landfall site at the two transects plotted on previous figure, and results of innomar survey in terms of thickness of movable sediment layer

6.6. GRANULOMETRY OF MOVABLE SEDIMENT WITHIN ISOLATED SANDY POUCH

Particle size distribution was carried out **on only one sample along the Spanish landfall**, called VC-024. This sediment sample was collected in the sandy veneer at its maximum thickness (over 2.43 m BSF[3]). Resulting graphs are reported in [16].

Sediment at the upper layer of the movable seabed (from 0 BSF to 1m BSF) is mainly made of sand (99%) with 1% of gravel. The median particle diameter is D_{50} = 0.5 mm (i.e. coarse sand according to the Wentworth sediment classification).

Considering this mean grain diameter of sand of 0.5 mm, ripples height (Yalin [22]) is about Δ_r =2.5 cm to 10 cm, and ripples length λ_r = 25 cm to 50 cm.

The deepest layer (from 2m BSF to 2.43 m BSF) is mainly made of gravel (61%), cobble (21%) and sand (17%). The median particle diameter is D_{50} = 13 mm (i.e cobble according to the Wentworth sediment classification).

[3] BSF = Below Sea Floor

6.7. LOCAL HYDRODYNAMICS

Analysis of metocean conditions at Spanish landfall area was carried in [1] in terms of currents due to tide and wind forcings, as well as in term of wave conditions. Here are reminded the main results that are used further on to calculate the corresponding bed shear stress applied on seabed over a representative year (2012).

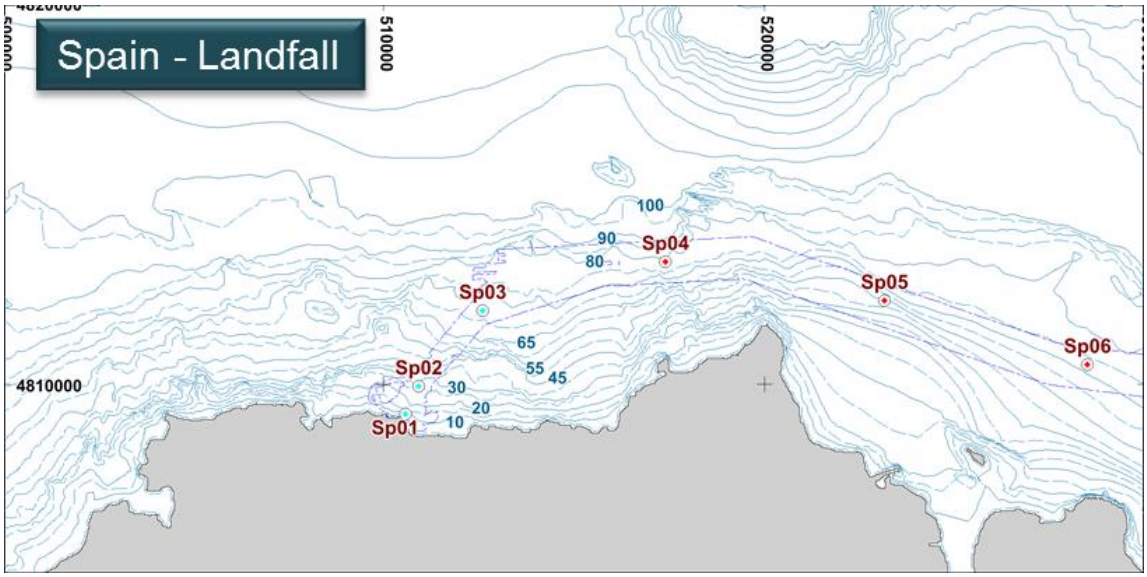

Figure 93. Locations of points where currents and wave climate were analyzed, from [1]

6.7.1. Tidal currents

In front of the Spanish landfall, offshore, the total direction is mainly directed towards the East (point Sp03) and turns in direction East-South-East as one approaches the coast (point Sp02). At the closest point to the coast (Sp01), 2 main directions appear (East-South-East and West-North-West). The intensity remains lower than 0.3 m/s near the sea bottom and can exceed 0.35 m/s close to the surface. The main part of the signal is not generated by the tide but by the current induced by the atmospheric parameters.

6.7.2. Usual wave conditions

In front of the Spanish landfall (points Sp02, Sp03) the main directions are North-West with a narrower spread around the main direction near the coastline. Near the coastline (point Sp01), the direction changes due to refraction, the waves come mainly from the North. The highest H_s (> 3 m) and the longest periods (12-18 s) appear frequently during winter months whereas the summer season sees waves with lower H_s (0.5 to 1.5 m) and shorter period.

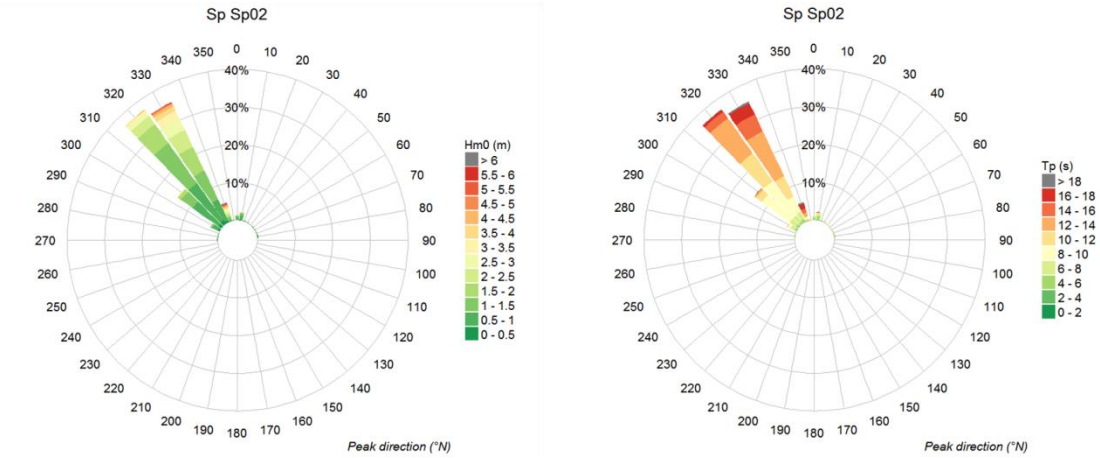

Figure 94. Annual wave rose – Point Sp02 – Spanish landfall

6.8. ASSESSMENT OF POTENTIAL SEABED MOBILITY ABOVE THE SANDY POUCH

6.8.1. Calculation of bed shear stress at the Spanish landfall

To assess the capability of the granular sediment trapped in the sandy pouch to move, calculations of bed shear stresses:

- due to the action of tides and winds (TAU_C);
- due to the combined action of tides, winds and waves (TAU_C+W or TAU_MAX);

are carried out over the year 2012, at Spanish landfall location SP02.

Comparison with threshold bed shear stresses related to 3 types of grain is made and allows to assess times (in percent per year) of potential motion of seabed sediment along the Spanish landfall thus, to qualify the potential mobility of the seabed along the Spanish landfall.

6.8.1.1. Critical shear stress

To take into account the variability of sand granulometry along the route, three grain sizes are considered. The following tables give, for each of the grain size, the critical bed shear stress.

Table 19 – Critical bed shear stress

Mean grain diameter (D50)	Critical bed shear stress (TAU_CR)
2 mm	1.28 N/m^2
1 mm	0.52 N/m^2
0.5 mm	0.25 N/m^2

6.8.1.2. Bed shear stress due to wind, current and wave action (TAU_C+W and TAU_MAX)

Bed shear stress due to wind, current and wave action (TAU_C+W and TAU_MAX) is calculated at Sp02 over 2012, following the same methodology as in 3.3.3

6.8.2. Assessment of potential seabed mobility along the Spanish landfall

At Sp02, the following parameters were plotted on a graph (Figure 95):

- Time series of TAU_C over 2012 (red line);
- Time series of TAU_C+W over 2012 (green line);
- Time series of TAU_MAX over 2012 (dashed dark red line);
- TAU_CR (D_{50} = 0.5 mm) (orange line) ;
- TAU_CR (D_{50} = 1 mm) (light orange line);
- TAU_CR (D50 = 0.2mm) (yellow line)

Table 20 – Yearly percentage of time where critical bed shear stress is exceeded for different assumptions of mean grain diameter for the sediment pouch at Spanish landfall

Location	D50 = 0.5 mm	D50 = 1 mm	D50 = 2 mm
SP02	41%	17%	2.7%

Concerning the isolated sandy and gravelly veneer within the Spanish landfall area, wave action (TAU_MAX) can put surficial coarse sand in suspension and rework the observed seabed features (ripples) 41% of the year. This important potential of mobility of sand (even if coarse sand) tends to indicate that local hydrodynamics potentially transport sand almost half of the year, allowing thin sand veneer to possibly run over the bedrock, only stopped when trapped in bedrock cavities.

Concerning the underneath coarser particles, potential of mobility is drastically lower: only major storm can possibly rework deeply the 2.5 m layer.

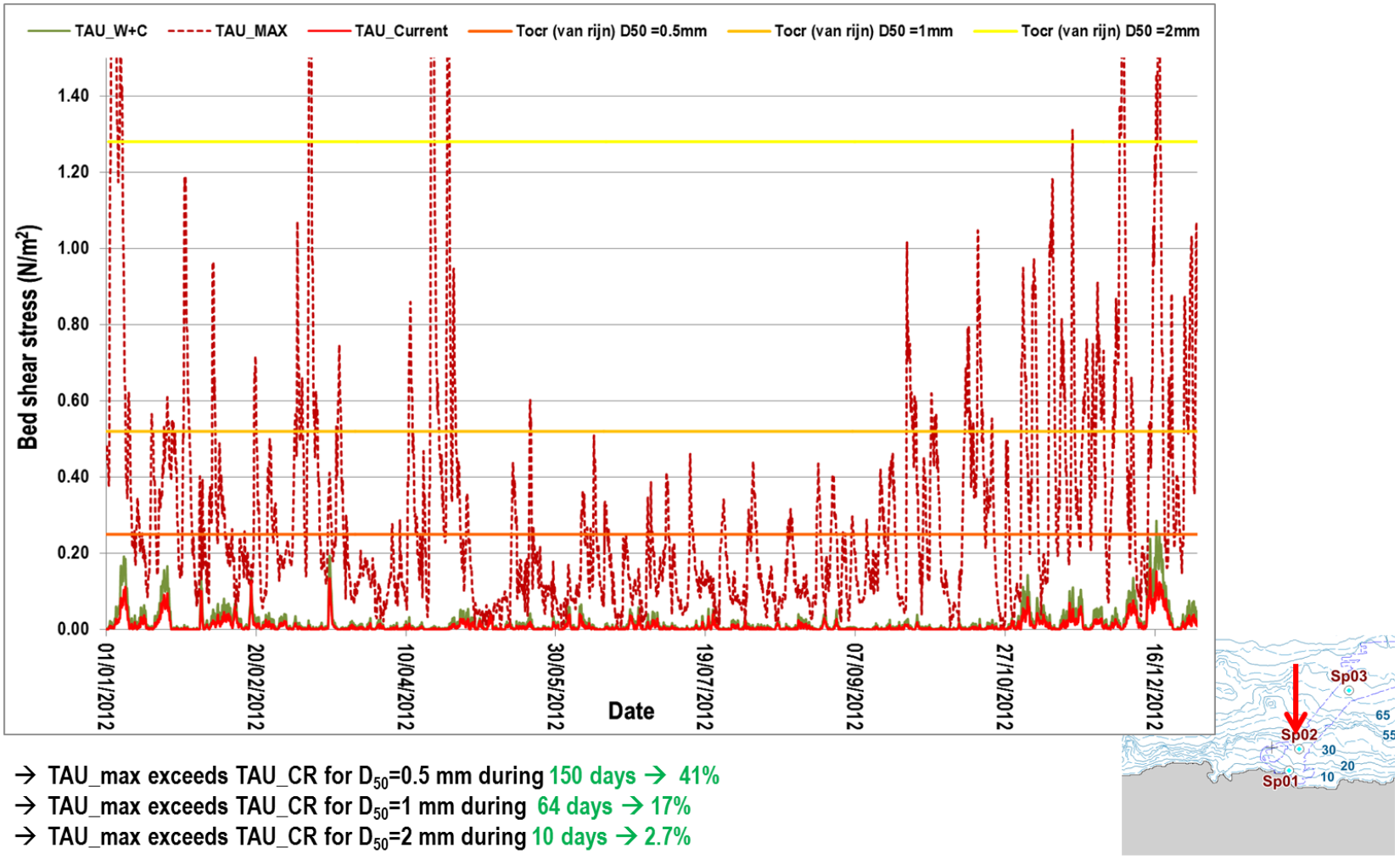

***Figure 95.** Plotted bed shear-stresses at Sp02 over 2012, to be compared to TAU_CR for grains of D_{50} = 0.5mm, of D_{50} = 1 mm and of D_{50} = 2 mm*

6.8.3. Summarized table of seabed mobility and bed level change along the Spanish landfall

Previous results are put into perspective with the characteristics of the Spanish landfall mainly the mean diameter, the existence of bed forms and the thickness of erodible layer as shown in the following table.

Table 21 – Potential mobility at Spanish landfall

Section	Metocean analysis point	Bed forms	Thickness of erodible layer	D50 (mm) at surficial layer	Seabed mobility (% of a year)	Seabed level change
SL[4]	Sp02, Sp01	Mainly bedrock, with isolated patchy sand and gravel veneer/ Ripples at seabed surface of sand pouch Height < 10cmr	Reaches 2.5m	Sand and Gravel trapped in bedrock cavities. D50 = 0.5 mm at surficial layer	Surficial sand in sandy pouch are possibly reworked 41% of the year	In sandy pouch made of sediment trapped in bedrock cavities, seabed changes are equal to height of sand ripples < 10 cm.

No significant seabed level change are expected at the Spanish landfall, due to the rocky nature of the seabed.

[4] SL for Spanish Landfall

6.9. STABILITY OF SHORELINE AT SPANISH LANDFALL

As shown on aerial pictures presented Figure 96 and Figure 97, the area where the cable is supposed to land is a very rocky embayment.

According to a simple comparison of historical aerial pictures we can assume the apparent stability of the coastline. Shoreline accretion or recession at the Spanish landfall is expected to be negligible over the cable life span.

In accordance with INELFE, we did not pursue further the investigations concerning the coastal stability.

Figure 96. ***Aerial picture of the coastline in October 2004, from Google Earth***

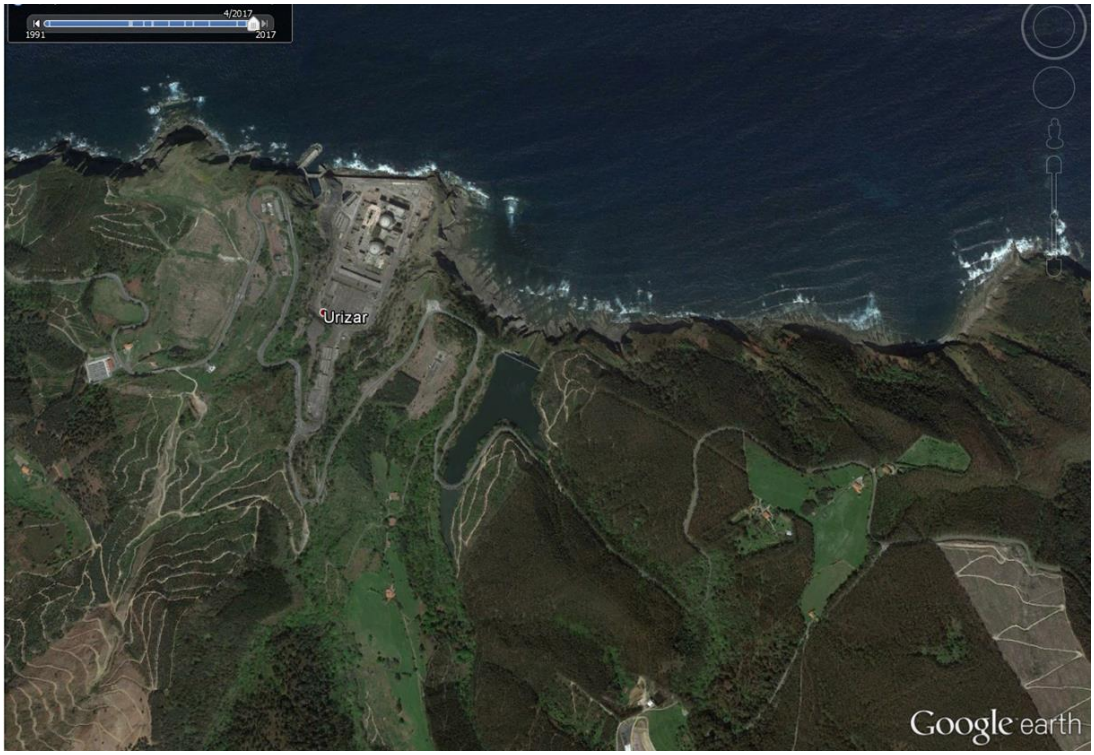

Figure 97. ***Aerial picture of the coastline in April 2017, From Googl Earth***

REFERENCES

[1] ARTELIA, November 2017, Biscay Gulf Interconnector Project – Metocean study report

[2] SOGREAH, 2011, Etude de gestion de la bande côtière à 2040

[3] Jossand R., 2004. Etude de l'évolution du trait de côte et de l'impact des ouvrages de défense contre la mer de Lacanau-Océan pour la définition de nouvelles solutions de défense. Rapport de Master, spécialité 3GC, Univ. Bordeaux I

[4] Commune de Lacanau, Département de la Gironde, Région Aquitaine,2015. Stratégie locale de gestion de la bande côtière de Lacanau - Programme d'actions et de prévention de l'érosion, Version 8 du 23.10.2015

[5] Mairie de Lacanau, avec le soutien du GIP Littoral Aquitain et de l'Observatoire de la Côte Aquitaine, 2012, 2ème Forum sur l'érosion du trait de côte. Support de présentation

[6] Aubie S, Mallet C. and Favennec J. with collaboration of Hoareau A.., 2011. Caractérisation de l'aléa érosion (2020-2040) de la Côte Aquitaine dans le cadre de l'étude stratégique du trait de côte. Observatoire de la côte aquitaine, Rapport BRGM/RP-59095-FR, 97p.

[7] Bernon N., Mallet C. Belon R. J. with collaboration of Hoareau A., Bulteau T. and Garnier C, 2016. Caractérisation de l'aléa recul du trait de côte de la Côte Aquiaine aux horizons 2025 at 2050 . Rapport final. BRGM/RP-66277-FR, 99p.

[8] Mallet C., Garnier C., Maugard F., Millescamps B., Mugica J., Nahon A., Rosebery D., avec la collaboration de Bassibey A., Bouchet C., Capdeville B., Chartier E., Devoti J., Duport B., Maia J., Perrocheau E., Rambaud D., Raynaud V., Robert D. (2014). Compte-rendu des observations post-tempêtes sur le littoral Aquitain (décembre 2013 – janvier 2014). Rapport final. BRGM/RP-63182-FR, 81 p.

[9] SHOM and CETMEF, 2012, Statistiques des niveaux marins extrêmes des côtes de France (Manche et Atlantique)

[10] Marine Survey Report, MMT for INELFE, Revision A March 2017, Biscay HVDC WI Route Survey – Capbreton Canyon, Gulf of Biscay, September - November 2016 (102354-INE-MMT-SUR-REP-SURVEYRE)

[11] Garlan T. and Marchès E,, undated. Nature sédimentaire des fonds marins / SRM GDG (SHOM)

[12] Mazière A., 2011, Evolution morphologique et processus sédimentaires actuels de plateau continental interne sud-aquitain : Etude comparée des zones de La Salie-Biscarosse et de la zone de la tête du Canyon de Capbreton, PhD thesis, University of Bordeaux I

[13] Gillet H., 2012. High resolution morphobathymetric analysis and short-term evolution of the Capbreton canyon head, Report for recommendations concerning a project of submarine VHV cable installation

[14] Loubrieu B., Mazé J.P., 2012. Morphology analysis of the Cap Breton Canyon, Ifremer-RTE contract DV/SC12.01

[15] Mallet C., Garnier C., Maugard F., Millescamps B., Mugica J., Nahon A., Rosebery D., avec la collaboration de Bassibey A., Bouchet C., Capdeville B., Chartier E., Devoti J., Duport B., Maia J., Perrocheau E., Rambaud D., Raynaud V., Robert D., 2014. Compte-rendu des observations post-tempêtes sur le littoral aquitain (décembre 2013 – janvier 2014). Rapport final. BRGM/RP-63182-FR, 81 p., 109 fig., 1 ann

[16] Geotechnical report, MMT for INELFE, For client review October 2017, Biscay HVDC WI Route Survey (102534-INE-MMT-SUR-REP-GEOTECH)

[17] Mallet C. Thinon I., Idier D. Gillet H., Rosebery D. (2016). Projet d'interconnexion électrique France-Espagne via le Golfe de Gascogne. Avis technique concernat la route maritime. Rapport BRGM/RC-65979-FR. 47p

[18] Soulsby R., 1994, Dynamics of Marine Sands: A Manual for Practical Applications, HR Wallingford editions.

[19] Mazières A., 2014, Evolution morphologique et processus sédimentaires actuels du plateau continental interne sud-aquitain : Etude comparée des zones de La Salie-Biscarosse (sud des passes d'Arcachon) et de la zone de la tête du Canyon de Capbreton. Thèse de doctorat. Ecole doctorale des Sciences et Environneents, Université de Bordeaux.

[20] EID Méditerranée et Service Maritime et de Navigation du Languedoc-Roussillon, 2005 . Guide technique n°9 « Connaissance et gestion de l'érosion littorale », SDAGE Rhône-Méditerranée – Corse, 55p 1 annexe,.

[21] CIRAC P., BERNE S., CASTAING P., WEBER, O. 1999. Processus de mise en place et d'évolution de la couverture sédimentaire superficielle de la plate-forme nord-aquitaine, Oceanologica Acta Vol. 23 – n° 6

[22] YALIN M.S, 1985. On the determination of Ripple Geometry. Journal of Hydraulic Engineering, Vol.III,n° 8.

APPENDIX A

STUDY ON THE LONG-TERM HYDROSEDIMENTARY STABILITY OF THE NEARSHORE SEABED LOCATED BETWEEN THE CAPBRETON CANYON AND THE COASTLINE. I-SEA 2017.

APPENDIX B

BED SHEAR-STRESS MAPS (TIDAL +WIND CURRENTS)

APPENDIX C

SEABED MOBILITY POTENTIAL ALONG THE OFFSHORE ROUTE